Multi-layer distributed control of complex systems with communication constraints : application to irrigation channels

Le-Duy-Lai Nguyen

Communauté
UNIVERSITÉ Grenoble Alpes

THÈSE

Pour obtenir le grade de

DOCTEUR DE LA COMMUNAUTÉ UNIVERSITÉ GRENOBLE ALPES

Spécialité : **AUTOMATIQUE-PRODUCTIQUE**

Arrêté ministérial : 25 Mai 2016

Présentée par

Le-Duy-Lai NGUYEN

Thèse dirigée par **Monsieur Laurent LEFÈVRE**
et co-encadrée par **Monsieur Denis GENON-CATALOT**

préparée au sein **Laboratoire de Conception et d'Intégration des Systèmes (LCIS - EA 3747)**
dans **l'École Doctorale Électronique, Électrotechnique, Automatique et Traitement du Signal (EEATS - ED 220)**

Contrôle distribué multi-couches des systèmes complexes avec contraintes de communication : application aux systèmes d'irrigation

Multi-layer distributed control of complex systems with communication constraints: application to irrigation channels

Thèse soutenue publiquement le **19 Décembre 2017**,
devant le jury composé de :

Monsieur, Jean-Marc THIRIET
Professeur - GIPSA-Lab, Univ. Grenoble Alpes, Président
Monsieur, Eric DUVIELLA
Professeur - IMT, Ecole des Mines de Douai, Rapporteur
Monsieur, Michel ROBERT
Professeur - CRAN, Univ. de Lorraine, Rapporteur
Monsieur, Bastien CHOPARD
Professeur - CUI, Univ. de Genève, Examinateur
Monsieur, Laurent LEFÈVRE
Professeur - LCIS, Institut Polytechnique de Grenoble, Directeur de thèse
Monsieur, Denis GENON-CATALOT
Maître de conférence - LCIS, Univ. Grenoble Alpes, Co-Encadrant

Multi-layer distributed control of complex systems with communication constraints: application to irrigation channels

Le-Duy-Lai NGUYEN

Supervisors: **Prof. Laurent LEFÈVRE**
Assoc. Prof. Denis GENON-CATALOT

Univ. Grenoble Alpes, Grenoble INP*, LCIS, 26000 Valence, France
* Institute of Engineering Univ. Grenoble Alpes
Address: 50, Rue Barthélémy de Laffemas - BP54
26902 VALENCE Cedex 09 - FRANCE

This dissertation is submitted for the degree of
Doctor of Philosophy

December 2017

I would like to dedicate this thesis to my loving and lovely family,
especially, my wife Vy-Nha and my two princes Gia-An and Gia-Khang.

Acknowledgements

It is a great milestone in one's life to engage in the doctoral study and success the Ph.D. degree. This doctoral thesis, like most research works, is the result of a curious and inquisitive spirit, coupled with plenty of hard work and persistence. Naturally, it was difficult at times, but overall, the fulfilling moments far exceeded the hardship – and I owe that in a world of people, to whom I will always be grateful. Without their generous supports throughout, this thesis would not become possible.

First of all, I would like to express my sincere gratitude to my supervisors Prof. Laurent LEFÈVRE and Assoc. Prof. Denis GENON-CATALOT for their continuous support of my Ph.D. study and related research, for their patience, motivation, and immense knowledge. Their guidance helped me in all the time of research period and writing of this thesis. They are knowledgeable and helpful mentors who have not only given me advice on the academic side, but also shared a lot of experience in life. Their patience and high availability when I needed assistance in research benefited me greatly. It has been an honor to be their Ph.D. student. They have taught me, both consciously and unconsciously, how good automatic control and computer science can be combined. I appreciate all their contributions of time, ideas, and funding to make my Ph.D. experience productive and stimulating. The joy and enthusiasm that they have for their research were contagious and motivational for me, even during tough times in the Ph.D. pursuit. I am also thankful for the excellent example, they have provided as successful scientists and professors.

Besides my supervisors, I would like to thank the reading committee members: Prof. Eric DUVIELLA and Prof. Michel ROBERT, for their insightful comments and encouragement, but also for the hard question which incanted me to widen my research from various perspectives. They spent their valuable time examining my research work and provided many insightful suggestions. I would also like to thank the other members of my oral defense committee, specially Prof. Jean-Marc THIRIET, Prof. Bastien CHOPARD, for their time, interest, and helpful questions.

The financial support of the Artemis Arrowhead European project under grant agreement number 332987 is acknowledged. With the forty-two month scholarship from this project, I did not have to worry about my living expenses, and therefore was able to concentrate on studies and research.

Many thanks to the "Syndicat d'Irrigation Drômois" (SID, www.siid.fr), which has provided the information such as the overview, structure, figures and control objectives of the Bourne river irrigation network. We also wish to thank the working group "Arrowhead Project" within

Schneider Electric Grenoble, particularly Mr. Claude LEPAPE, Domain Leader of Energy Management and Analytics Optimization and Mr. Alfredo SAMPERIO, Project Leader of Task 1.4, for their support throughout the completion of research works.

I would also like to thank the members inside and outside the MACSY-COSY group. Mr. LEFÈVRE, Mr. GENON-CATALOT and Mr. André LAGREZE drove me to disastrous excursion and leisure activities many times when I stayed in the Laboratory LCIS during the three years. Mr. Antoine SAILLOT taught me techniques on the control of linear dynamic systems. Discussion with Mrs. Ionela PRODAN gave me new insights into some problems from centralized to decentralized control of complex systems. In addition, I enjoyed the friendship with other members in our group: Mr. Youness LAMI, Mr. Yoann HERVAGAULT, Mr. Benjamin VINCENT. We have shared lots of exciting moments together. I also thank Mr. El Mehdi KHALFI for inspirational discussions with me regarding the knowledge in the field of multi-agent systems. My sincere thanks also go to Mr. Christophe DELEUZE, and Mr. Yves GUIDO, who provided me an opportunity to join their team as teaching assistant, and who gave access to the network department facilities. Without their precious support it would not be possible to conduct this research.

My time at LCIS was made enjoyable in large part due to the many friends and groups that became a part of my life. I am grateful for the time spent with roommates and friends, for my backpacking buddies and our memorable trips in the mountains, countryside for Youness LAMI and Benjamin VINCENT's hospitality as I finished up my degree, and for many other people and memories. My time at LCIS was also enriched by the graduate ESISAR student group.

Finally and most importantly, I should express my gratitude to my family. Their supports, encouragement and love have been accompanying me for so many years. I am indebted to their diligent work and great contribution to the family. For my parents who raised me with a love of study and supported me in all my pursuits. I would like to thank my foster brother, Patrick TROUCHE, for supporting me spiritually throughout writing this thesis and my life in general. And most of all for my loving, supportive, encouraging, and patient wife whose faithful support during the final stages of this Ph.D. is so appreciated.

I thank my fellow lab-mates in LCIS for the stimulating discussions, for the sleepless nights we were working together before deadlines, and for all the fun we have had in the last four years. Also, I am grateful to Prof. Marc BUI in the institution "École Pratique des Hautes Études" (EPHE) for enlightening me the first glance of research.

Thank you.

Abstract

This thesis presents the control problems of irrigation network with communication constraints and a multi-layer approach to solve these problems in a distributed manner. Detailed discussions of each layer with analytical and simulation results are described throughout several chapters. They emphasize the potential interest of the multi-layer approach, more precisely its efficiency and reliability for supervision, multi-objective optimization and distributed cooperative control of complex water transport systems.

The first layer to be considered is the hydraulic network composed of free-surface channels, hydraulic structures and mesh subnetwork of pressurized pipes. By coupling the Saint-Venant equations for describing the physics of free-surface fluid and the Lattice Boltzmann method for the fluid simulation, a discrete-time nonlinear model is obtained for the channels. The hydraulic structures are usually treated as internal boundaries of reaches and modeled by algebraic relationships between the flow and pressure variables.

To enable the exchange of the information among the control system's components, a communication network is considered in the second layer. Solving challenging problems of heterogeneous devices and communication issues (e.g., network delay, packet loss, energy consumption) is investigated in this thesis by introducing a hybrid network architecture and a dynamic routing design based on Quality of Service (QoS) requirements of control applications. For network routing, a weighted composition of some standard metrics is proposed so that the routing protocol using the composite metric achieves convergence, loop-freeness and path-optimality properties. Through extensive simulation scenarios, different network performance criteria are evaluated. The comparison of simulation results can validate the interest of this composition approach for dynamic routing.

Finally, the third layer introduces an optimal reactive control system developed for the regulatory control of large-scale irrigation channels under a Distributed Cooperative Model Predictive Control (DCMPC) framework. This part discusses different control implementation strategies (e.g., centralized, decentralized, and distributed strategies) and how the cooperative communication among local MPC controllers can be included to improve the performance of the overall system. Managing the divergent (or outdated) information exchanged among controllers is considered in this thesis as a consensus problem and solved by using an asynchronous consensus protocol. Based on the multi-agent system paradigm, this approach to distributed control provides a solution guaranteeing that all controllers have a consistent view of some data values needed for action computation. A particular benchmark of an irrigation channel is

investigated in simulations. The comparison of simulation results validates the benefits of the distributed cooperative control approach over other control strategies.

Keywords - irrigation network, Saint-Venant (SV) equations, Lattice Boltzmann (LB) method, Networked Control System (NCS), Low power and Lossy Network (LLN), hybrid architecture, dynamic routing, Routing Protocol for Low power and lossy network (RPL), composite metric, distributed control, cooperative control, asynchronous consensus, Multi-Agent System (MAS).

Résumé

Cette thèse présente une contribution sur les problèmes de contrôle de réseaux d'irrigations en tenant compte des contraintes de communication grâce à une approche multi-couches d'intelligence distribuée. Les analyses détaillées de chaque couche avec les résultats analytiques et les simulations seront décrites dans les différents chapitres. Ils mettent l'accent sur l'intérêt de l'approche multicouches, plus précisément sur son efficacité et sa fiabilité pour la supervision, l'optimisation multi-objectifs et le contrôle coopératif distribué sur des systèmes complexes de transport d'eau.

La première couche analysée est le réseau hydraulique composé de canaux d'écoulements à surface libre, de sous-réseaux maillés de tuyaux sous pression et des structures hydrauliques. En intégrant les équations de Saint-Venant pour décrire l'écoulement physique des fluides en surface libre et la méthode de Lattice Boltzmann pour la simulation du fluide, nous obtenons un modèle non linéaire discret pour les canaux à surface libre. Les structures hydrauliques sont généralement traitées comme des limites internes des biefs (tronçons) et modélisées par des relations entre les variables de flux et de pression.

Permettant l'échange d'informations entre les éléments du système de contrôle, le réseau de communication sera considéré comme la deuxième couche. La résolution des problèmes d'hétérogénéités des systèmes et des communications (par exemple les retards de diffusion dans le réseau, la perte de paquets, la consommation d'énergie) sera étudié en introduisant une architecture de réseau hybride avec un routage dynamique basé sur les exigences de Qualité de Service (QoS) des applications de contrôle. Pour le routage dynamique dans le réseau, une composition pondérée de certaines métriques standards est proposée afin que le protocole de routage utilisant cette métrique composite converge sans boucle avec une « route » optimum. Grâce à différents scénarios de simulation, plusieurs critères de performance du réseau ont été évalués. La comparaison des résultats de simulation permet de valider l'intérêt de cette approche de composition pour le routage dynamique.

Une troisième couche propose un système de contrôle réactif optimal développé pour la régulation du réseau d'irrigation dans un modèle étendue à grande échelle : Distributed Cooperative Model Predictive Control (DCMPC). Cette partie aborde la mise en œuvre de différentes stratégies de contrôle (centralisées, décentralisées et distribuées) et intègre la communication coopérative entre les contrôleurs MPC locaux afin d'améliorer les performances globales du système. La gestion de la divergence dans l'échange d'informations entre les contrôleurs est considérée dans cette thèse comme un problème de consensus et résolue en utilisant un protocole de consensus asynchrone. Cette approche du contrôle distribué basée sur le paradigme des systèmes multi-agents, fournit une solution garantissant que tous les contrôleurs aient une

vue cohérente de certaines valeurs des données nécessaires pour le calcul de décision. Un cas d'application sur un canal d'irrigation est étudié dans les simulations. La comparaison des résultats de simulations valide les avantages de l'approche du contrôle distribué coopératif par rapport aux autres stratégies de contrôle.

Mots-clés - réseau d'irrigation, équations de Saint-Venant (SV), méthode de Lattice Boltzmann (LB), système de contrôle en réseau (NCS), réseau à faible puissance et à perte (LLN), architecture hybride, routage dynamique, protocole de routage pour réseau à faible puissance et à perte (RPL), métrique composite, contrôle distribué, contrôle coopératif, consensus asynchrone, système multi-agent (MAS).

Publications

International conference papers

1 L. Nguyen, L. Lefevre, D. Genon-Catalot, V. T. Pham, and C. Raïevsky, "Optimal reactive control of hybrid architectures: A case study on complex water transportation systems," in 19th IEEE International Conference on Emerging Technologies and Factory Automation (ETFA), 2014, Barcelona, Spain, pp. 1–8.

2 L. Nguyen, A. J. Rojas, D. Genon-Catalot, A. Lagreze, and L. Lefevre, "Signal-to-noise ratio for irrigation canal networked control system," in 2015 IEEE Conference on Control and Applications (MSC), 2015, Sydney, Australia, pp. 1637–1643.

3 L. Nguyen, L. Lefevre, and D. Genon-Catalot, "A composite metric for dynamic routing in networked control systems using a hybrid architecture," in IEEE 14th International Conference on Industrial Informatics (INDIN), 2016, Poitiers, France.

4 L. Nguyen, L. Lefevre, D. Genon-Catalot, and Y. Lami, "Asynchronous information consensus in distributed control of irrigation canals," in 21st IEEE Conference on Emerging Technologies and Factory Automation (ETFA), 2016, Berlin, Germany, pp. 12–15.

5 L. Nguyen, I. Prodan, L. Lefevre, and D. Genon-Catalot, "Distributed Model Predictive Control of Irrigation Systems using Cooperative Controllers," in The 20th World Congress of the International Federation of Automatic Control (IFAC), 2017, Toulouse, France.

Journal papers

6 L. Nguyen, L. Lefevre, and D. Genon-Catalot, "Composite metric design for dynamic routing in networked control systems using a hybrid architecture," IEEE Transactions on Industrial Informatics, 2017. Submitted.

Technical reports for Artemis ArrowHead European project

- TR201409 - Optimal reactive control of complex water systems
- TR201509 - Communication issues in the control of large-scale irrigations systems

- TR201606 - Information consensus and cooperation in networked control systems
- TR201611 - Distributed cooperative Model Predictive Control of irrigation systems

Table of contents

List of figures

List of tables

Nomenclature

Channel modeling and control

BC	Bourne channel as an example of free-surface channel, page 12	
BGK	Bhatnagar–Gross–Krook collision model, page 7	
D1Q3	One-dimension three-velocities Lattice Boltzmann model, $i = \{1,2,3\}$, page 7	
LB	Lattice Boltzmann method, page 7	
SV	Saint-Venant equations, page 7	
α_g, α_w	Coefficient of gate or weir, page 22	
Δl	Lattice spacing in one-dimension, page 9	(m)
Δt	Time step, page 9	(s)
Ω_i	Collision term considered for a spatial direction i, page 17	
ϕ	Ratio of the wave speed to the lattice speed, page 19	
τ	Relaxation time corresponding to the viscosity in a fluid model, page 17	
θ	Gate opening, page 22	(m)
B	Surface width or top width, page 9	(m)
B_g, B_w	Width of gate or weir, page 22	(m)
F	Force term, page 14	
f_i	Density distribution of particles considered for a spatial direction i, page 16	
F_r	Froude number, page 19	
g	Acceleration of gravity, page 10	(m/s^2)
h	Water height, page 9	(m)
I	Bed slope, page 9	(m/m)

J	Friction at the bottom of a reach, page 14	
L	Length of channel, page 19	(m)
l	Longitudinal abscissa measured on the flow axis, page 9	(m)
N	Number of discretized points l_j, page 19	
n	Manning-Strickler coefficient, page 14	$sm^{-\frac{1}{3}}$
Q	Water flow rate at a point, page 10	(m^3/s)
Q_p	Discharge withdrawn by the pumping station, page 22	(m^3/s)
u	Average velocity in a cross-section of the flow, page 10	(m/s)
v	Velocity at a point of the flow, page 10	(m/s)
v_i	Velocity of particles considered for a spatial direction i, page 16	

Communication networks

(DO)DAG	(Destination-Oriented) Directed Acyclic Graph, page 45
6LoWPAN	IPv6 over Low power Wireless Personal Area Network, page 35
B-F	Bellman-Ford algorithm, page 42
ETX	Expected Transmission count metric, page 47
HP	Hop count of a Path metric, page 47
IETF	Internet Engineering Task Force, page 39
LLN	Low power and Lossy Network, page 45
LoWPAN	Low power Wireless Personal Area Network, page 35
NCS	Networked Control System, page 35
NE	Node remaining Energy metric, page 47
PWS	Path Weight Structure, page 41
QoS	Quality of Service, page 35
RFC	Request for Comments, managed by IETF, page 39
ROLL WG	Routing Over LLN Working Group, page 45
RPL	Routing Protocol for Low power and lossy network, page 35
WSAN	Wireless Sensor/Actuator Network, page 36

Multi-agent based coordination and cooperation

DMPC	Distributed model predictive control, page 57
MAS	Multi-agent system, page 58
NSP	A non-negative, stochastic and primitive matrix, page 70
1_n	Vector $1_n = [1\ 1\ \ldots\ 1]^T$, page 67
$\breve{\mathcal{G}}$	Union of a set of graphs, page 68
$\chi^{\textcircled{i}}$	Information vector of the controller i, page 61
$\mathcal{A}$	Adjacency matrix, page 67
$\mathcal{C}$	Set of controllers, page 65
$\mathcal{E}$	Set of edges, page 68
$\mathcal{G}_A$	Graph associated to the matrix A, page 68
$\mathcal{M}_i$	Neighbor set of the controller i, page 61
$\mathcal{N}$	Index set of controllers, page 65
τ	Time scale for the consensus process, page 61
τ_u	Updating instants of controllers for the consensus process, page 66
θ	Gate opening, page 60
$\tilde{\mathcal{G}}$	All possible graphs defined for a group of n controllers, page 68
C_i	A controller C_i, page 60
$d_{ij}(\tau)$	Time-varying communication delay between controllers i and j, page 67
h_{ds}	Water height at the downstream of a gate, page 61
h_{us}	Water height at the upstream of a gate, page 61
n	Number of reaches, page 60
Q	Flow rate at downstream as controlled variable, page 60
Q_g	Flow rate through a gate, page 61
t_a	Event-based discrete-time instants in the control system, page 66

Distributed model predictive control

DCMPC	Distributed Cooperative Model Predictive Control, page 83

$\theta^{\textcircled{i}}$	Gate opening of the reach $\textcircled{i}$, page 88
$\textcircled{i}$	Index of a reach or a controller, page 88
C_i	Controller for the control of the reach $\textcircled{i}$, page 88
$h_{ds}^{\textcircled{i}}$	Water height at downstream of the gate, page 88
$h_{us}^{\textcircled{i}}$	Water height at upstream of the gate, page 88
$J^{\textcircled{i}}$	Local cost function considered for the reach $\textcircled{i}$, page 91
$J_{coop}^{\textcircled{i}}$	Cooperative cost function considered for the reach $\textcircled{i}$, page 95
L_i	Length of a reach, page 88
L_{p_i}	Location of pumping station in the reach $\textcircled{i}$, page 88
n	Number of reaches, page 88
$Q^{\textcircled{i}}$	Flow rate at the downstream end of the reach $\textcircled{i}$, page 88
$Q_p^{\textcircled{i}}$	Pumping dischange in the reach $\textcircled{i}$, page 88

Other symbols

$\mathbb{R}$	Set of real numbers, page 19
$\mathbb{R}_{n\times n}$	Set of all $n \times n$ real matrices, page 68

Introduction

A multi-layer approach to distributed control problems for irrigation channels with communication constraints

The irrigation always is a major concern for human societies and it is more serious with rapid urbanization and climate change [3]. Currently, the performance of irrigation channels manually operated can no longer meet new challenges of irrigated areas in both water conservation and operating aspects [22, 78, 63, 77, 100]. The automation of engineering works is a possible way of improving the operational management [3, 78]. Automatic control systems can be designed to achieve desired objectives of water resource management while reducing investment and operating costs [91, 78, 103, 130, 18, 67, 87, 80]. From these perspectives, this thesis presents the control problems of an irrigation network with limited communication and a multi-layer approach to solving these problems in a distributed manner. As an interdisciplinary subject, it uses the concepts from automatic control, hydraulic engineering, and computer networks in an attempt to bring together these advantages. The detailed discussions for each layer and the demonstration with analytical and simulation results are described throughout several chapters.

The first layer to be considered is the hydraulic network composed of free-surface channels, hydraulic structures and mesh subnetwork of pressurized pipes [67]. By adopting a model-based control strategy [108], the control of this large-scale complex system requires a tractable model, which adequately captures system dynamics and the interactions among subsystems (different irrigation channel models are surveyed in [77, 163]). Based on the top-down approach to deal with the system complexity, **the first chapter** presents a "modular modeling" that involves partitioning the system into different scalable and reusable subsystems (i.e., modules) and making use of well-defined modular interfaces (the approach is detailed in [81]). Modules are independently modeled and contained in a Model Library as model components, which can be re-used for other water systems. For instance, the reach component in the Model Library is a discrete-time nonlinear model for a reach obtained by coupling the Saint-Venant (SV) equations for describing the physics of free-surface fluid [25, 73, 67, 6, 77] and the Lattice Boltzmann (LB) method for fluid simulation [54, 70, 158, 98]. As demonstrated in [98, 79, 95], the chosen LB method is an efficient and powerful numerical tool (in terms of accuracy, numerical stability and computational time) to simulate the free-surface flows respecting the conservation laws of macroscopic variables. Other components of the Model Library are hydraulic structure models. The hydraulic structures are usually treated as internal boundaries of reaches and modeled by

using algebraic relationships between the flow and pressure variables [98, 67]. Eventually, the complete model of a considered system is built by selectively assembling appropriate components from the Model Library. The channel model can be used as a forecasting model to predict some water quantities (e.g., water heights, flow rates) at different points along the channels at a time, corresponding to specified initial conditions [98]. The advantages of the "modular modeling" approach are the flexibility and the effectiveness of the modeling process in terms of model construction, testing, and reuse-ability of system components [81].

To enable the exchange of the information among the control system's components, a communication network is considered in the second layer. In networked control systems [7, 157, 40], an efficient communication between their components plays an important role in achieving global objectives [156, 131, 39]. However, the study of the network architecture and the interactions between networked components is challenging due to the presence of heterogeneous devices and communication issues such as time delay, data packet loss, etc. [50, 157]. Solving these problems is investigated in **the second chapter** by introducing a hybrid network architecture [62, 154, 132] and a dynamic routing design ([132], Section 5.2) based on Quality of Service (QoS) requirements of control applications. A hybrid network refers to any network that contains two or more different communications standards or multiple topological structures [107, 52, 109]. In terms of QoS, some applications (and users) demand just the performance, which is guaranteed from the network "as the best that could be done under the circumstances", others may require the satisfaction of stronger performance criteria (such as dropped packet rate, out-of-order delivery, error rates, bit rate, throughput, transmission delay, availability, jitter, etc.) (see more details in [132], Section 5.4). Eventually, the second chapter focuses on the ways to provide QoS that meet the requirements of control applications when integrating all control system components in a hybrid network [51, 148]. The dynamic routing is a process determining the optimal path that data packets should follow through a network to arrive at a specific destination [132] and it uses routing algorithms and protocols to monitor and respond to changes in network topology [55, 30]. The purpose of dynamic routing is to help prevent packet delivery failure, improving network performance and relieving network congestion [132]. For network routing design in order to satisfy the QoS requirements of control applications, a weighted composition of some standard metrics is proposed so that the routing protocol using the composite metric achieves convergence, loop-freeness and path-optimality properties [16, 17, 51, 48, 69]. This composition method shows the correlation between combined routing metrics and required network performance criteria. In this chapter, the composition approach is analytically demonstrated on the application of composite metrics with the Routing Protocol for Low-power and lossy network (RPL) [145, 155], specified by Internet Engineering Task Force (IETF - www.ietf.org). Simulations of the dynamic routing in the hybrid network are also performed and different network performance criteria are evaluated through extensive simulation scenarios. The comparison of simulation results can validate the benefits of this composition approach for dynamic routing in networked control systems.

As the irrigation network is a large-scale complex system, the control of this system is chosen in the distributed way in order to increase the scalability and reliability [96, 91, 103, 130, 46, 87,

137]. In distributed control, accounting for the interactions of subsystems, the coordination and/or the cooperation of controllers requires exchanging the information among controllers [26, 4, 42, 134]. However, challenges arise when controllers may lose the synchronization and when the shared information may encounter the divergence due to the switching topology and the imperfection in communication [61, 23]. Managing the divergent (or outdated) information is considered in **the third chapter** as an information consensus problem and solved by using an asynchronous consensus protocol [106, 66, 161, 64, 114, 34, 149, 28]. Based on multi-agent system (MAS) paradigm, the consensus approach provides a solution guaranteeing that all controllers have a consistent view of some data values needed for action computation [114, 93, 113]. By exploring information exchange topologies under proposed communication assumptions (e.g., directed graphs, connectivity, and asynchronism) [28], we find the necessary and sufficient conditions for the information consensus to be reached asymptotically using the defined asynchronous protocol. The designed consensus protocol can be integrated into the distributed scheme so that the shared information among controllers asymptotically converges to the newest values after applying an action. As a result, the performance of the control system is improved in comparison with the decentralized or distributed implementation strategies where interaction information is not up to date. Some simulation scenarios are given to illustrate the efficiency of this approach for the distributed control of irrigation channels modeled by the Lattice Boltzmann method.

Finally, the third layer introduces the optimal reactive control system developed for the regulatory control of large-scale irrigation channels under a Distributed Cooperative Model Predictive Control (DCMPC) framework [91, 78, 103, 130, 18, 46, 67, 87, 13]. Whereas different approaches to the control of irrigation systems have been developed and applied to real channels all over the world (as surveyed in [77, 80, 18]), the DCMPC is chosen because the channel control requires taking into account system inputs/outputs, the interactions among subsystems, and the structural/operational constraints and processing the delay compensation [9, 108]. **The fourth chapter** discusses different control implementation strategies (i.e., centralized, decentralized and distributed strategies) and how the cooperative communication among local controllers can be included to improve the performance of the overall system. In the proposed DCMPC scheme, each controller shares the interaction variable (e.g., the flow rate through a controlled gate) for action computation of the upstream neighbor and a coordination variable (e.g., its set-points) for the cooperation with the downstream neighbor. For simulations, a particular benchmark of an irrigation channel modeled by the Lattice Boltzmann method is considered. The comparisons of simulation results among the proposed control approaches validate the benefits of the distributed cooperative control approach. The numerical results show up the improvement of some global performance criteria such as response time, overshoot limit, but larger computation delay in distributed cooperative control with regard to decentralized control. By these results, we have extended the state-of-the-art in the control of irrigation channels with the coherent combination of the modeling by the Lattice Boltzmann method and the centralized/decentralized/distributed model predictive control approaches.

Outline and contribution of the thesis

Motivated by challenging control and communication problems in distributed control of large-scale irrigation channels, this thesis presents a multi-layer approach to solving these problems through several chapters organized as follows:

- **Chapter 1** contributes the component-based modeling of irrigation channels using the Lattice Boltzmann method. Modularity in modeling involves the modularized and parameterized modeling technique and the creation of a Model Library. The proposed modular approach reduces the system design and review cycle that can significantly improve the design consistency of a large-scale system. In simulations, it takes less time and enables a more efficient co-simulation. The model has a decisive role in the understanding and diagnosis of irrigation channels.

- **Chapter 2** investigates in designing a hybrid network to cope with the heterogeneity of wide-area networked control systems and the communication issues. In the hybrid network, a composite metric is proposed for dynamic routing in order to satisfy different QoS requirements of control applications. The resulting network model can be used to dynamically compute the QoS-related costs (or probabilities) of different paths between the components of networked control systems (NCSs). These are the important concerns when considering the information exchange in NCSs.

- **Chapter 3** aims to solve updating problems of the information shared among controllers in a networked control system with communication constraints. These problems are considered as an information consensus problem and solved by using an asynchronous consensus protocol. The advantages of this approach are that, even when the neighboring controllers lose the direct communication, the shared information is still able to be updated with the benefit of consensus convergence. The integration of the consensus protocol into a control scheme is demonstrated that it still guarantees the control performance, but with the robustness of the changes in communication topology due to link/node failures and time delays.

- **Chapter 4** aims to implement and compare different control schemes in which costs, constraints, profiles are taken into account in decentralized and distributed constrained optimization problems (i.e., via the MPC design); and the cooperation among local MPC controllers can be included in order to improve the performance of the overall system.

In brief, the original contributions of this thesis are as follows:

- combining the LB method for fluid simulation and “modular modelling” approach, we provide a parameterizable Model Library of a large-scale irrigation system suitable for adequately capturing its dynamics and the interactions among the subsystems. This Model Library can be reused for other water systems;

- to cope with the heterogeneity and the communication issues when integrating all components of a wide-area networked control system into a unified network infrastructure, we

propose a hybrid network architecture and the dynamic routing with a composite metric over this network;

- to address challenging QoS requirements of control applications in network design, we show that several performance criteria related to the communication needs for control applications can be optimized by using a metric composition approach;
- for the convergence of the information shared among controllers, we design an asynchronous consensus protocol and establish conditions for a class of "leader-followers" systems to asymptotically reach the consensus under fixed or time-varying directed exchange topology;
- we propose a global topology for the "leader-switching" system to satisfy multiple information consensus problems;
- we integrate the consensus protocol into the DCMPC algorithm
- we propose a decentralized implementation of the control system where a local MPC controller for each subsystem is separately designed. They compute the action using only the local information;
- the distributed cooperative controllers are designed by taking into account the information shared by neighboring controllers (e.g., system output and set-points) to compute the action. They cooperate with their neighbors by minimizing the influence of an applied action with the regularization objective of their neighbors;
- extensive simulation results are provided through different scenarios, which validate the proposed predictive control schemes and highlights their strengths and weakness in terms of global performances.

These chapters emphasize the potential interest of the multi-layer approach, more precisely its efficiency and reliability for supervision, multi-objective optimization and distributed control of complex water transport systems.

Chapter 1

Modeling of irrigation channels using the Lattice Boltzmann method

The use of a hydraulic computing model allows making some simulations in order to deeply know about system operations, predict hydraulic variables, evaluate management rules, and diagnose malfunctions. This chapter provides an overview of the methods used for the modeling of free-surface hydraulic as found in natural rivers or artificial channels. The emphasis is on the application of the Lattice Boltzmann (LB) method to model free-surface flow characterized by fluid hydrodynamics. Organizationally, Section 1.1 introduces a general irrigation channel with various geometric and characteristic variables that are useful for hydraulic calculation. In the channel, the flow can be treated in different patterns (e.g., uniform or non-uniform) or in different functional regimes (i.e., steady or varied) corresponding to spatial and temporal variations. The Saint-Venant (SV) equations presented in Section 1.2 constitute a distributed-parameter model, which is commonly used to provide a detailed description of one-dimension (1D) free-surface flow. The detailed model makes it possible to understand the phenomena associated with the physical system. Using the SV model, the analysis of a steady-state regime of non-uniform flow is useful for considering the evolution of water heights (or flow rates) in the channel as a function of the boundary conditions. Section 1.3 is dedicated to the modeling of an irrigation channel using the LB method. The LB model allows generating the dynamics of a complex water system from various boundary conditions. In particular, the one-dimension three-velocities (D1Q3) LB model can be effectively used for the modeling of a reach (or a segment). For coupling different reaches, the hydraulic structures (such as gates, weirs, or mixed gates and spillway) are used as internal boundaries and modeled by mathematical relations between mesoscopic variables and hydraulic variables. In Section 1.4, the discrete-time LB equations are solved to simulate the flow of irrigation channel using Bhatnagar–Gross–Krook (BGK) collision model. We are particularly interested in the modularized and parameterized modeling technique, which is used to create a Model Library of system components (e.g., reach, gate, weir or mixed). As an example, a section of the Bourne channel in France is considered for the analysis and simulation schemes. The simulation results presented in Section 1.4.2 show the coherence of flow behavior corresponding

to the specified initial conditions and when introducing perturbations. Finally, Section 1.5 summarizes the aspects presented in this chapter.

1.1 Irrigation channels

The operational management of irrigation channels often is unsatisfactory due to the complexity of considered systems [3, 78, 63, 77, 11]. In traditional irrigation channels, water is conducted, from a source of supply (e.g., lakes, rivers, dams), along the main channels (possibly diverted to secondary channels) and then to distribution networks or to the natural drainage systems. An irrigation channel (or free-surface channel) generally is an open-channel hydraulic system providing a desired flow of water [77]. When the channel is directly connected to a water source such as a lake or a river, the water supply is fairly reliable in normal weather [39]. Even though, water must be regulated to avoid using so much water in one area while other areas suffer. For this purpose, some hydraulic structures are required to regulate the flow and deliver the correct amount of water to different branches of the system and onward to the irrigated fields. There are four main types of hydraulic structures [39, 138, 67]: erosion control structures, distribution control structures, crossing structures and water measurement devices. Erosion control structures (e.g., drop structures or chutes) are required to reduce the bottom slope of channels lying on steeply sloping land in order to avoid high velocity of the flow and risk of erosion. Distribution control structures (e.g., gates, weirs, or mixed gates and spillway) are installed at appropriate locations in order to control the water heights, flow rates or volumes at some points along the channel. Crossing structures (e.g., flumes, culverts, and inverted siphons) are necessary to carry irrigation water across roads, hillsides, and natural depressions. The most commonly used water measurement devices are water level and flow-rate meters. From the main or secondary channels, pumping stations are used to withdraw water upward into the distribution network (e.g., mesh pressurized network or field ditches). Occasionally, when an irrigation channel traverses a great distance or must navigate through the changes in elevation, temporary reservoirs are commonly built to store water and then refill irrigation channels through dams. Popularly, the drainage system at channel downstream removes the excess of water from the channels (e.g., caused by oversupply, rainfall, high water level in the river).

The channel managers usually face different operational management problems. Their main objectives are: *(1) improving irrigation water management in order to increase productivity; (2) save water, minimize energy consumption and exploration costs; while (3) guaranteeing the safety of the infrastructure* among others. The automation of hydraulic structures is a possible way to achieve the desired objectives of operational management while reducing or sometimes eliminating human intervention. In principle, automatic control of such a system requires the description of the system dynamics represented by a model. However, modeling the complete system is a difficult task due to the complexity (e.g., dimensionality, uncertainty, and information structure constraints) and because unknown external perturbations may affect its behavior.

1.1.1 Characterization of irrigation channels

Generally, the irrigation channel is a very large and complex system characterized by important time delays between inputs and outputs (due to water transportation), strong non-linear dynamics (mainly around the hydraulic structures), unknown or unmeasurable perturbations (e.g., inflows created by rainfall, high river level and outflows created by stealthy withdrawal, infiltration and evaporation losses), and interactions between subsystems. We recall briefly in the next sections the definition of some common parameters and variables, which can be used for system modeling.

1.1.2 Geometric parameters

We limit our study to a free-surface channel (e.g., single bed river or irrigation channel) characterized by fixed banks and bottom bed, a surface subjected to atmospheric pressure, and the watercourse can be reasonably considered as rectilinear (see Fig. 1.1). The geometry of the channel can then be perfectly defined by a succession of cross-sections, perpendicular to the direction of flow (i.e., flow axis) [138]. Assuming that the free (or open-air) surface is horizontal from one channel bank to the other and velocities are homogeneous in a cross-section, the bank-to-bank and vertical components of the flow can be neglected. As a result, this leads to one-dimensional modeling (or 1D model) that allows all geometric parameters and hydraulic variables to be considered as functions of the abscissa $l\ (m)$ measured on the flow axis and the time $t\ (s)$ [138, 67]. For simplicity, we denote a function, for example, $f(l,t)$ by f.

Definition 1.1.1. *Geometric parameters* [138, 67].

As shown in Fig. 1.1,

- the surface width or top width, denoted by $B\ (m)$, is the width of the channel at the level of the free surface,
- the water height, denoted by $h\ (m)$, is the maximum water height measured between the bottom bed and the free surface,
- the wetted perimeter, denoted by $P\ (m)$, is the perimeter of a cross-section excluding the length of the free surface,
- the wetted section area, denoted by $S\ (m^2)$, is the portion of the section wetted by the water in the cross-section of the channel,
- the hydraulic height, denoted by $D_h = S/B\ (m)$, corresponds to the ratio between the wetted section area and the top width of the channel,
- the hydraulic radius, denoted by $R_h = S/P\ (m)$, is the ratio between the wetted section area and the wetted perimeter,
- the bed slope, denoted by $I\ (m/m)$, is commonly expressed as the ratio in of the difference between upstream and downstream heights to the length of the channel,

- the free-board of the channel is the anticipated height of the bank above the highest water level, it is required to guard against over-topping by waves or unexpected increase in water level.

The parameters B, h, P, S, and R_h depend on the flow rate (therefore, they are not geometric constants) whereas I is a geometric constant. According to the shape of their cross-section, the channel is called rectangular, trapezoidal, triangular, circular, parabolic or irregular (as shown in Fig. 1.1.b). The most commonly used cross-sections in irrigation and drainage systems are rectangular or trapezoidal forms with small side slope (e.g., usually less than 5%¸ [138]). When the cross-section, bed slope and roughness do not vary according to the flow axis, the channel is prismatic.

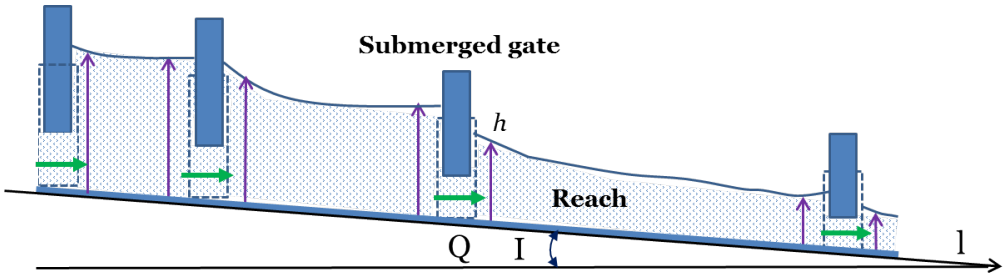

a) Longitudinal view of a free-surface channel shows the flow axis ***l***, bed slope ***I***, water height ***h***, and discharge ***Q***.

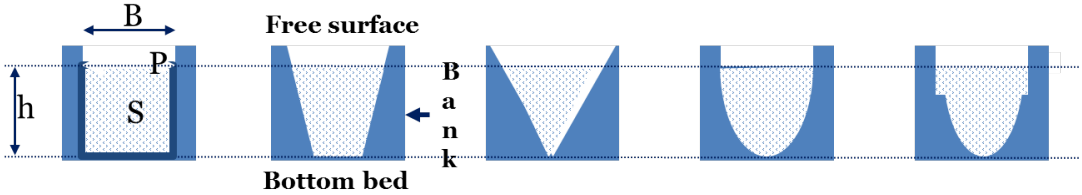

b) Different cross-sections of a free-surface channel include the definition of wetted perimeter ***P***, wetted section **S**, water height ***h***, and top width ***B***.

Fig. 1.1 The common parameters and variables are used to characterize a free-surface channel.

1.1.3 Hydraulic variables

Some hydraulic variables needed to quantify the motion of water (or fluid) are:

Definition 1.1.2. *Hydraulic variables* [138, 67].

- the velocity at a point of the flow, denoted by $v = \frac{\Delta l}{\Delta t}$ (m/s) (where Δl is 1D lattice spacing and Δt is time step), is the velocity of the particle passing at this point in the mean time,
- the average velocity, denoted by u (m/s), is the average of all velocities in a cross-section,
- the flow rate, denoted by $Q = Bhu$ (m^3/s), is the volume of water flowing through a cross-section perpendicular to the flow axis per unit time.

In addition, the study of fluid dynamics involves other parameters characterizing the environment such as the acceleration of gravity, denoted by g (m/s^2); the pressure, denoted by ρ (N/m^2);

the viscosity, denoted by μ $(kg/m*s)$; the various force terms, denoted by F (N/kg), etc. The density of the water, denoted ρ_w, is 1000 (kg/m^3) in the case of clear water without suspended matter. The water in motion also exerts a perpendicular thrust and a tangential frictional force on the banks of the channel. The solution of a dynamic fluid problem typically involves the calculation of various characteristic variables of the fluid (e.g., flow depth, flow rate, velocity, pressure, density, etc.) as functions of space and time.

1.1.4 Classifications of the flows

The free-surface flows can be classified and described in various ways, according to the variability of hydraulic characteristics (e.g., flow heights and velocities) with respect to time and space.

Definition 1.1.3. *Classifications of the flows* [138, 67].

The fundamental types of flows related to free-surface hydraulics are:

- Variability over time:
  - *Steady (or permanent) flow* - the flow heights and velocities do not change over time or are assumed to be constant during the considered time interval. Note that the flow in the channels is rarely permanent. Nevertheless, the temporal variations are, in some cases, slow enough so that the flow can be considered as a succession of steady state (i.e., defined as a quasi-permanent regime).
  - *Unsteady (or non-permanent) flow* - the flow heights and velocities do change with time.
- Variability in space:
  - *Uniform flow* - the flow heights and velocities remain invariable in various sections of the channel. A truly uniform flow is rarely found in rivers, but rather in channels of great length, with constant cross-section and slope.
  - *Varied (or nonuniform) flow* - the flow heights and velocities change along the length of the channel. A varied flow may be accelerated or decelerated depending on whether the velocities increase or decrease in the direction of movement. Varied flow can be further classified as either rapidly or gradually varied.
    - *Rapidly varied flow* - the flow heights and velocities change abruptly (sometimes with discontinuities) over a comparatively short distance. This is usually manifested in the vicinity of a singularity, such as a weirs, shrinkage, hydraulic jump or sudden drop.
    - *Gradually varied flow* - the flow heights and velocities only change over a long distance.

Besides, we also use the definition of *continuous flow* when the flow rate is constant throughout the channel. This is the case for a steady flow. Therefore, the continuous flow can be described using the continuity equation for the steady flow. Whereas the *spatially varied* or *discontinuous flow* is considered when the flow rate is nonuniform along the channel. This

happens when water enters and/or leaves the channel along the course of the flow. The flow can be described using the continuity equation for continuous unsteady flow.

The classifications of flows are also based on the states of flow. The behavior of a free-surface flow is governed by the effects of viscosity and gravity. Surface tension has a minor contribution and does not play a significant role to be a governing factor in most circumstances. Depending on the effect of viscosity, relatively to inertial forces (as represented by the Reynolds number), the flow can be either laminar, turbulent, or transitional (see more details in [117, 79]).

1.1.5 Example of an irrigation channel

We introduce the Bourne channel (BC) in France as an example for the system analysis and modeling. The block diagram of the BC irrigation network presented in Fig. 1.2 shows multiple sections (i.e., reaches) of a primary channel interconnected through the Gates (G), Mixed gates and spillways (M) or Pumping stations (P). The main trunk, BC, connects further two secondary channels (S2, S3). For system modeling, the irrigation network is decomposed into three types of system components: (1) the first category includes the reaches of primary channel and secondary channels; (2) the second category contains the hydraulic structures (such as G, M, and P) interconnecting the reaches; (3) the third category is a mesh subnetwork of pressurized pipes (the modeling of pipe network is ignored in this thesis).

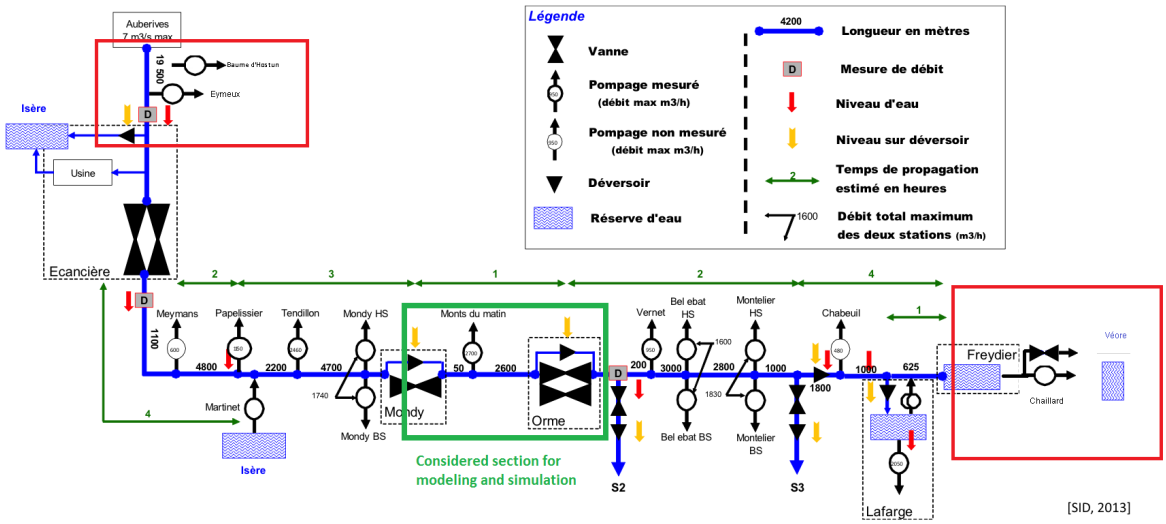

Fig. 1.2 Synoptic view of the Bourne channel (BC), which is used as an example of the free-surface channel.

The Bourne channel has several problems, whether technical, economic or compliance. Although endowed with a historical seniority since the $17th$ century, the construction of numerous engineering structure was carried out for many years and the services of agricultural crops are popularly started from the 18th century. The BC main channel of 46 km in length (excluding subnets of secondary and tertiary channels) is used for the irrigation of large cultivation areas (about $25,000$ hectares) with gravitational and aspersion techniques. The water in the channel is taken from the Bourne river at the dam of Auberives. The upstream flow is regulated and limited to 7 (m^3/s); the complement of the water level, if necessary, is taken by pumping in the

Isère river. Along the channel, the pumping stations withdraw the water in order to supply a mesh sub-network of pressurized pipes. The total length of pressurized pipes can attain nearly 1000 (km). Finally, at the top of the plots, the water is distributed to irrigated lands on demand. Moreover, when the irrigation is no longer necessary in the favorable seasons, the water is re-conducted to turbines for the electricity production and the electricity is sold to the "Réseau de Transport d'Électricité" (RTE). The control structures attached to the free-surface channel are gates or mixed. Actually, the measuring instruments are probes or meters of old technology for the evaluation of levels and flow-rates at some locations. Two downstream reservoirs conserve the unused water at the end of the main channel. The socio-economic context of the BC have been the subject of a more precise description, thus making it possible to formulate the problematic of the distributed control of an irrigation network under communication constraints (see more details in [89]).

1.1.6 Necessity of a model for the irrigation channel

Technical improvement of channel management requires the knowledge of the hydrodynamic behavior of the flow and the characteristics of installed hydraulic structures. Hydrodynamic models sufficiently detailed enable a good understanding of the overall hydraulic characteristics of large-scale irrigation schemes [67, 77]. They are useful for the evaluation of the impacts of different operational options on hydraulic performance and main problems faced by the managers of irrigation channels. In particular, automatic control techniques such as Model Predictive Control (MPC) make use of the models for the controller design [9, 108, 91, 130, 87, 137, 13]. The benefits of a hydrodynamic model offered to channel managers can be to:

- avoid resorting to experimentation field and thus disrupting the functional operation,
- test and evaluate channel management rules through simulations on the model and to develop control methods,
- reproduce existing management rules and diagnose malfunctions.

Numerous models exist to represent the hydrodynamic behavior of a free-surface flow. These models can principally be grouped into two families.

- *Empirical or conceptual approach (Experience ⇒ Model).* This is a macroscopic approach which considers the system as a whole and focuses only on global behavior.
- *Deterministic or theoretical approach (Model ⇒ Experience).* This approach consists of decomposing a system and its operations into sub-systems and micro-phenomena, modeling them and then constructing a recomposition model. These models are based on the principles and equations of mechanics in order to represent some hydraulic phenomena of the system.

For the irrigation channels, we adopt the deterministic approach for system modeling because the resulting mechanical models can study the real motion of the water. In addition, this approach is motivated by many works (as surveyed in [163, 67, 77]) and the validation theoretically or

through experimentation [73, 104, 67]. This makes it possible to increase the performance of the control and supervision systems.

1.2 Modeling of an irrigation channel using classical Saint-Venant equations

We consider a non-permanent and non-uniform flow of an irrigation channel supposed to be rectangular. The equations of Barré de Saint-Venant established in 1871, also called 1D Shallow Water equations (1DSW), are mostly used to model unsteady flow gradually varied with free-surface channels (see [36], [67], Section 2.1 and Appendix A). These hyperbolic partial differential equations are in fact derived from the depth-integrating of the Navier–Stokes equations with some assumptions and simplifications (presented in [67], Section 2.1). They consist in two relations, the first being the mass conservation (also called, continuity equation) and the second, the momentum balance (also called, dynamic equation) as follows:

$$\partial_t(h) + \partial_l(hu) = 0, \tag{1.1}$$

$$\partial_t(hu) + \partial_l(\frac{1}{2}gh^2 + hu^2) = F, \tag{1.2}$$

where: h is the water height, u is the depth-average velocity of the flow, g is the acceleration of gravity, and F is force term. Different external forces (e.g., forces of gravity, pressure or friction) representing the interactions of the system with the environment can be integrated into SV equations. Especially used for simplicity, a simple force term, F, is calculated by using the bed slope I and the friction J at the bottom of the channel [162], that is:

$$F = gh(I - J). \tag{1.3}$$

Commonly, the friction, J, is deduced by the Manning-Strickler empirical formula [98, 67]:

$$J = \frac{n^2u^2}{(\frac{Bh}{(B+2h)})^{\frac{4}{3}}}, \tag{1.4}$$

with n $(sm^{-\frac{1}{3}})$ is the *Manning-Strickler coefficient*.

Following Eqs. (1.1) and (1.2), we can initialize the water height profile along the channel using the boundary conditions. Assuming that the upstream flow rate and the downstream water height are fixed at the constant values Q_0 and h_0, the water height profile of the steady flow (i.e., $\partial_t h = 0$ and $\partial_t u = 0$) in the channel of length L is expressed by:

$$\partial_l h = \frac{gh(I - J)}{gh - u^2}, \tag{1.5}$$

where, the boundary conditions: $h(L) = h_0$, $u = \frac{Q_0}{Bh}$ and $J = \frac{n^2 Q_0^2}{B^2 h^2 \left(\frac{Bh}{B+2h}\right)^{\frac{4}{3}}}$. The solution can be obtained by integrating the ordinary differential equation for $h(l)$.

As shown in Eq(s). (1.5), the uniform flow (i.e., $\partial_l h = 0$ and $\partial_l u = 0$) in a channel is attained when the condition $I = J$ holds (i.e., the friction forces equilibrate the gravitational forces). The relationship between uniform water height, h_e, and the steady-state water flow, Q_e, is deduced by using the Eq(s). (1.4) and the definition $Q_e = Bh_e u$ as follows:

$$Q_e = \sqrt{I}\frac{Bh_e}{n}\left(\frac{Bh_e}{B+2h_e}\right)^{\frac{2}{3}}, \tag{1.6}$$

Assumptions 1.2.1. *Assumptions for the SV equations* ([67], Section 2.1)

The fundamental assumptions necessary for the SV equations to be valid are the followings:

- the flow is considered as one-dimensional, rectilinear and the variation of channel width along the flow axis is small,
- the vertical pressure distribution vertically is hydrostatic and the vertical acceleration is negligible,
- the velocity is uniform over the cross-section, the average velocity is used in the calculation,
- the average bed slope is small (so that the cosine of elevation angle may be replaced by unity),
- the effect of friction can be taken into account through resistance laws used for steady flow or the viscosity is negligible,
- finally, the channel is supposed to transport clear water.

The resolution of the Eqs. (1.1) and (1.2) allows to define the temporal variations of the water heights h or flow rates q along the flow axis l. The analytical resolution of the SV equations is impossible in most real cases, but the numerical resolution is now quite common on microcomputers using finite difference methods (such as Preissmann Implicit Scheme) or finite element methods (introduced in [67], Section 2.2). For these methods, the initial and boundary conditions are needed for the computation. The choice of boundary conditions depends on the flow characteristics since a change in the boundary conditions may change the flow characteristics. We can choose either the water height or the flow rate at the channel upstream or downstream as boundary conditions.

The modeling method using SV equations has been validated on an experimental channel located at the University of Evora in Portugal in the Gignac experimental platform project (2000–2006) financed by Cemagref ([68, 67], Section 11), on Arrêt-Darré/Arros dam-river system located in the Southwest region of France [104], on the "Sector B-XII del Bajo Guadalquivir", Lebrija, Spain [73], and otherwise, on lab experimentations [79, 6].

1.3 Modeling of an irrigation channel using Lattice Boltzmann method

1.3.1 Hydrodynamic model of free-surface flow

As demonstrated in [117, 98, 79, 95], the LB method is an efficient and powerful numerical tool (in terms of accuracy, numerical stability and computational time) to simulate the free-surface flow while respecting the conservation laws of macroscopic variables (as described by the Eqs. (1.1) and (1.2)). The variables used in the LB model are the density distributions

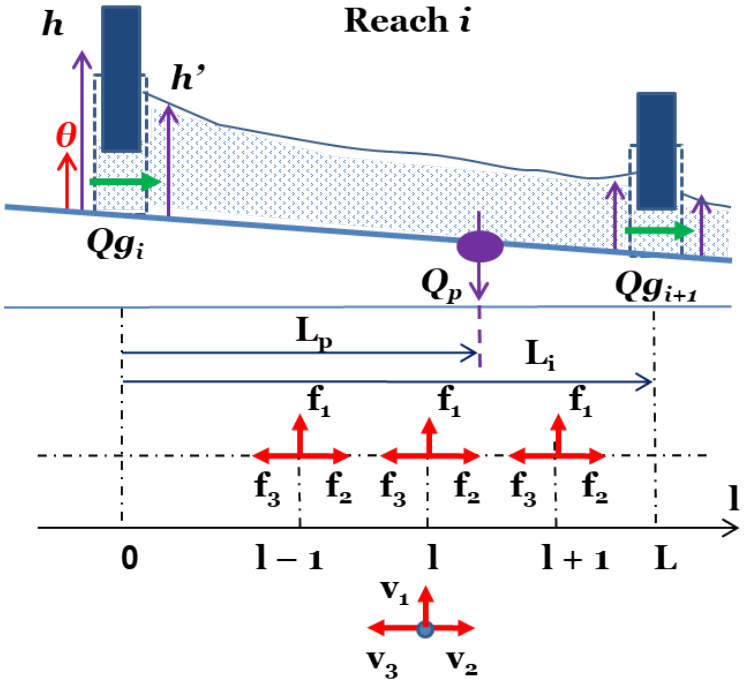

Fig. 1.3 Modeling a reach of length L using Lattice Boltzmann (LB) method illustrates the density distributions, f_i, the velocities of particles, v_i, in a spatial direction i, $i = \{1,2,3\}$.

(denoted by f_i for a spatial direction i), representing the density of particles which enter into a site l at a time t with a velocity (denoted by v_i for the particles from the direction i) [54]. According to [98], Section 2.2, the one-dimension three-velocities (D1Q3) LB method is effectively used to model the irrigation channel in one dimension l and with three velocities $[v_1\ v_2\ v_3]$ corresponding to three directions $i = \{1,2,3\}$ (as illustrated in Fig. 1.3), where: $[v_1\ v_2\ v_3] = [0\ v\ (-v)]$, $v = \frac{\Delta l}{\Delta t}$ (Δl is lattice spacing, Δt is time step). Based on the theory of cellular automata [19], the dynamics of the flow are described by the intrinsic interactions among particles. These interactions can be represented by two consecutive phases [98]: (1) *the collision phase* - at the time t, a density distribution f_i^{in} of particles from the direction i entering into a site with velocity v_i collide with other particles from other directions entering into the same site; (2) *the streaming phase* - during the next time step $(t + \Delta t)$, a new density distribution f_i^{out} of particles emerging from the collision phase move to a new lattice site with a new velocity. These phases can be mathematically

expressed by:

$$\begin{array}{lll} \text{Collision:} & f_i^{out}(l,t) & = f_i^{in}(l,t) + \Omega_i(f^{in}(l,t)), \\ \text{Streaming:} & f_i^{in}(l + v_i\Delta t, t + \Delta t) & = f_i^{out}(l,t), \end{array} \tag{1.7}$$

where: $i = \{1,2,3\}$, Ω_i represents the collision term depending on the vector of all distributions $f_i^{in}(l,t)$, denoted by $f^{in}(l,t)$. Among the models used in the study of collision, the Bhatnagar-Gross-Krook (BGK) collision model is known for its stability and flexibility in describing free-surface flow properties (see the details in [54], Section 10.7). Using this model, the collision term, Ω_i, is expressed by a relaxation of density distributions, f_i, with respect to the local equilibrium distributions, f_i^e, that is:

$$\Omega_i(f^{in}(l,t)) = \frac{1}{\tau}(f_i^e(l,t) - f_i^{in}(l,t)), \tag{1.8}$$

where: τ is the relaxation time corresponding to the viscosity in a fluid model.

As in SV modeling, the LB density distributions must verify for each site and at each time step, the conservation of mass (related to the water height, h), momentum (related to the flow rate per unit of section width, given by hu), and momentum tensor, that is:

$$\begin{array}{ccccc} \sum_{i=1}^3 f_i^{in} & = & \sum_{i=1}^3 f_i^{out} & = & h \\ \sum_{i=1}^3 v_i f_i^{in} & = & \sum_{i=1}^3 v_i f_i^{out} & = & hu \\ \sum_{i=1}^3 v_i^2 f_i^{in} & = & \sum_{i=1}^3 v_i^2 f_i^{out} & = & \frac{1}{2}gh^2 + hu^2 \end{array} \tag{1.9}$$

The equilibrium density distributions must also satisfy these conservations as follows:

$$\begin{aligned} \sum_{i=1}^3 f_i^e &= h \\ \sum_{i=1}^3 v_i f_i^e &= hu \\ \sum_{i=1}^3 v_i^2 f_i^e &= \frac{1}{2}gh^2 + hu^2 \end{aligned} \tag{1.10}$$

Solving these equations Eq(s). (1.10) allows determining the equilibrium density distributions, f_i^e, as functions of the macroscopic variables h and u, as follows:

$$\begin{aligned} f_1^e &= h - \frac{1}{2v^2}gh^2 - \frac{1}{v^2}hu^2 \\ f_2^e &= \frac{1}{4v^2}gh^2 + \frac{1}{2v}hu + \frac{1}{2v^2}hu^2 \\ f_3^e &= \frac{1}{4v^2}gh^2 - \frac{1}{2v}hu + \frac{1}{2v^2}hu^2 \end{aligned} \tag{1.11}$$

In order to increase the accuracy of the resulting simulation scheme, different external forces representing the interactions of the system with the environment, can be integrated into the LB models. For instance, force models described by Zou [162], or by Gou [38], or by Exact Different

Method [56] can be added to the free-surface LB models (see more details in [98] and [54], Section 6). For a channel model designed for supervision and control purposes, a simple force is appropriate [162]. This simple force term is evaluated at the current site by a discretization of the classical force terms in the water flow equations (see the Eq(s). (1.3)).

With the choice of D1Q3 for lattice topology, modeling a free-surface flow using the LB method in the presence of the simple external force results in the local dynamics [98]:

$$f_i(l+v_i\Delta t, t+\Delta t) = f_i(l,t) + \frac{1}{\tau}(f_i^e(l,t) - f_i(l,t)) + \omega_i \frac{\Delta t}{c_s^2} v_i F \tag{1.12}$$

where: ω_i and c_s are the parameters determined by the geometry of the lattice so that the isotropy of the model is preserved [162]. The following values are chosen for ω_i and c_s: $\omega_1 = \frac{2}{3}$, $\omega_2 = \omega_3 = \frac{1}{6}$, $c_s^2 = \sum_{i=1}^{3} \omega_i v^2 = \frac{v^2}{3}$.

The Eq(s). (1.12) can be put in the form of a representation by directions as follows:

$$\begin{array}{rcl} f_1(l,t+\Delta t) & = & f_1(l,t) + \frac{1}{\tau}(f_1^e - f_1(l,t)) \\ f_2(l,t+\Delta t) & = & f_2(l-v\Delta t,t) + \frac{1}{\tau}(f_2^e - f_2(l,t)) - \frac{\Delta t}{2v}F \\ f_3(l,t+\Delta t) & = & f_3(l+v\Delta t,t) + \frac{1}{\tau}(f_3^e - f_3(l,t)) + \frac{\Delta t}{2v}F \end{array} \tag{1.13}$$

The global dynamics of the LB model (i.e., the dynamics of the density distributions at all points of the lattice) at a time $t+\Delta t$ are defined as the functions of density distributions at preceding instants and neighboring points. By applying the values of equilibrium density distributions calculated by the Eq(s). (1.11) to the Eq(s). (1.13), the global dynamics can be expressed as follows:

$$\begin{array}{rcl} f_1(l,t+\Delta t) & = & f_1(l,t) + \frac{1}{\tau}(f_1^e - f_1(l,t)) \\ & = & \frac{1}{\tau}[(\tau - \frac{1}{2\phi^2})\,(1 - \frac{1}{2\phi^2} - \frac{F_r}{\phi})\,(1 - \frac{1}{2\phi^2} + \frac{F_r}{\phi})] \begin{bmatrix} f_1(l,t) \\ f_2(l,t) \\ f_3(l,t) \end{bmatrix} \\ & = & A_1 \begin{bmatrix} f_1(l,t) \\ f_2(l,t) \\ f_3(l,t) \end{bmatrix} \\ f_2(l,t+\Delta t) & = & f_2(l-v\Delta t,t) + \frac{1}{\tau}(f_2^e - f_2(l-v\Delta t,t)) + \frac{\Delta t}{2v}F \\ & = & \frac{\Delta t}{2v}F + \frac{1}{\tau}[(\frac{1}{4\phi^2})\,(\frac{1}{4\phi^2} + \frac{F_r}{2\phi} + \tau - \frac{1}{2})\,(\frac{1}{4\phi^2} - \frac{F_r}{2\phi} - \frac{1}{2})] \begin{bmatrix} f_1(l-v\Delta t,t) \\ f_2(l-v\Delta t,t) \\ f_3(l-v\Delta t,t) \end{bmatrix} \\ & = & \frac{\Delta t}{2v}F + A_2 \begin{bmatrix} f_1(l-v\Delta t,t) \\ f_2(l-v\Delta t,t) \\ f_3(l-v\Delta t,t) \end{bmatrix} \end{array}$$

$$\begin{aligned} f_3(l,t+\Delta t) &= f_3(l+v\Delta t,t)+\tfrac{1}{\tau}(f_3^e-f_3(l+v\Delta t,t))-\tfrac{\Delta t}{2v}F \\ &= -\tfrac{\Delta t}{2v}F+\tfrac{1}{\tau}[(\tfrac{1}{4\phi^2})\,(\tfrac{1}{4\phi^2}+\tfrac{F_r}{2\phi}-\tfrac{1}{2})\,(\tfrac{1}{4\phi^2}-\tfrac{F_r}{2\phi}+\tau-\tfrac{1}{2})]\begin{bmatrix} f_1(l+v\Delta t,t)\\ f_2(l+v\Delta t,t)\\ f_3(l+v\Delta t,t)\end{bmatrix} \\ &= -\tfrac{\Delta t}{2v}F+A_3\begin{bmatrix} f_1(l+v\Delta t,t)\\ f_2(l+v\Delta t,t)\\ f_3(l+v\Delta t,t)\end{bmatrix}, \end{aligned} \tag{1.14}$$

where: $\phi=\frac{v}{\sqrt{gh}}$ is the ratio of the wave speed to the lattice speed, and $F_r=\frac{u}{\sqrt{gh}}$ is the Froude number.

By normalizing the time step Δt, $t-\Delta t=k-1$, $t=k$, $t+\Delta t=k+1$ and denoting lattice positions $l_{j+1}=l_j+v\Delta t$, $l_{j-1}=l_j-v\Delta t$, the dynamics of free-surface flow can be represented as a discrete-time systems using state-space representation as follows:

$$x(k+1)=\mathrm{A}(x(k))x(k)+\mathrm{F}, \tag{1.15}$$

where: the discrete-time local states, $x(k)\in\mathbb{R}^{3N\times 1}$, of the channel of length L (corresponding to N discretized points l_j, $j=1,\ldots,N$) are defined by:

$$\begin{aligned} &x(k)= \\ &[f_1(l_1,k)\;\; f_2(l_1,k)\;\; f_3(l_1,k)\ldots f_1(l_j,k)\;\; f_2(l_j,k)\;\; f_3(l_j,k)\ldots f_1(l_N,k)\;\; f_2(l_N,k)\;\; f_3(l_N,k)]^T, \end{aligned} \tag{1.16}$$

the state matrix, $\mathrm{A}\in\mathbb{R}^{3N\times 3N}$, and the matrix related to forces, F, are determined by:

$$\mathrm{A}=\begin{bmatrix} A_1 & 0 & 0 & \cdots & 0 & 0\\ 0 & 0 & 0 & \cdots & 0 & A_2\\ 0 & A_3 & 0 & \cdots & 0 & 0\\ 0 & A_1 & 0 & \cdots & 0 & 0\\ A_2 & 0 & 0 & \cdots & 0 & 0\\ 0 & 0 & A_3 & \cdots & 0 & 0\\ 0 & 0 & A_1 & \cdots & 0 & 0\\ 0 & A_2 & 0 & \cdots & 0 & 0\\ 0 & 0 & 0 & \cdots & 0 & 0\\ & & & \vdots & & \\ 0 & 0 & 0 & \cdots & A_1 & 0\\ 0 & 0 & 0 & \cdots & 0 & 0\\ 0 & 0 & 0 & \cdots & 0 & A_3\\ 0 & 0 & 0 & \cdots & 0 & A_1\\ 0 & 0 & 0 & \cdots & A_2 & 0\\ A_3 & 0 & 0 & \cdots & 0 & 0 \end{bmatrix} \quad \textit{and} \quad \mathrm{F}=\begin{bmatrix} 0\\ \frac{\Delta t}{2v}F\\ -\frac{\Delta t}{2v}F\end{bmatrix} \tag{1.17}$$

Note that it is a nonlinear system represented by: $x(k+1) = \mathrm{A}(x(k))x(k)$, since the elementary matrices A_i depend on the Froude number and ϕ, which themselves depend on the macroscopic variables h and u determined by:

$$\begin{aligned} h &= \sum_{i=1}^{3} f_i = f_1 + f_2 + f_3 \\ q &= hu = \sum_{i=1}^{3} v_i f_i = v(f_2 - f_3) \end{aligned} \tag{1.18}$$

The Chapman–Enskog expansion on the LB model, Eq(s). (1.15), allows recovering the SV continuity and dynamic equations, Eqs. (1.1) and (1.2), as demonstrated in [70]. Their results show the good applicability of the LB method in solving the SV equations.

1.3.2 Boundary conditions used to generate the dynamics of the irrigation channel

The LB method allows integrating a wide variety of boundary conditions. For instance, these conditions can be imposed by either defining macroscopic conditions (e.g., water height or flow rate at the boundaries) or using lattice-type boundary conditions (e.g., bounce-back, periodic or reflexive conditions) (see more details in [54], Section 5). Due to the non-respect of conservation laws for some lattice-type boundary conditions (reported in [79, 41]), we have chosen in this study to directly impose the macroscopic variables at the boundaries.

We consider a reach of length L (corresponding to N discretized points l_j, $j = 1,\ldots,N$) as shown in Fig. 1.4. Unknown density distribution, $f_2(l_1)$, at the site l_1 and unknown density distribution, $f_3(l_N)$, at the site l_N, are calculated differently in the case where either the water height, h, or the flow rate, Q, is imposed at upstream or downstream ends of the reach.

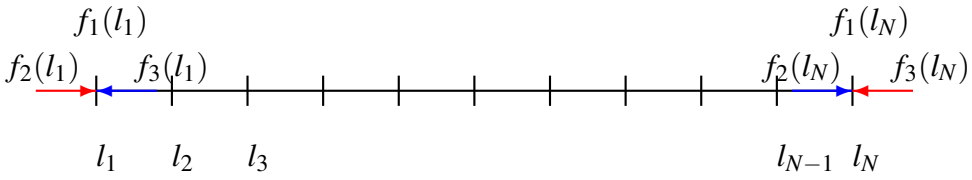

Fig. 1.4 Unknown density distribution, $f_2(l_1)$, at the site l_1 and unknown density distribution, $f_3(l_N)$, at the site l_N, are calculated differently according to the boundary conditions.

The Eq(s). (1.18) can be applied in these cases to determine the unknown density distributions:

- Water flow rate, Q_1, imposed at upstream l_1

$$vB(f_2(l_1) - f_3(l_1)) = Q_1 \quad \Rightarrow \quad f_2(l_1) = \frac{Q_1}{vB} + f_3(l_1) \tag{1.19}$$

- Water flow rate, Q_N, imposed at downstream l_N

$$vB(f_2(l_N) - f_3(l_N)) = Q_N \quad \Rightarrow \quad f_3(l_N) = f_2(l_N) - \frac{Q_N}{vB} \tag{1.20}$$

- Water height, h_1, imposed at upstream l_1

$$f_1(l_1) + f_2(l_1) + f_3(l_1) = h_1 \quad \Rightarrow \quad f_2(l_1) = h_1 - f_1(l_1) - f_3(l_1) \tag{1.21}$$

- Water height, h_N, imposed at downstream l_N

$$f_1(l_N) + f_2(l_N) + f_3(l_N) = h_N \quad \Rightarrow \quad f_3(l_N) = h_N - f_1(l_N) - f_2(l_N) \tag{1.22}$$

However, the oscillation of water heights or flow rates causes a fast change in density distributions and vice-versa. A relaxation algorithm as described in [98], Section 5.4 may be necessary in some situations to prevent numerical instabilities.

1.3.3 Coupling D1Q3 LB models of multiple reaches

The operational management of irrigation channels is done through controlled hydraulic structures and well-defined control policies. These hydraulic structures are used as inter-connectors between the reaches, but also to measure or control the hydraulic variables. Among the inter-connectors, we have classical distribution control structures (e.g., submerged gates, weirs, mixed gates and spillway), but also pumping stations and branching structures such as T or Y junctions. These various inter-connectors can be modeled by mathematical relations, which can integrate the state of inter-connectors and the variation of hydraulic variables.

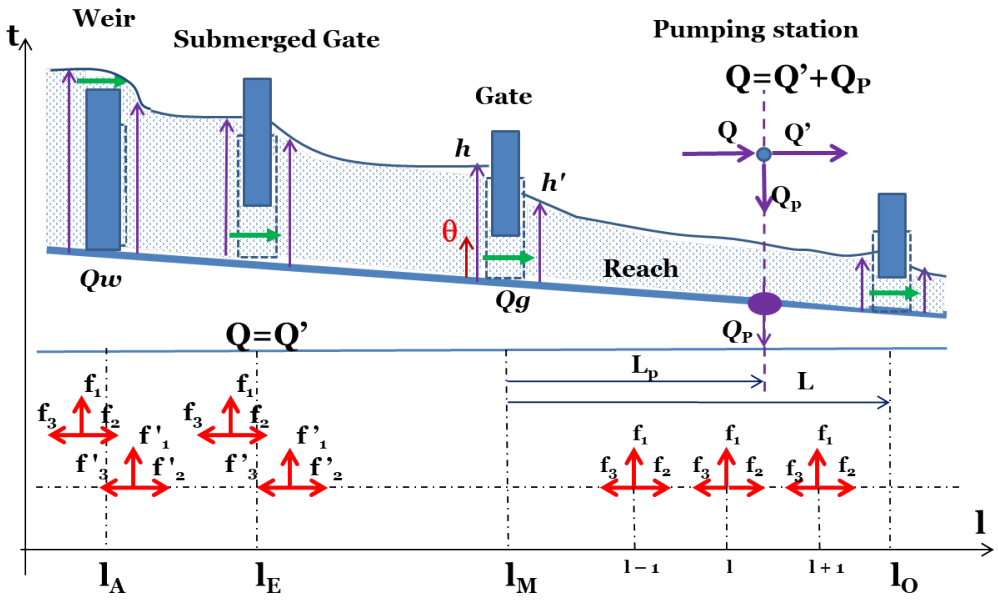

Fig. 1.5 Lattice schemes are presented for some interconnections between two reaches. The flow rate through a gate, Q_g, (or a weir, Q_w, or mixed, Q_m), are expressed by the relations with water heights at upstream, h, and downstream, h', of the gate (or weir or mixed). For the pumping station, the flow rates before, Q, and after, Q', the pump are normally deduced by the pumping flow rate such that: $Q = Q' + Q_p$.

- *Submerged gate* - In a submerged gate as presented in Fig. 1.5, the flow rate through the gate, Q_g, is calculated by the well-known gate equation ([67], Section 6.2), which is based on the difference between the water heights at upstream, h, and downstream, h', of the gate, that is:

$$Q_g = B_g \alpha_g \theta \sqrt{2g(h-h')}, \tag{1.23}$$

where: B_g is the gate width, α_g is the gate coefficient, θ is the gate opening, and g is the acceleration of gravity.

- *Overshot weir (also, immovable spillway)* - it can be considered as level thresholds to be reached before having a flow to the downstream and thus guarantee a minimum height at upstream. The flow rate through the overshot weir, Q_w, can be written ([67], Section 6.2) as follows:

$$Q_w = \begin{cases} B_w \alpha_w \sqrt{2g(h-h_w)^3}, & if \quad h \geq h_w \\ 0, & otherwise \end{cases} \tag{1.24}$$

where: B_w is the weir width, α_w is the weir coefficient, h is water height at upstream of weir and h_w is the weir level.

- *Mixed of gates and spillway* - it is common to use a mixed structure consisting of different elements (e.g., a gate and a spillway or two gates) placed in parallel to interconnect two reaches. The flow rates, Q_M, through a mixed of two gates, g_1, g_2, and one spillway, w, for example, are described by following equations:

$$\begin{aligned} Q_M &= Q_{g_1} + Q_{g_2} + Q_w, \\ Q_{g_1} &= B_{g_1} \alpha g_1 \theta g_1 \sqrt{2g(h_1 - h_1')}, \\ Q_{g_2} &= B_{g_2} \alpha g_2 \theta g_2 \sqrt{2g(h_2 - h_2')}, \\ Q_w &= \begin{cases} B_w \alpha_w \sqrt{2g(h-h_w)^3}, & if \quad h \geq h_w \\ 0, & otherwise \end{cases} \end{aligned} \tag{1.25}$$

- *Pumping station* - the flow rate and water height just before, Q and h, and after the pump, Q' and h', are described by the following equations:

$$\begin{aligned} Q &= Q' + Q_p, \\ h &= h', \end{aligned} \tag{1.26}$$

where: Q_p is the flow rate withdrawn by the pump.

- *Branching junction* - in the case of the main channel that splits into two branches or diverts to secondary channels (see Fig. 1.6), the water heights are the same for three branches

whereas the upstream flow rate is divided into two parts as follows:

$$\begin{aligned} h &= h' = h'', \\ Q &= Q' + Q''. \end{aligned} \tag{1.27}$$

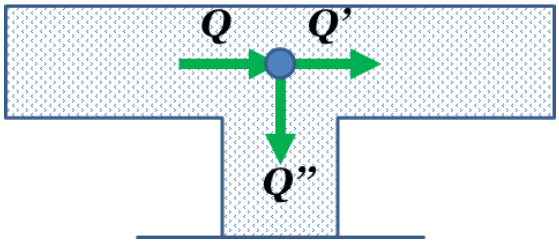

Fig. 1.6 The main channel diverting to a secondary channel is represented by a T branching junction. The upstream flow rate is divided into two parts: $Q = Q' + Q''$.

When coupling two reaches modeled by the D1Q3 LB method, some of the distribution functions before, (f_i), and after, (f_i'), the interconnection are unknown. The unknown LB variables can be determined by solving the equations describing the physical properties of the coupling (as presented in Eqs. (1.23) to (1.27)) and the definition of macroscopic variables (see Eq(s). (1.18)). For example, the coupling of two reaches by a submerged gate requires that the unknown distributions, f_3 and f_2' for two reaches, must be computed using the gate equation, Eq(s). (1.23), and the definition of water height, h, and flow rate through the gate, Q_g as Eq(s). (1.18). As a result, we obtain f_3 and f_2' by solving following equations:

$$vB(f_2 - f_3) = Q_g \quad \Rightarrow \quad f_3 = f_2 - \frac{Q_g}{vB} \tag{1.28}$$

$$vB(f_2' - f_3') = Q_g \quad \Rightarrow \quad f_2' = f_3' + \frac{Q_g}{vB} \tag{1.29}$$

In the same manner for other "inter-connectors" (such as weirs, pumping stations or branching junctions), a system of (non)linear equations can be solved by numerical methods to obtain the unknown variables.

1.3.4 Validation of D1Q3 LB method

Some laboratory validations (as reported in [79, 95]) have been experimentally realized on the micro-channel at LCIS (at Valence, France). Geometrical parameters of the micro-channel are described in [79] such as the length $8(m)$, the width $0.1(m)$, the rated water height $0.1(m)$ and some other network parameters (e.g.,). A first test for the force term is performed on a steady flow in a micro-channel with deformed bottom [79]. A second test verifies the speed of wave propagation for the model [79]. The last test compares the steady case of the LB model to the exact solution of the SV equations [79]. The modeling methodology is validated through comparison to the traditional practices and further correlated to the lab measurements. A comparative study between the LB method and some conventional methods (e.g., Finite Volume

and Preissmann methods) shows some advantages of the LB method in terms of performance and precision. For example, it is 30 times faster than the Finite Volume method and 90 times faster than the Preissmann method (see the details in [79]). By integrating appropriate forces (e.g., Zhou's force and Guo-Chopard's force), the resulting model gives better precision. All these results show the potential of LB approach to simulate a realistic complex irrigation network.

1.4 Fluid simulations

The LB modeling requires a lot of data from the channel (e.g., geometry of the channel, longitudinal profile, roughness coefficient) that are not always available in large-scale channels. In this work, some terms have been neglected in the equations in order to create a simplified model of free-surface flow [98]. The successive simulations of the obtained model are necessary for calibration and validation using data gathered on a practical channel. The resulting simulator can be used as a management and diagnostic tool for the efficient water management of the considered channel. For example, the LB simulation results of the hydrodynamic model can help for the comprehension of local behaviors with regards to global states. On this basis, the control engineer investigates the new features for the designed controllers, making the model compatible with predefined mathematical criteria or the refinement of initial conditions.

1.4.1 Modularity in modeling of free-surface channels using a library

In the literature, the works related to LB modeling of irrigation channels usually consider the system of one, two or multiple reaches as a whole [95, 79, 98, 67]. Therefore, the resulting models are difficult to apply to other systems, due to the complex interconnection considered in these systems. This section proposes a modular approach using parameterized modeling blocks gathered in a *Model Library*. The proposed modular approach reduces the system design and review cycle. This can significantly improve the design consistency for large-scale systems. In simulations, it takes less time and enables a more efficient co-simulation. The concepts allow the decomposition of complex systems into tractable subsystems and a set of interactions. Subsystems are the modeled using the LB method or mathematical equations and the sub-models are added to a Model Library as components. These components are re-usable and scalable for generating a parameterized complete model. For the irrigation channel, the modular modeling methodology is used to generate the Model Library of reaches and control structures. As an example, a Simulink/MatLab model library created for an irrigation channel is shown in Fig. 1.7.

1.4.2 Simulation schemes and results

As a demonstration of the modeling methodology, we perform Simulink/MatLab simulations for a section of the Bourne channel, from the Mondy gate (a mixed gate and spillway structure) to the branching junction with secondary channel S2 (see Fig. 1.2 and Fig. 1.8). This section

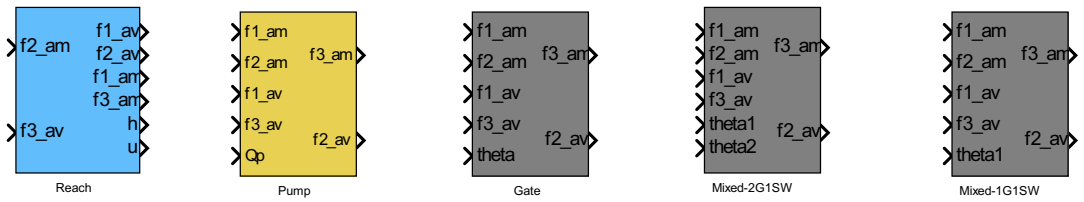

Fig. 1.7 A Simulink/MatLab Model Library is created for the modeling and the simulation of an irrigation channel.

consists of three segments interconnected by a pumping station at "Monts du Matin" and a mixed structure (composed of two gates and one spillway) at "Orme". The flow rate and level meters are available at certain locations and periodically give the flow rates and water heights at different points in the considered section. By coupling different components of the Model Library (shown in Fig. 1.7) such as reach, pump, and mixed components through their interactions, a model of the considered section is created as shown in Fig. 1.9. Based on the model, the simulations require the geometric information of the corresponding section and boundary conditions at upstream and downstream ends to perform the hydraulic calculations for steady or transient flow. The selected geometric and simulation parameters are presented in Tables 1.1, 1.2 and 1.4. In simulations, we use a global flow axis with the beginning at Auberives barrage (see Fig. 1.2). Consequently, the relative location of the first considered section is between $3.25e4$ m to $3.62e4$ m. Assuming that the boundary conditions of the first considered section impose the water flow rate at the upstream end of Mondy gate, Q_M, and the water height at the S2 junction, h_S as in Table 1.3 and Fig. 1.10.

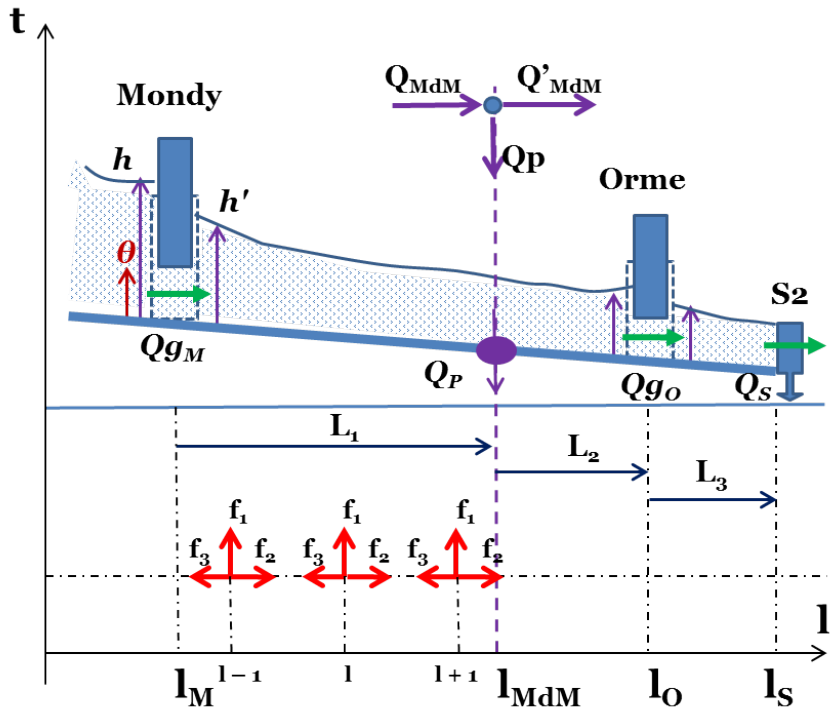

Fig. 1.8 A section of Bourne channel is considered for modeling and simulation.

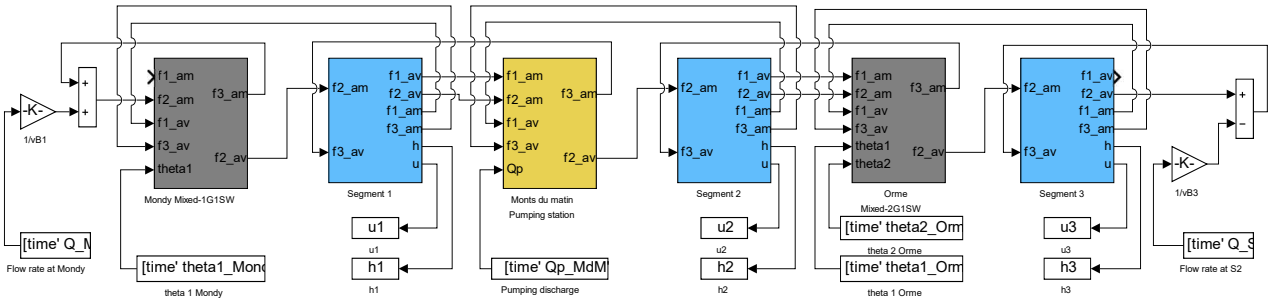

Fig. 1.9 A Simulink/MatLab model is created for the simulation of the first considered section.

Table 1.1 Geometric parameters of the irrigation channel.

Segment	Length (L)	Width (B)	Slope (I)	Manning coef. (n)	Space st. (Δx)
1	100 m	5.12 m	2.400e-4	0.033	100 m
2	2600 m	5.20 m	2.441e-4	0.033	100 m
3	1000 m	5.40 m	2.440e-4	0.033	100 m

Table 1.2 Structural parameters of mixed hydraulic structures.

Mixed structure	Gate width (Bg)	Gate coeff. (α)	Spillway width (Bsw)	Spillway height (Hsw)	Spillway coeff. ($\alpha_s w$)
at Mondy	3.97 m	0.66	0.80 m	1.3 m	0.35
at Orme	2.8 m & 0.9 m	0.66	1.91 m	1.7 m	0.35

Table 1.3 Boundary conditions and initial values are used in simulation scenarios.

h_S	θ_{1-Orme}	θ_{2-Orme}	Q_P	$\theta_{1-Mondy}$	Q_M
$1.64m$	$0.20m$	$0.20m$	$0m^3/s$	$0.60m$	$2m^3/s$

Table 1.4 Simulation parameters of the irrigation channel.

Simulation time (T_s)	Time step (Δt)	Relaxation time (τ)
8000 s	10 s	0.55

For numerical time-interpretation of the resulting equations, the system firstly needs to be initialized at steady state of flow by the following procedure:

- Choose the initial water height of steady flow at S2, $h_S(l_S,0)$, the steady flow rate is calculated by $Q_S(l_S,0) = B_3 * h_S(l_S,0) * u$ (in the case of a rectangular section, otherwise $Q_S(l_S,0) = S(h_S(l_S,0)) * u$).
- Integrate the steady-flow Eq(s). (1.5) with the boundary conditions at S2 to obtain the water height $h_S(l)$, the steady-state profile for $l \in [l_O, l_S]$.
- Using the gate relation Eq(s). (1.23), calculate the flow rate through the mixed at Orme, $Qg_O(l_O,0)$, by selecting gate openings, θ_{1-Orme} and θ_{2-Orme}.
- Integrate the Eq(s). (1.5) with the boundary conditions at Orme to obtain the water height $h(l)$, the steady-state profile for $l \in [l_{MdM}, l_O]$.
- The flow rate at "Monts du Matin", Q_{MdM}, is calculated by the pump relation, Eq(s). (1.26) where the pumping flow rate is $Q_P(l_P,0)$.
- Integrate the Eq(s). (1.5) with the boundary conditions at "Monts du Matin" to obtain the water height $h(l)$, the steady-state profile for $l \in [l_M, l_{MdM}]$.
- By selecting the initial flow rate at the Mondy gate, $Q_M(l_M,0)$, and the gate opening, $\theta_{1-Mondy}$, Eq(s). (1.23) can determine the water height at upstream of the Mondy gate.
- The initial water height profile for the considered section is initialized.

The initial values used in simulations are presented in Table 1.3 and an overview of the initialized section is shown in Fig. 1.11. Starting with this equilibrium profile for the considered section,

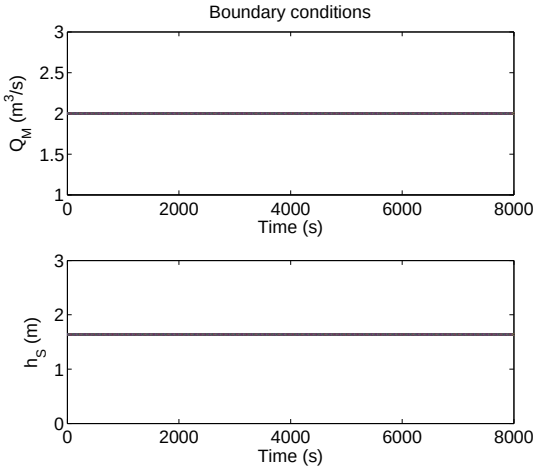

Fig. 1.10 Boundary conditions impose the water flow rate at Mondy gate, Q_M, and water height at S2 junction, h_S for the first considered section.

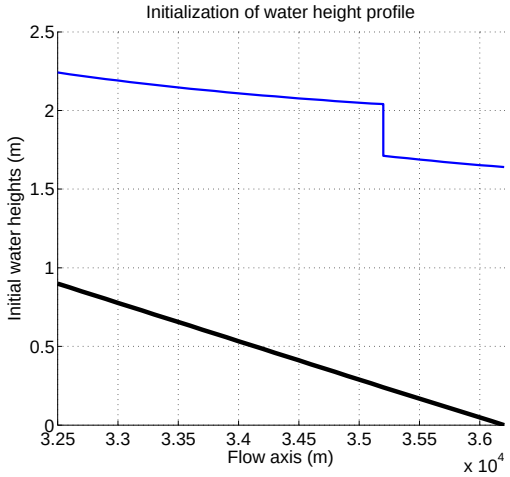

Fig. 1.11 The first considered section is initialized. The specified flow axis (i.e., $3.25e4\ m$ to $3.62e4\ m$) is relative to global flow axis beginning at Auberives barrage.

we propose the following scenario for the simulation of the transient behavior of the LB model.

At time $t = 80\ (s)$, the opening of the Mondy gate, $\theta_{1-Mondy}$, is changed in a way to linearly increase the flow rate at the upstream by 50% from its initial value $Q_M(l_M, 0)$ at time 1000 (s). At time $t = 1200\ (s)$, the gate openings at Orme, θ_{1-Orme} and θ_{2-Orme}, increase gradually to 0.3 (m) at $t = 2000\ (s)$. At "Monts du Matin", the pumping flow rate is increased from 0 (m^3/s) to 0.2 (m^3/s) between $t = 5000\ (s)$ and $t = 5500\ (s)$ and stabilized. The simulation scenario is illustrated in Figs. 1.17 and 1.18.

The simulations are done with Matlab R2016b®on a computer Intel®Core™i5-4310U CPU 2.0GHz. The simulation results presented in Fig. 1.12 (for water height profile along the section) and Fig. 1.13 (for flow rate profile) show a coherent behavior of the considered section. Indeed, we see that (1) there is a wave propagation phenomenon at a constant speed from the upstream to the downstream; (2) the water heights change when the flow passes through the mixed structures at "Mondy" and at "Orme"; and (3) the discontinuity of flow rates corresponds to the withdrawal of the pumping station at "Monts du Matin". The first coherent results motivate a model of a more complex section or the whole channel, which can potentially be constructed in the same way (see Section 1.4.3).

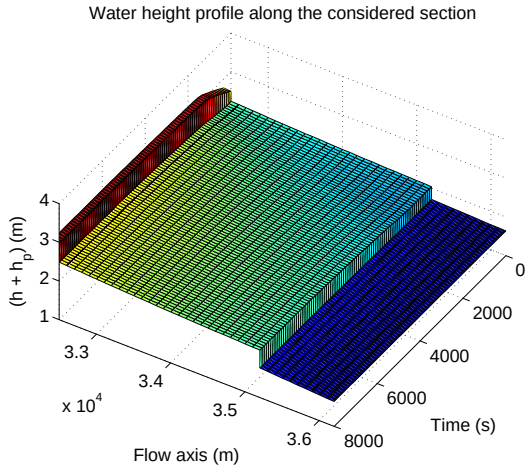

Fig. 1.12 Simulation results - Water height profile in the first considered section. The specified flow axis (i.e., 3.25e4 m to 3.62e4 m) is relative to global flow axis beginning at Auberives barrage.

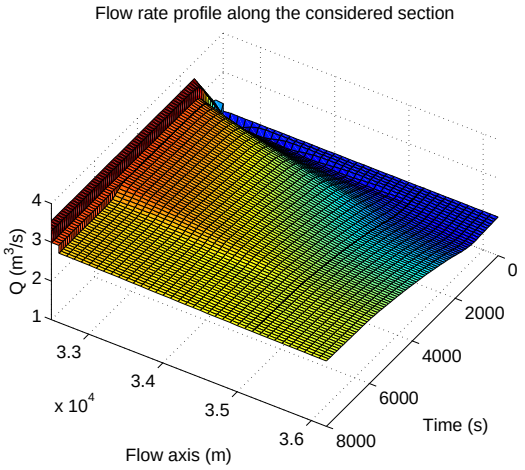

Fig. 1.13 Simulation results - Flow rate profile in the first considered section. The specified flow axis (i.e., 3.25e4 m to 3.62e4 m) is relative to global flow axis beginning at Auberives barrage.

Finally, let us remark that the model still needs to be calibrated and validated during the field campaigns, with surveys and orders from channel operators and precise corresponding experimental measurements.

1.4.3 Considering a real irrigation channel and data requirements for model setup

Another more complex section of the Bourne channel (shown in Fig. 1.2) from the Auberives barrage to the branching T junction with the secondary channel $S2$, is considered for the simulation to illustrate hydraulic aspects. This section (with a length of approximately 37 (km)

long) comprises twelve reach segments, three mixed control structures, and eight pumping stations withdrawing the water along the main channel. For reliable hydraulic simulations, some adequate data on water conveyance and distribution infrastructure are needed to put into the model. The collected field data can be classified into three main categories: (1) channel geometry, longitudinal profile, and environment parameters; (2) the details of control structures and their operations; (3) flow characteristics such as water heights, flow rates through gates and pumping flow rates. All of these data are not available in Bourne channel. We have used the maximum information provided by the "Syndicat d'Irrigation Drômois" (SID) operator on the irrigation network topology, channel geometry, details of control structures, and operation rules. The canal geometry and longitudinal profiles were determined for the whole channel length and cross-section data were measured at fixed intervals by a campaign of channel surveying (files supplied by SID operator). Control structures such as submerged gates, mixed structures were carefully located and their dimensions were measured. Moreover, their detailed features such as gate levels, opening heights and their conditions were noted for each structure. The global parameters necessary for the modeling of the considered section are summarized in Tables 1.1 to 1.5.

The modeling of the considered section using the LB method is described in Section 1.3. Similarly, the model of the second considered section is created as shown in Fig. 1.14 by coupling different components of the Model Library (shown in Fig. 1.7) such as reach, pump and mixed components through their interactions.

Table 1.5 Global simulation parameters for the considered section of BC.

Parameter	Value	Comment
Total length	36200 m	
Number of reaches	12	
Number of controlled structures	3	Orme, Mondy, Ecanciere
Number of pumping stations	8	Baume d'Hostun, Eymeux, Meymans, Papelissier, Martinet, Tendillon, Mondy, Monts du Matin
Number of discretized points	374	Space lattice $dx = 100m$
Simulation time	8000 s	Time step $dt = 10s$

As mentioned in Section 1.4.2, for numerical time-interpretation of the resulting equations, the considered section firstly needs to be initialized at steady state of flow by the similar procedure applied on the overall section using the boundary conditions and initial values given in Fig. 1.11. An overview of the initialized section is shown in Fig. 1.16.

Based on the section model, a simulation scenario is proposed for hydraulic presentation. For example, assuming that the gate openings of three mixed controlled structures change as described in Fig. 1.17, the flow rate at Auberives evolves from 0 to 2.2 (m^3/s) in time between 0 and 1000 (s) and pumping flow rates at different pumping stations evolve as shown in Fig. 1.18. Other parameters are fixed at their equilibrium values. The simulations are also done with Matlab R2016b®on a computer Intel®Core™i5-4310U CPU 2.0GHz. The

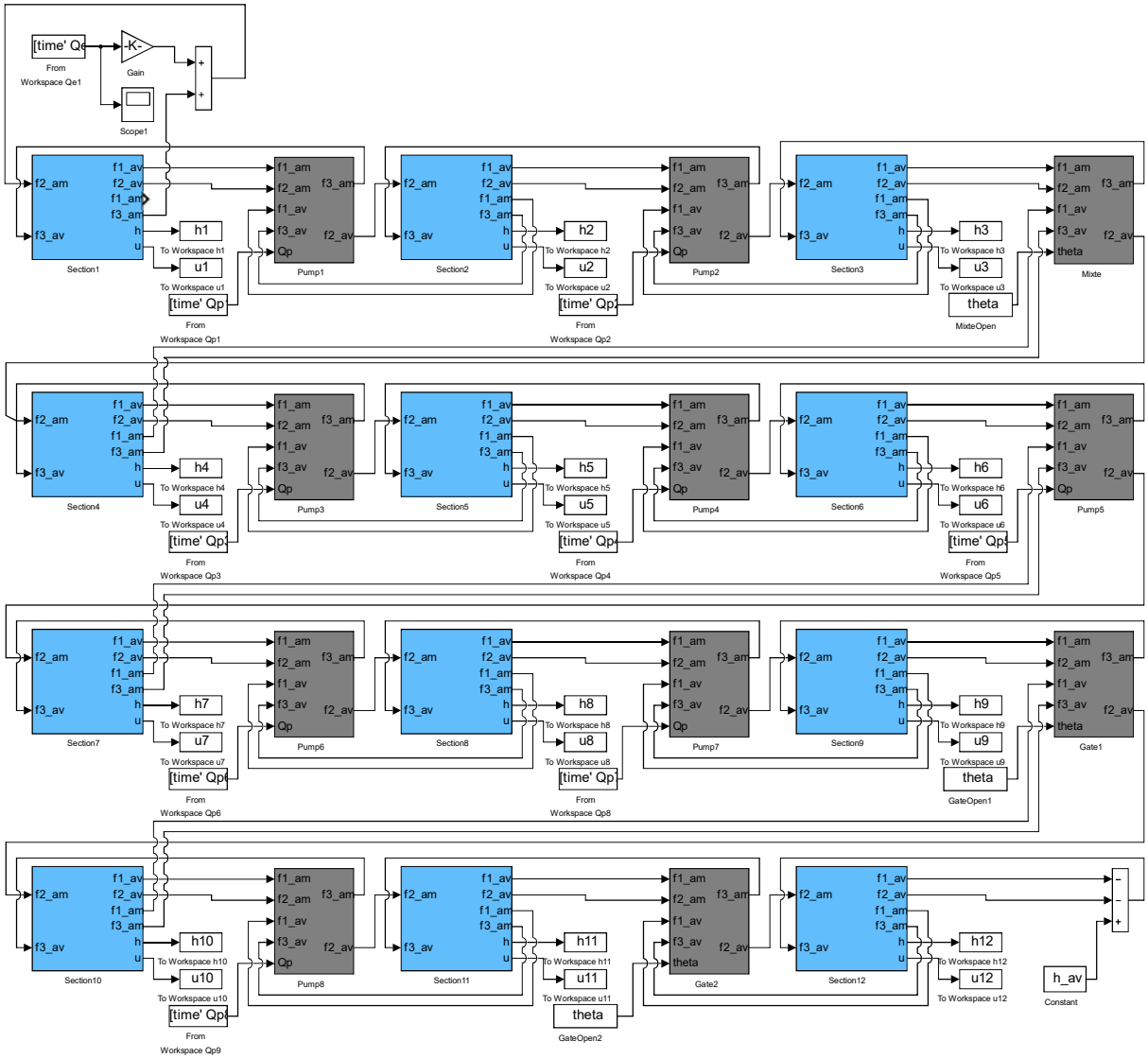

Fig. 1.14 A Simulink/MatLab model is created for the simulation of the second considered section using the Model Library.

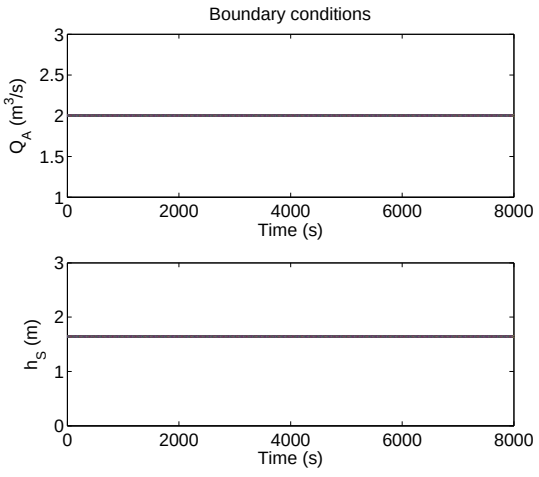

Fig. 1.15 Boundary conditions are imposed for the second considered section.

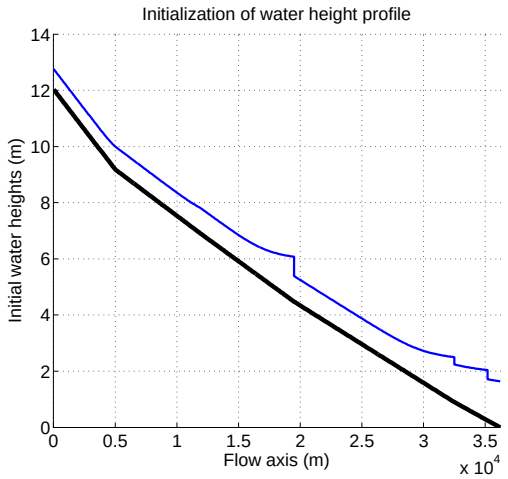

Fig. 1.16 The second considered section is initialized.

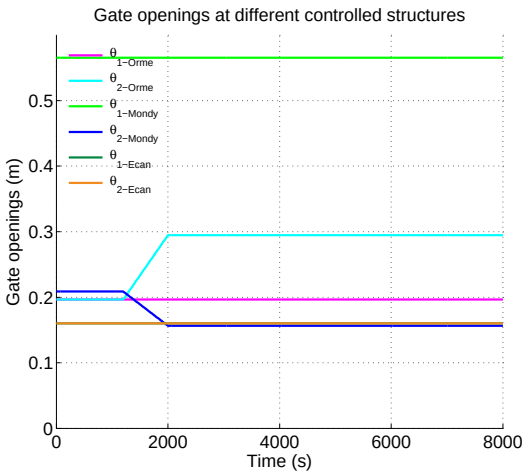

Fig. 1.17 Simulation scenario - Gate openings of different controlled structures in the second considered section.

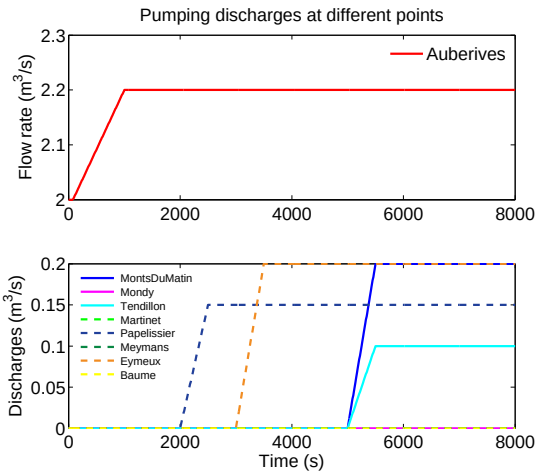

Fig. 1.18 Simulation scenario - Pumping discharges at different points of the second considered section.

simulation results of this scenario are shown in Fig. 1.20. According to simulation results, we see that there is a wave propagation phenomenon at constant speed from the upstream to the downstream of the considered section; the water heights change when the flow passes through the mixed structures at “Ecanciere”, “Mondy” and at “Orme”; and the discontinuity of flow rates corresponds to the withdrawal of the pumping stations at “Monts du Matin”, “Mondy”, “Tendillon”, “Martinet”,“Papelissier”, “Meymans”, “Eymeux”, “Baume”.

In consequence, based on LB method and the parameters of the flow (e.g., channel geometry, environment parameters, the details of control structures and their operations, and flow characteristics), it is possible to determine the longitudinal profile of the water line at various sections in the channel and thus, to localize the phenomena which generate and perhaps quantify the flow and perturbations themselves. Therefore, the natural animation of the flow in the channel can be supported by modeling the evolution in time and in space of the flow and disturbances generated by the different situations.

From a complexity point of view, with the code written in Simulink/Matlab and the specified computer used to perform these simulations, the computation time is 7 (s). The computation time estimated for the flow in future 24 (h) is 84 (s). A simulation over one year for the above network described with 374 sites requires about 8.5 (h) of CPU times. In addition, a C++ implementation typically is 100 times faster without any code optimization (as discussed in [98]). It can reduce the time needed for the 1-year simulation to the order of a few minutes of CPU times with the same spatial and temporal resolutions. Even for real-scale complex irrigation networks (e.g., with more secondary channels, hydraulic structures, pumping stations, reservoirs, etc.), the simulations can respect real-time requirements. This computing efficiency may be useful for scale-reduced experimental micro-channels typically characterized by fast dynamics associated with low frictions and short reaches (e.g., only a few meters long) or for other application examples of fluid flow (see more details in [79]). Moreover, the D1Q3 LB method is analyzed in detail and compared with other numerical schemes (such as an implicit finite difference scheme

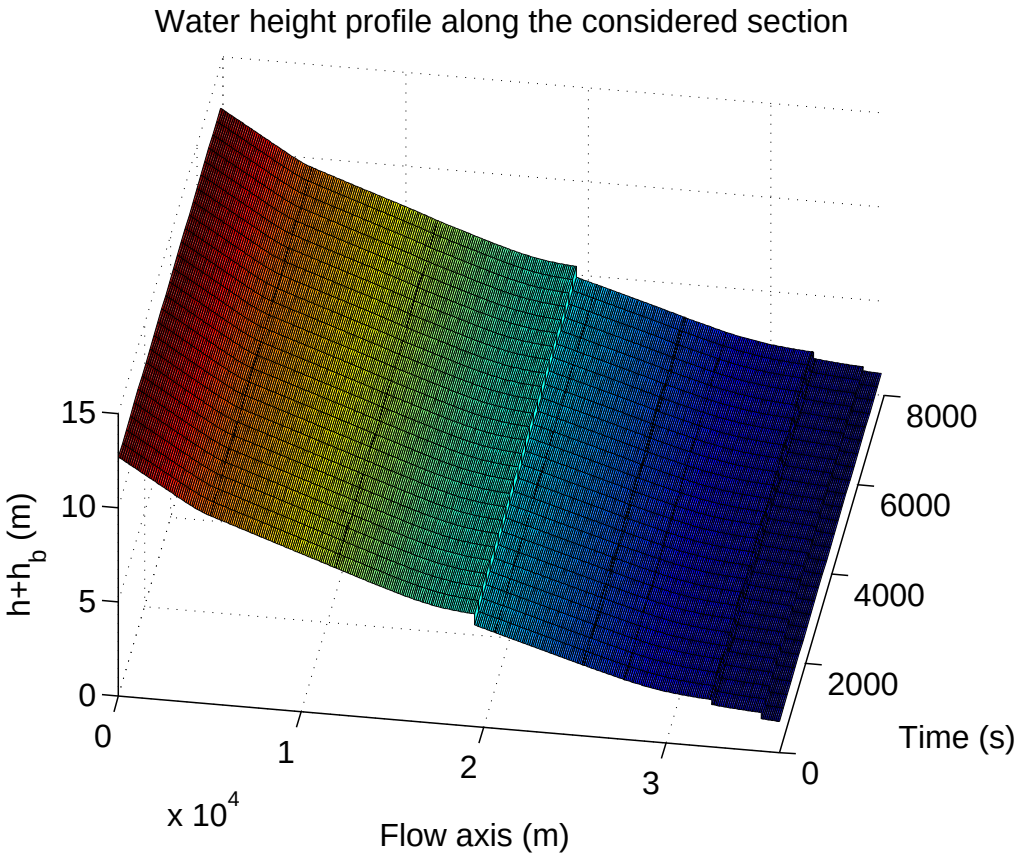

Fig. 1.19 Simulation results - Water height profile along the second considered section corresponds to the specified simulation scenario.

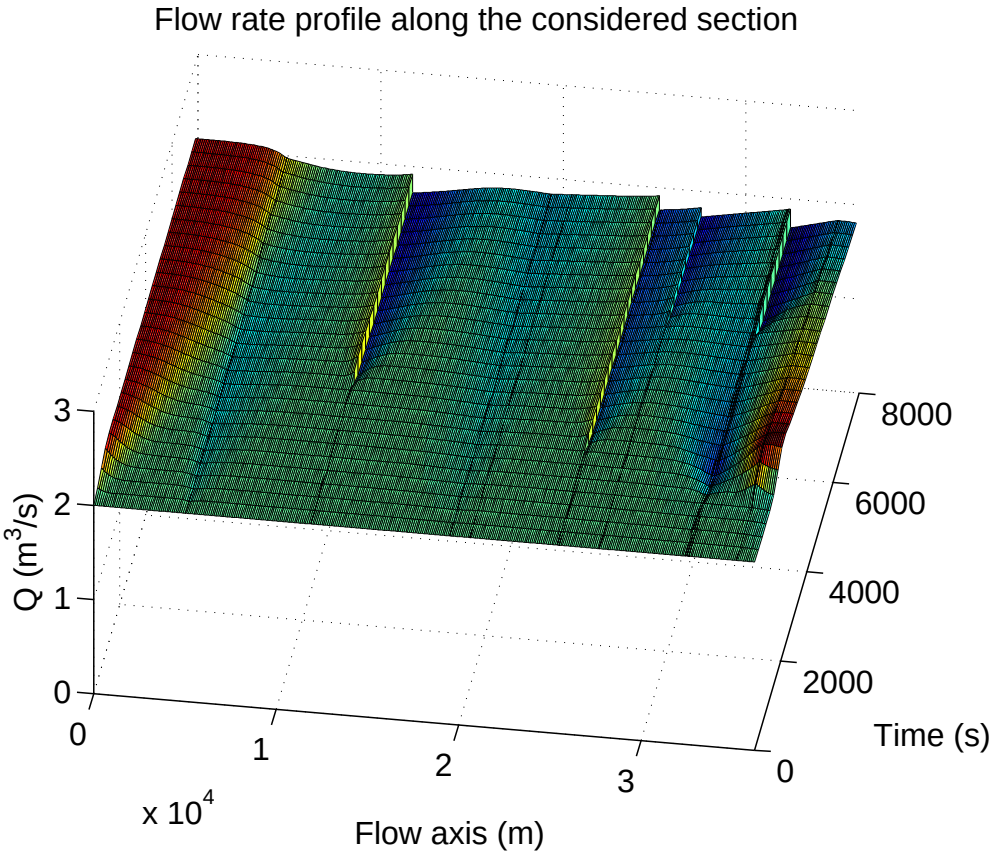

Fig. 1.20 Simulation results - Flow rate profile along the second considered section corresponds to the specified simulation scenario.

and a finite volume approach) in [98]. This work has shown that the LB method is 10 times faster than the Finite Volume method and 100 times faster than the Preissmann method (see [98], Section 5). With appropriate forces (Zhou force and Guo-Chopard strength), the LB model gives the better precision, but the numerical stability region of the LB model is limited by the Courant condition and sub-critical flow conditions.

1.5 Summary

In this chapter, we have presented the LB method with its application to the modeling and the simulation of the free-surface flow in irrigation channels. Geometric parameters and hydraulic variables characterizing an irrigation system are first introduced to provide a synthesis of physical quantities in the modeling framework. The SV (or 1DSW) equations are briefly represented as a classical distributed-parameter model for transient free-surface flow. The LB approach to solving the SV equations is introduced in details. It is a mesoscopic technique bridging the molecular movements and macroscopic physical variables. The aspects concerning boundary conditions were discussed in 1D for network-type conditions, but also for conditions that allow directly imposing macroscopic variables. A coupling methodology to interconnect several 1DSW models is developed by introducing mathematical relations of LB variables and hydraulic variables. Taking into account the boundary conditions, internal interconnections and the interactions with the environment, fluid simulations show the potential of the LB approach to simulate a realistic complex network of irrigation channels.

Chapter 2

Composite metric design for the dynamic routing in networked control systems using a hybrid architecture

Networked control systems (NCSs) allow integrating components (e.g., controllers, sensors, actuators) and algorithms of control systems into a global network infrastructure. Based on this infrastructure, the control information (e.g., reference inputs, controlled variables, system inputs/outputs, feedback values, and collected data) can be exchanged among the components through wired and/or wireless communication subnetworks. A hybrid network architecture involving different types of subnetworks to be interconnected is needed so that the components can share, collaborate and cooperate efficiently to accomplish different tasks. Therefore, an efficient communication among the system components plays an important role in achieving global objectives. This chapter aims to design a hybrid network to cope with the heterogeneity of wide-area NCS and a composite metric for the dynamic routing over the hybrid network in order to satisfy different Quality of Service (QoS) requirements of control applications. The resulting network model can be used to dynamically compute the QoS-related costs (or probabilities) of different paths between NCS components. These are the important concerns while considering the information exchange in NCSs.

To describe the motivation and deal with the routing problem of complex communication network, the following sections will present: (1) the challenging communication constraints possibly imposed on a wide-area NCS, an example is given by the Bourne channel (BC) case (Section 2.2.1); (2) the benefits of a hybrid network using IPv6 over Low power Wireless Personal Area Network (6LoWPAN) technology to unify the communication among NCS components (Section 2.2.2, and Section 2.2.3); (3) different QoS requirements of control applications can be imposed to the network services (Section 2.2.4); (4) the design of a composite metric used by a dynamic routing protocol for satisfying these requirements (Section 2.3); (5) a case study for the design of a composite metric used by Routing Protocol for Low power and lossy network (RPL) over a network with mesh topology (Section 2.4); and finally (6) the simulations of this case study in some extensive scenarios.

2.1 Introduction

Networked control systems (NCSs) are evolving into *distributed* NCSs, which integrate distributed components (e.g., controllers, sensors, actuators), and distributed algorithms of control systems into a global network infrastructure [157, 107, 39]. This vision is even more realistic with the proliferation of the ubiquitous Internet of Things (IoT) [120]. Indeed, the sensing/actuating devices in NCSs can greatly benefit from the recent IoT developments. Many works have been done in order to emphasize the complementary contributions in both fields of automatic control and wireless sensor/actuator networks (WSANs). In particular, two lines of research have significant practical implications [157, 39]: (1) *network-aware control* that aims at modifying control algorithms to cope with the imperfection in communication; and (2) *control-aware networking and communication* that attempts to modify network protocols and radio links for better real-time control performance. As an example of the former category, research works have discussed the control methodologies in NCSs [131], the modeling, analysis, and design of NCSs (see [26, 4] and reference therein). Especially, many works were interested in system stabilization and control in the presence of communication constraints [60, 65, 115, 90, 10]. Whereas the works in the latter category have investigated in a joint design of control algorithm and network protocol [107, 21, 30, 97] or introduced network configurations adapted to control systems [26, 24]. However, these works have considered control algorithms without [97] or with simple routing strategies such as multi-path static routing [4, 24]. Moreover, the components of wide-area NCSs are commonly heterogeneous devices integrated into different types of networks. They demand to pay much more attention in network design, especially routing design to enable the interoperability and Quality-of-Service (QoS) satisfaction. The co-design of NCS and network often requires making some assumptions on network models with probabilities of delays or packet loss for different paths [24]. There is little information available on the routing optimization process combining multiple criteria (i.e., metrics) in NCSs. More concrete methods also need to be investigated on the computation of delay (or packet loss) probability in network models.

In certain wide-area NCSs, communication constraints might require *a unified communication among components within a global network*. For the design of this network, the present chapter aims at presenting the approaches to two problems:

- *multiple applications on the same network infrastructure*: by introducing a hybrid network to cope with the heterogeneity of NCSs and the 6LoWPAN technology suitable for a resource-limited network (e.g., including devices with low-power, limited memory and processing capabilities);

- *QoS satisfaction*: by designing a composite metric for dynamic routing over the hybrid network in order to satisfy different QoS requirements of control applications.

As an example, one ArrowHead project demonstrator focusing on distributed control of Bourne Channel (BC) irrigation network in Drôme - France, is used to introduce an NCS with specific communication constraints (see detail in [89]). The BC communication setting is shown in Fig. 2.1.

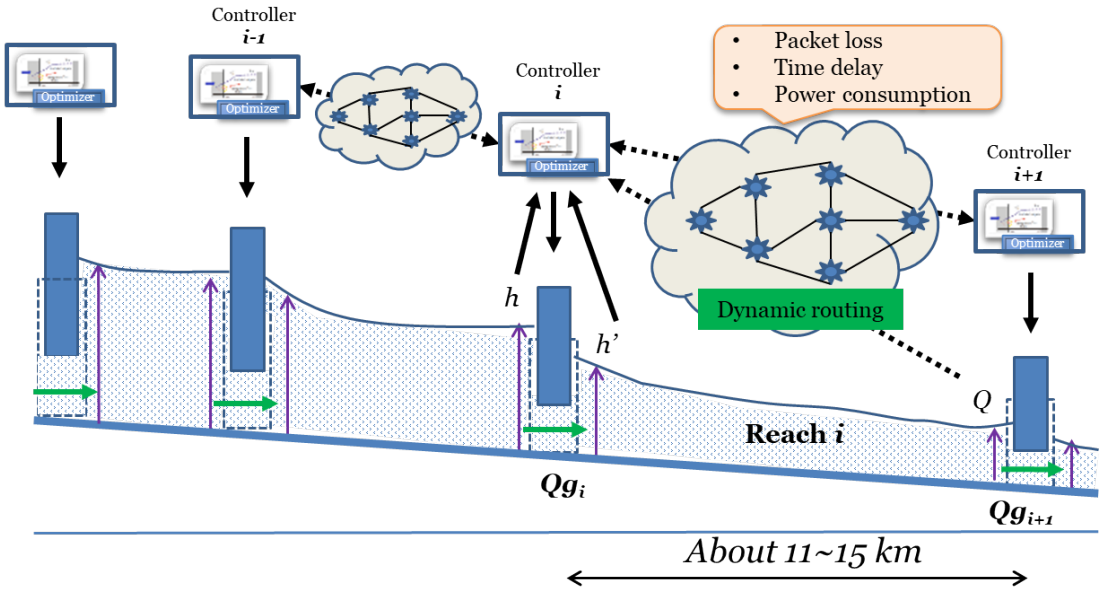

Fig. 2.1 Communication setting of primary Bourne Channel (BC) in which the large network coverage and the wide communication range require the implementation of a large number of intermediate nodes that motivate a unified communication of control system components within a hybrid network.

2.2 Motivation: A hybrid network for NCSs

2.2.1 Communication constraints in NCSs

A study of networking aspects is always necessary for the design of wide-area NCSs. With regards to the needs of data exchange, each controller designed for a distributed NCS may have three basic actions [21]: (1) gather the information recorded by sensors; (2) interact with other controllers for coordination and cooperation; and (3) send control signals to the actuators. To achieve these actions, controllers commonly make use of efficient transmission techniques for point-to-point communication, sometimes over a long range and under challenging limitations on data rate, operational energy consumption, etc. [21, 131]. To give an example, some communication constraints are encountered in large-scale BC control system such as *long communication range and large network coverage*, *wireless-imposed network type*, *heterogeneous and resource-limited devices*, *dynamic topology*, and *lack of regular maintenance*. The serious difficulties in the current state of the BC control system are frustrating some technological proposals in terms of interoperability, scalability, network design, and operations. Particularly for network routing, some standard protocols used in Internet stack (e.g., Routing Information Protocol - RIP, Open Shortest Path First - OSPF) or the protocols, especially designed for WSANs (e.g., Adhoc On-Demand Distance Vector - AODV, Dynamic MANET On-demand routing protocol - DYMO, Dynamic Source Routing - DSR) perform much worse for this task as discussed in [124] and some routing protocols are compared on the basis of different criteria in [55]. Dealing with these challenges requires the network design to adopt constraint-based networking technologies (such as LoRa® technology from Semtech providing long-range communications) or to optimize the dynamic routing process.

2.2.2 A hybrid network for heterogeneous components of the NCS

An NCS with communication constraints described above will take advantage of the unified communication among components within a hybrid network. This type of network refers to any network that contains two or more different communications standards or multiple topological structures [62, 154, 132]. It enables different types of subnetworks to be interconnected so that the components can share, coordinate and cooperate efficiently to accomplish different tasks. A hybrid network for NCS (as shown in Fig. 2.2) is commonly composed of traditional WSNs [92, 154], embedded networks (as defined in [122], Section 1.1) and Internet Protocol (IP) networks (e.g., local network infrastructure connected to the Internet) [132]. Although each subnetwork is

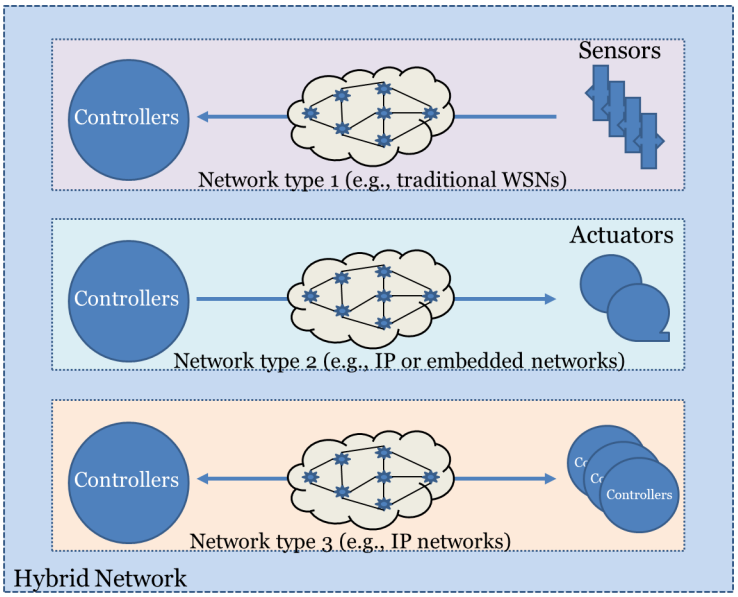

Fig. 2.2 An example of a hybrid network for NCS. It can be composed of traditional WSNs, embedded networks, and Internet Protocol (IP) networks. Intermediate nodes can route any data packets.

different in nature, but the network services are required to be homologous through the hybrid network.

To benefit from available technologies and the large-scale deployment of the Internet, it may be expected that NCS components should be integrated into Internet-connected networks [124]. In this integration, each component playing the role of a node in the global network, is able to dynamically join the Internet. In addition, with recent technological progress materializing IoT, the future Internet is foreseen to be extended as a worldwide network of interconnected devices or objects (as mentioned in [124]). Wireless network technology continues to play an ever-increasing role in data network architecture throughout the large range of electronic component markets. However, deploying an NCS configured to access the Internet (see Fig. 2.3) raises new challenges, which need to be tackled before such an integration. [124] highlighted and discussed the challenges newly emerging on the capabilities of WSAN devices such as the mobility management, quality of service (QoS), and network configuration in addition to their usual sensing/actuating functionality. Many open challenges remain, mostly due to the complex

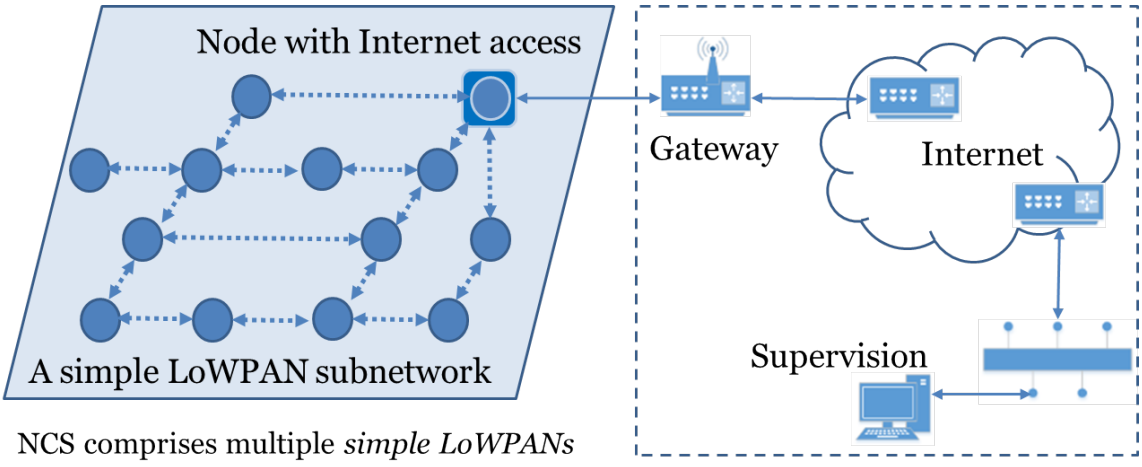

Fig. 2.3 A hybrid network architecture composed of multiple Simple LoWPANs is proposed for NCS due to low mobility between subnetworks [122].

deployment characteristics and the stringent requirements imposed by various desired services of such hybrid network. For example, the control applications cannot directly profit by IP technology because of limited processing and transmission capabilities of nodes, non-permanent power source, small packet size or the overhead of IP header, etc. The promising 6LoWPAN technology allows IP networking for resource-limited devices.

2.2.3 6LoWPAN technology suitable for the NCS hybrid network

As surveyed in [122], some possible technologies can be considered while addressing the Internet integration of WSANs such as ZigBee (ZigBee Alliance), Machine-to-Machine (ETSI M2M), Future Internet (e.g., EU 4WARD project) and 6loWPAN (IETF). Nevertheless, non standard or especially non-IP networks tailored to specific applications seem inappropriate for building a global infrastructure. If all of the system components are connected through a single open standard protocol (e.g., IP), they might benefit without any extra effort, by seamless connectivity, unique addressability, and rich applicability. This shows a strong trend of convergence on standardization, both in industry and in academia, that is clearly steering towards *an Internet-based approach*. The 6LoWPAN and ROLL WGs of IETF are actively performing this standardization by specifying the 6LoWPAN technology and RPL protocol.

The design of a hybrid network for NCSs can take advantage of 6LoWPAN compared to other technologies (e.g., WiFi, ZigBee) such as scalability, self-organization, and low-power consumption [55, 122]. More advantages are presented in [122], Section 1.1.1. The 6LoWPAN is expected to become a standard networking technology supported on any constrained network [122]. By this motivation, it shows up a wide range of interesting research proposals (e.g., RFC4919, RFC6568, RFC6606) and applications using 6LoWPAN (as surveyed in [55], and [122], Section 1.1.4). They offer solutions for making networks more reliable, adaptable, durable and manageable.

2.2.4 Different QoS requirements of control applications

A hybrid network is technologically realizable. However, one of the important concerns for the hybrid network design is the selection of network performance criteria. Whereas "QoS is the description and/or measurement of the performance of a network service as seen by network users" [51, 132], selecting network performance criteria for the hybrid network can be based on QoS requirements of control applications. For instance, the level meters or pressure meters in mesh-pressurized subnetworks require *minimum power consumption and minimum aggregation delay* to reach their controllers. The control signals from controllers are expected to reach actuators (e.g., gate control motors) with the *minimum packet loss rate, minimum aggregation delay*, and in certain cases (e.g., with pressure regulating valves), *minimum power consumption*. Whereas the controllers are implemented on devices usually attached to a power source, they only require *minimum aggregation delay and packet loss rate*.

Eventually, the QoS-based performance criteria considered in the NCS hybrid network are *packet loss rate*, *network latency*, and *network lifetime*. The challenging factors influencing on network performance in the hybrid network are the varying channel characteristics, bandwidth allocation, fault tolerance levels and hand-off support for heterogeneous wireless networks. Network software may help to address those challenges by using dynamic routing.

2.3 Dynamic routing design for the hybrid network

There is a state-of-the-art introduction to various dynamic routing mechanisms (e.g., flooding, shortest path, distance vector routing, link state routing, etc.) in [132], Section 5.2. Especially for 6LoWPAN networks, the work [55] presented a survey of existing routing protocols, a taxonomy of routing requirements and parameters for evaluating routing algorithms. The RPL presented in Section 2.4 is one of the common protocols used for the routing in 6LoWPAN networks [122].

2.3.1 Network model and formal representation of metrics

It is crucial for routing design to address the relationship between routing metrics, path calculation algorithms, and packet forwarding schemes. For this goal, they should be properly represented in a network model.

Definition 2.3.1. *Network model and Path Weight Structure* [152].

According to [126], refined thereafter by [152], a network can be modeled by a strongly connected and directed graph $G(H,L)$, also called *digraph*, where:

- H is a set of nodes;
- L is a set of edges representing links between nodes.
- Let $H = \{X_1, X_2, \ldots, X_n\}$ be a node set of the graph G of n nodes. For $i, j, s, d \in \{1, \ldots, n\}$,
  - a link from node X_i to node X_j, denoted by l_{ij} or $(X_i, X_j) \in L$, has link cost, $c(l_{ij})$ or $c(X_i, X_j)$;

- a path p from node X_s to node X_d, denoted by $p(X_s, X_d)$, has path cost, $c(p)$;
- a set of all paths from X_s to X_d discovered by a routing protocol, R, is denoted by $R(X_s, X_d)$

From the network model, the routing using a metric m can be mathematically represented as an algebra on top of a quadruplet: $(\mathscr{P}, \oplus, c, \preceq)$, called *Path Weight Structure* (PWS), where $\mathscr{P}$ is a set of all possible paths, $\oplus$ is the path concatenation operation, c is a function that maps a path to a cost based on metric m and $\preceq$ is an order relation.

A metric is specified in a domain, for example, *integer, real, [1,+∞], etc*. It can be either recorded or aggregated along a path [139]. For a same aggregated metric, the path cost may be different depending on the aggregation rule such as additive, multiplicative, or concave. For a path p of n_p nodes, denoted by $p(P_1, P_2, \ldots, P_{n_p})$, a metric is additive if: $c(p) = c(P_1, P_2) + \cdots + c(P_{i_p}, P_{i_p+1}) + \cdots + c(P_{n_p-1}, P_{n_p})$, multiplicative if: $c(p) = c(P_1, P_2) * \cdots * c(P_{i_p}, P_{i_p+1}) * \cdots * c(P_{n_p-1}, P_{n_p})$, and concave if: $c(p) = Max\{c(P_1, P_2), \ldots, c(P_{i_p}, P_{i_p+1}), \ldots, c(P_{n_p-1}, P_{n_p})\}$ or $Min\{c(P_1, P_2), \ldots, c(P_{i_p}, P_{i_p+1}), \ldots, c(P_{n_p-1}, P_{n_p})\}$. Metric order relation defines weighted comparison of paths leading to the next hop selection.

The following section presents the requirements for a routing protocol using a designed metric to operate correctly. These requirements can be expressed by the mean of PWS properties.

2.3.2 Requirements for the routing protocol using a designed metric

Applying a designed metric to a routing protocol cannot always guarantee the correct network operations. According to [152], in order to guarantee correct network operations, the routing protocol must satisfy three basic requirements: consistency, loop-freeness, and path-optimality. From the network model (see Definition 2.3.1), the routing requirements for a network can be formulated using PWS as follows:

Definition 2.3.2. *Routing requirements: consistency, loop-freeness, and path-optimality* [152].

- A routing protocol, R, is *consistent* if all paths discovered by R are *consistent*. For a path p discovered by R, assumed to contain n_p nodes, denoted by $p(P_1, P_2, \ldots, P_{n_p})$, p is *consistent* if for any P_{i_p}, $i_p \in \{1, \ldots, n_p - 1\}$ on path p, P_{i_p} must forward packets (sent from P_1 to P_{i_p}) to the next hop P_{i_p+1} on path p;
- A routing protocol R is *optimal* if R chooses the optimal path among all paths discovered by R, to route packets. Following PWS formulation, $(\mathscr{P}, \oplus, c, \preceq)$, the optimal path p_{min} from nodes X_s to X_d discovered by R, $p_{min} \in R(X_s, X_d) \subseteq \mathscr{P}$, is defined by: for any $p_k \in R(X_s, X_d) : c(p_{min}) \preceq c(p_k)$;
- A loop-free path p is defined by: for any $X_i, X_j \in H$, $i, j \in \{1, \ldots, n\}$ on path p, if $i \neq j$ then X_i is different from X_j. Loop-freeness is the most important requirement for a routing protocol.

Formally, these routing requirements are verified by considering *isotonicity* and *monotonicity* properties of PWS defined as follows:

Definition 2.3.3. *Isotonicity* and *monotonicity* properties [152].

According to [152], *isotonicity* is defined as: $\forall p,q,r \in \mathscr{P}$, quadruplet PWS $(\mathscr{P},\oplus,c,\preceq)$ is *left-isotonic*: if $c(p) \preceq c(q)$ then $c(r \oplus p) \preceq c(r \oplus q)$, or *right-isotonic*: if $c(p) \preceq c(q)$ then $c(p \oplus r) \preceq c(q \oplus r)$, or *strict-isotonic*: if it is left-isotonic and right-isotonic. *Monotonicity* is defined as: $\forall p,r \in \mathscr{P}$, quadruplet PWS $(\mathscr{P},\oplus,c,\preceq)$ is *left-monotonic*: if $c(p) \preceq c(r \oplus p)$, or *right-monotonic*: if $c(p) \preceq c(p \oplus r)$, or *strict-monotonic*: if it is left-monotonic and right-monotonic.

Important following lemma related to isotonicity and monotonicity, is presented from Sobrinho [127], Proposition 1 and reported by [152], Section III.B, for a hop-by-hop routing:

Lemma 2.3.1. *Sobrinho's Theorems* [127, 126, 152]

The *strict isotonicity* and *monotonicity* are sufficient for correct hop-by-hop routing based on optimal paths.

Proof. See [127], Proposition 1 and [152], Section III.B. □

Then, the necessary and sufficient conditions are relaxed by Yaling [152] for different protocols ([152], Table I). Since the chapter focuses on the specific RPL routing within a 6LoWPAN network, the Yaling's theorem [152] presented in Lemma 2.4.1 are used to establish the requirements related to PWS properties for RPL routing protocol. The following section recalls different methods involved in the metric composition approach.

2.3.3 Metric composition methods

To cover QoS requirements imposed by control applications while taking into account the characteristics and constraints of the underlying network, the routing protocol must adopt an appropriate routing metric [139]. Whereas primary standardized metrics could achieve a specific performance criterion, the combination of multiple primary metrics might lead to the optimization of various performance aspects [136, 155, 152]. The Gouda methods [37] addressed this combination question by defining two distinct approaches, namely *lexical metric composition* and *additive metric composition*.

Definition 2.3.4. *Metric composition methods* proposed by Gouda [37].

Following the formulation of quadruplet $(\mathscr{M},\oplus,c,\prec)$ defined in [37], two routing metric sets are considered: $(\mathscr{M}_1,\oplus_1,c_1,\prec_1)$ and $(\mathscr{M}_2,\oplus_2,c_2,\prec_2)$, where: $\prec_i$, $i \in \{1,2\}$ is an order relation over a set of metric values $\mathscr{M}_i$, $\oplus_i$ is the path (or link) cost aggregation operation and c_i is the function that maps a path (or a link) to a cost. A relation $\prec_{lex}$ over the set $\mathscr{M}_1 \times \mathscr{M}_2$ is called *a lexical composition* for the ordered pair $(\prec_1,\prec_2)$ if and only if, for every (m_1,m_2) and (m'_1,m'_2) in $\mathscr{M}_1 \times \mathscr{M}_2$, the following relation: $(m_1,m_2) \prec_{lex} (m'_1,m'_2) \Leftrightarrow (m_1 \prec_1 m'_1) \vee [(m_1 = m'_1) \wedge (m_2 \prec_2 m'_2)]$ is obtained. The additive composition relation $\prec_{add}$ over the set $\mathscr{M}_1 \times \mathscr{M}_2$ is defined as by: $(m_1,m_2) \prec_{add} (m'_1,m'_2) \Leftrightarrow (m_1+m_2) \prec (m'_1+m'_2)$.

The lexical metric combination intentionally provides a strict priority between inspected metrics and it is not necessary for the primary metrics to hold the same order relation. However,

in the case where the most prioritized metric is not equal (e.g., it is not associated with a limited set of integer values), the second-order metric will likely never be considered. The second approach, "additive metric combination", is more interesting when combining multiple metrics with the same order relation (either $\prec$ or $\succ$). This additive manner when combining multiple metrics allows tuning some performance criteria by using weight factors (e.g., α_i, $i \in \{1,2\}$ for the metric m_i). Nevertheless, it imposes the same properties for all considered metrics such as domain, aggregation rule, and order relation. Therefore, the primary routing metrics with different properties are usually transformed into *derived metrics* holding the same properties before combining them into an additive composite metric.

2.3.4 A composite routing metric

To design a composite metric based on a combination of multiple primary metrics, the works [155, 51, 136] have mentioned some issues to be considered for general applications. In particular, the composite metric must hold monotonicity and isotonicity properties (see Definition 2.3.3) so that the protocol achieves the consistency, loop-freeness and optimality properties (see Definition 2.3.2 and Lemma 2.3.1). Other concerns are about scalability, path stability, continuity (i.e., small variations in metric values must result in small variations in the composite metric value) [136, 155].

In the considered hybrid network, assuming that three routing metrics are used in combination to deal with some network QoS requirements of control applications aforementioned. All of these metrics are strict monotonic and strict isotonic. Then, they will be used in an additive composition. Given that the strict priority between these metrics does not seem absolutely necessary, the additive metric combination (presented in Section 2.3.3) is more appropriate.

Proposition 2.3.1. *A composite metric for the hybrid network.*

Based on the additive composition of primary metrics, the proposed composite metric is defined as follows:

$$m_h = \alpha_1 * m_1 + \alpha_2 * m_2 + \alpha_3 * m_3, \tag{2.1}$$

where: $\alpha_i \in \mathscr{R}, i \in \{1,2,3\}$ such that: $\alpha_i \in [0,1]$ and $\sum_{i=1}^{3} \alpha_i = 1$, and m_1, m_2, m_3 are the primary isotonic and monotonic metrics. Based on the composite metric definition, the cost of a path p is calculated as follows:

$$c_h(p) = \alpha_1 * c_1(p) + \alpha_2 * c_2(p) + \alpha_3 * c_3(p), \tag{2.2}$$

The metric m_h, defined by Eq(s). (2.1), is isotonic and monotonic. By Lemma 2.3.1, the hop-by-hop routing protocol using the metric m_h satisfies three routing requirements: consistency, loop-freeness and path optimality (see Definition 2.3.2).

Proof. According to the formulation of PWS quadruplet $(\mathscr{P}, \oplus, c, \preceq)$ (see Definition 2.3.1), three derived metrics can be represented as $(\mathscr{P}, \oplus, c_i, \preceq), i = \{1,2,3\}$. The function c_h (by Eq(s). (2.2))

that maps a path to a cost based on additive composite metric m_h, is defined as the addition of weighted terms c_i. From monotonicity and isotonicity properties of each metric m_i, $i \in \{1,2,3\}$, those are (by Definition 2.3.3): $\forall p,q,r \in \mathscr{P}$,

$$\begin{aligned}
\alpha_1 * c_1(p) &< \alpha_1 * c_1(r \oplus p) \\
\alpha_2 * c_2(p) &< \alpha_2 * c_2(r \oplus p) \\
\alpha_3 * c_3(p) &< \alpha_3 * c_3(r \oplus p) \\
c_h(p) = \sum_{i=1}^{3} \alpha_i * c_i(p) &< \sum_{i=1}^{3} \alpha_i * c_i(r \oplus p) = c_h(r \oplus p)
\end{aligned}$$

where: $0 \leq \alpha_i \leq 1$, and $\sum_{i=1}^{3} \alpha_i = 1$. Therefore, m_h is *left-monotonic*. Similarly, the *right-monotonicity* property is proved for the metric m_h. In the same manner, the costs of paths p,q,r are computed by Eq(s). (2.2) and the left-isotonicity property of each metric m_i, $i \in \{1,2,3\}$ deduce following inequalities:

$$\begin{aligned}
\alpha_1 * c_1(p) < \alpha_1 * c_1(q) \quad &\Rightarrow \alpha_1 * c_1(r \oplus p) < \alpha_1 * c_1(r \oplus q) \\
\alpha_2 * c_2(p) < \alpha_2 * c_2(q) \quad &\Rightarrow \alpha_2 * c_2(r \oplus p) < \alpha_2 * c_2(r \oplus q) \\
\alpha_3 * c_3(p) < \alpha_3 * c_3(q) \quad &\Rightarrow \alpha_3 * c_3(r \oplus p) < \alpha_3 * c_3(r \oplus q) \\
c_h(p) < c_h(q) \quad &\Rightarrow c_h(r \oplus p) < c_h(r \oplus q).
\end{aligned}$$

Therefore, m_h is *left-isotonic*. Similarly, *right-isotonicity* property: $c_h(p) < c_h(q) \Rightarrow c_h(p \oplus r) < c_h(q \oplus r)$ can be obtained for m_h. □

2.3.5 Challenges in the design of a composite metric

The diversity of network QoS requirements motivates the design of a composite metric to cope with routing problems in the hybrid network. However, the non-trivial composition method (e.g., linear composition) is challenging because of the strong difference of metric definitions, the complex computation of dynamic paths for wide-area network and fast adaptation in the routing decision [122]. It could lead to routing instability, non-optimal paths, increased latency, and packet loss due to small temporary loops [139, 136]. As discussed in [122], Section 4.2, the design of routing metrics plays an important role in (1) capturing specific characteristics of the target network; (2) optimizing some performance aspects; (3) having an impact on different routing protocol (causing the problems of instability, sub-optimality, loop creation); and (4) ensuring the use of consistent path calculation mechanisms.

Therefore, not all metrics can be used on any network. A particular case study is considered in Section 2.4 to demonstrate the metric composition approach to RPL routing adapted for NCSs. The process of composite metric design usually includes: (1) the selection of the primary metrics in order to preserve their routing properties; (2) the metric (re)quantification and derivation; (3) the composition of derived metrics; and finally (4) the demonstration with a routing protocol for consistency, loop-freeness and path optimality (see Definition 2.3.2).

2.4 Case study: Networked control systems using the RPL routing protocol

This chapter, especially focuses on the dynamic routing design for the hybrid network using 6LoWPAN technology. Routing problems of the hybrid network (e.g., the limited resources of nodes, how to route information in a multi-hop network, mesh topology frequently changed due to mobility, unreliable radio links, and specific application requirements) concern with both Internet and 6LoWPAN topologies [124]. Consequently, the routing design for hybrid network involves considering properties of nodes and wireless links to provide the QoS as expected by control applications. The hybrid network using 6LoWPAN technology can take advantage of RPL protocol for dynamic routing because they are specified by two closely linked IETF Working Groups (i.e., 6LoWPAN and ROLL) and RPL is specified for a low-power and lossy network [55, 145].

Background. *RPL routing: requirements, architecture, algorithms, and protocols* [145, 55].

From the IETF point of view, requirements of control applications as discussed above can belong to two categories: "industry" [RFC5673] (low power, high reliability, ease of installation and maintenance); and "building" [RFC5867] (auto-configuration, manageability). Terminologically, the constrained network in RPL context is also called "Low power and Lossy Networks" (LLN) [RFC7102]. In hybrid network, the dynamic routing is chosen to operate at the network layer (called "route-over" in [RFC6606], pp. 4-6) in order to make the link-layer transmission techniques transparent to IP and to profit by hop-by-hop forwarding decisions. The IETF ROLL WG is developing a potential solution for routing problem in LLN by defining a routing protocol, called "IPv6 Routing Protocol for LLN" (RPL) [RFC6550]. RPL is a proactive, distance-vector routing protocol (based on distributed Bellman-Ford algorithm and hop-by-hop forwarding), especially optimized for multi-point to point data flows. It cannot only operate on 6LoWPAN, but also on a large number of physical networks (refer to [RFC3819]). Functionally, it specifies how to build a "Directed Acyclic Graph" (DAG) containing all devices and routers using an objective function (OF), a metric set and some constraints. The DAG is itself composed of one or many sub-acyclic graphs, called "Destination-Oriented Direct Acyclic Graph" (DODAG). Each DODAG has a root (or *sink* node) representing a single point for external destinations. The RPL paths are usually optimized for packets to be transmitted through this sink node. A routing metric is typically based on the network information such as distance, bandwidth, network load, hop count, delay, maximum transmission unit (MTU), reliability and communications costs (see more in [139]).

The NCS hybrid network is considered as a class of network in which both the routers (i.e., intermediate nodes) and devices are constrained (i.e., LLNs). In hybrid network, the RPL protocol is appropriate to provide a unified routing mechanism whereby multipoint-to-point traffic (e.g., from sensors towards a controller) and the point-to-multipoint traffic (e.g., from a controller to the actuators or other controllers) are supported. Following Lemma considers the necessary and sufficient conditions for the RPL protocol to satisfy three routing requirements: consistency, loop-freeness, and path-optimality (see Definition 2.3.2).

Lemma 2.4.1. *Yaling's Theorems* [152] *refines the* Lemma 2.3.1.

The class of protocols based on distributed Bellman-Ford algorithm and hop-by-hop forwarding can find the shortest path if and only if the corresponding PWS is *left-isotonic* (see [152], Theorem 7). For these protocols to achieve consistent and loop-free routing, the necessary and sufficient conditions are that the PWS is *left-monotonic* (see [152], Theorem 8 and 9).

Proof. See [152], Section VI (and refer back to [127]). □

Functionally, the specification of RPL protocol can be interpreted using network model and PWS (Definition 2.3.1). Within an RPL instance, the *rank* (i.e., the best path cost) is defined as the approximate distance value of a node to the DODAG root. The *Objective Function (OF)* defines how to map one or more metrics and constraints into the path cost (i.e., path cost definition). Based on distributed Bellman-Ford algorithm solving the shortest path routing problem, a node will select its parent node with the smallest distance value to DODAG root (i.e., the order relation is minimum). For example, considering the nodes $X,Y,Z \in H$, and Y and Z are potential parent nodes of X, the distance values of the paths through Y and Z are calculated such that: $rank_X(viaY) = rank_Y + c(X,Y)$ and $rank_X(viaZ) = rank_Z + c(X,Z)$, where $c(X,Y)$ is a link cost from X to Y (i.e., the aggregation rule of path cost in this case is additive). If $rank_X(viaY) < rank_X(viaZ)$ then $rank_X = rank_X(viaY)$ and Y is the parent node of X. The re-definition of link cost can generate the inconsistent or non-optimal routing. Consequently, when the metric is redefined in order to satisfy QoS requirements, it is required to demonstrate that the RPL routing protocol continue to guarantee the consistency, loop-freeness, and path-optimality properties (see Definition 2.3.2). The process of metric re-definition encompasses the selection, re-quantification, derivation and composition of several primary metrics.

2.4.1 Metric selection

Based on static and/or dynamic metrics, paths can be calculated by routing algorithms using qualitative or quantitative methods [139, 136]. Many primary metrics have been proposed in [139] for LLNs to capture different network characteristics and to meet the application requirements as shown in Table 2.1. *These metrics should be redefined or differently re-quantified for specific applications as the way presented in this chapter.*

Table 2.1 Primary routing metrics proposed in [139] and redefined in Section 2.4.2.

Metric	Domain	Aggr. rule	Order rel.
Node state/attrib. (NSA)	undefined	undef.	undef.
Node energy (NE)	[0,1]	concave	minimum
Hop count (HP)	[1]	additive	minimum
Link Throughput	integer	concave	minimum
Link Latency	(0,+∞)	additive	minimum
Link Quality Level (LQL)	[0,7]	additive	maximum
Link ETX	[1,+∞)	additive	minimum
Link Color	integer	concave	minimum

As an example, some communication constraints (presented in Section 2.2.1) and operational criteria for BC control and supervision are concerned such as *the reliability of the paths* (e.g., when sending control signal to actuators), *low energy consumption* (as always with battery-powered devices) and *short average delay* (e.g., for information gathering or control sending) in data transmission. These criteria can infer the selection of three primary metrics from Table 2.1 such as *link Expected Transmission count (ETX), Node remaining Energy (NE)* and *Hop count of a Path (HP)* (as illustrated in Fig. 2.4 and summarized in Table 2.2). *None of these*

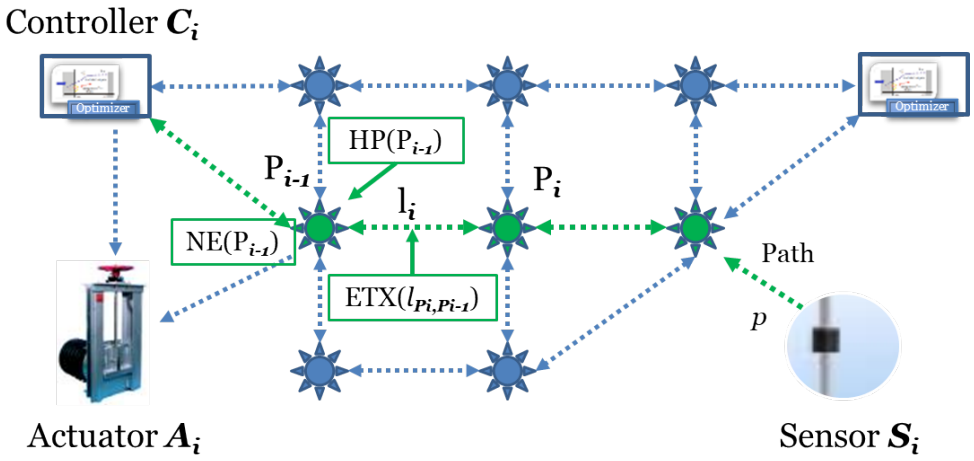

Fig. 2.4 An example of the data communication from level sensor S_i to controller C_i in the hybrid network: a path $p(S_i,\ldots,P_i,\ldots,P_1,C_i)$ is taken as an example. For a node P_i on the path p, the path cost from P_i to C_i is calculated by: $c(P_i,C_i) = c(P_i,P_{i-1}) + c(P_{i-1},C_i)$.

Table 2.2 An example of routing metrics used in NCS hybrid network.

Metric	Expected network performance
Node Energy (NE)	Network lifetime
Hop count (HP)	Network latency (also, energy consumption)
Link ETX (ETX)	Packet loss rate (also, transmission rate)

primary metrics by itself is suitable for use in the hybrid network to satisfy QoS requirements of control applications. Therefore, to achieve specific objectives of NCS using one homologous RPL instance, a composite metric (i.e., a weighted combination of primary metrics) should be considered. Besides, other approaches refer to the operations of RPL routing with multiple instances separately, each uses one primary metric for a specific data flow. Nevertheless, that needs the coordination of root nodes globally to do the unilateral allocation of instance identification (see more detail of RPL Instance IDs in [139]).

2.4.2 Metric quantification

For a routing problem using shortest path, the strong difference of metric domains, aggregation rules and order relations require the re-definition and derivation of the primary metrics in order to be used in composition method. The following Lemma is helpful for how to redefine a metric.

Lemma 2.4.2. *PWS properties of a metric* [51]

Any metric, (a) which is additive over the path; (b) provides a positive cost for any link, and (c) whose order relation is the "less than or equal" defined for real numbers, is strictly monotonic and strictly isotonic.

Proof. Following the PWS formulation $(\mathscr{P}, \oplus, c, \preceq)$ of an additive metric m, assuming that the path costs $c(p) > 0$, $c(q) > 0$ for any paths $p, q \in \mathscr{P}$, then $c(p \oplus q) = c(p) + c(q) > c(p)$ and $c(q \oplus p) = c(q) + c(p) > c(p)$. Therefore, the metric m is strictly monotonic by Definition 2.3.3. In the same manner, for any paths $p, q, r \in \mathscr{P}$ such that: $c(p) > 0, c(q) > 0, c(r) > 0$, we obtain: $c(p) < c(q) \Leftrightarrow c(p) + c(r) < c(q) + c(r) \Leftrightarrow c(p \oplus r) < c(q \oplus r)$ and $c(p) < c(q) \Leftrightarrow c(r) + c(p) < c(r) + c(q) \Leftrightarrow c(r \oplus p) < c(r \oplus q)$, By Definition 2.3.3, the metric m is strictly isotonic. □

Based on Lemma 2.4.2, the redefinition of selected primary metrics in Table 2.1 is necessary for obtaining (1) additive metrics over a path, (2) positive cost of any link, and (3) "less than or equal" order relations.

2.4.2.1 Link Expected Transmission Count (ETX)

In a control system, it is required that control signals must successfully reach the system actuators and the information exchanged between controllers must be accurate and stable. These requirements may be satisfied by imposing certain link reliability on the paths. As shown in Table 2.1, the primary metrics related to link reliability include Link Throughput, Latency, Quality Level and Expected Transmission Count (ETX). The easily measurable and adequate metric used in control application routing is *Link ETX*. It is commonly defined as the average number of transmissions (and re-transmissions) to successfully deliver a packet over a link. To avoid the complicated measurement and probability calculation, [51] proposed a Link ETX computation based on the number of packets delivered with or absence of acknowledgments (ACKs) (here, the control application is assumed to use the acknowledgment mechanism for link reliability). For a link l, the mathematical formula of *Link ETX* is given by:

$$ETX(l) = \frac{(transmitted\ packets)}{(packets\ with\ ACKs)} = \frac{(N_s + N_f)}{N_s}, \tag{2.3}$$

where N_s (and N_f) is the number of packets successfully delivered with acknowledgments (correspondingly, the absence of acknowledgments). A path of m links $l_i, i = \{1, \ldots, m\}$ has *Path ETX*: $ETX(p) = \sum_{i=1}^{m} ETX(l_i)$. Regarding the metric formulation (see Definition 2.3.1), the quadruplet PWS $(\mathscr{P}, \oplus, c, \preceq)$ represents a set of paths $\mathscr{P}$, capable of concatenation $\oplus$, the additive cost function c that maps the *link reliability properties* to Link ETX value, the order relation $\preceq$ is "less than or equal". As a result, the Objective Function related to Path ETX can be described as $min\{ETX(p)\}$, i.e., the best path is the one with a minimum value of Path ETX. Based on Lemma 2.4.2, this metric ETX is monotonic and isotonic.

2.4.2.2 Node remaining Energy (NE)

The energy issue is one of the most important concerns in control system due to the fact that a lot of devices are battery-powered and lack of regular maintenance (see Section 2.2.1). The nodes whose residual energy is lower than a threshold value, are disabled and create black-holes in the network unless certain redundancy is added to the network topology. In addition, the Link ETX metric discussed above usually provides for all data flow few similar paths which rapidly become congested. Concentrating data flow on mostly same paths results in energy exhaustion of nodes along the paths. The RPL protocol takes this issue into account by proposing another primary metric *Node remaining Energy (NE)* for path calculation algorithm. Many research works have considered different schemes such as node deployment, topology control, routing protocols, data reduction, duty/sleep schedule, etc. to provide a lowest energy-oriented path in routing selection (see [159, 1]). The energy-aware challenge is the complexity of a network that requires a dynamic constraint-based routing. Furthermore, there is no simple abstraction that adequately covers the broad range of power sources and energy storage devices used in existing LLN nodes such as mains-powered, primary batteries, energy scavengers, etc. The dynamic energy-aware metric is proposed by [139] as a useful percentage of remaining energy in *similar nodes*. The mathematical definition of this metric can be given in terms of measurable elements, either the energy or the power. In NCS example, assuming the current energy in battery E_{now} can be estimated, the remaining energy ratio of node X can be calculated by:

$$NE(X) = \frac{\textit{(initial energy)}}{\textit{(stored remaining energy)}} = \frac{E_0}{E_{now}}, \tag{2.4}$$

where E_0 is the initial energy of node battery. This metric is additive along the path, that is: for any path p of m nodes $X_i, i = \{1,\ldots,m\}$, $NE(p) = \sum_{i=1}^{m} NE(X_i)$. Regarding the metric formulation (see Definition 2.3.1), the quadruplet PWS $(\mathscr{P}, \oplus, c, \preceq)$ represents a set of paths $\mathscr{P}$, capable of concatenation $\oplus$, the additive cost function c that maps the *node energy properties* to NE value, the order relation $\preceq$ is "less than or equal". As a result, the Objective Function can be described as $min\{NE(p)\}$, i.e., the best path is the one with minimum Path remaining Energy. Based on Lemma 2.4.2, this metric NE is monotonic and isotonic.

2.4.2.3 Hop count of a Path (HP)

Many routing protocols use HP as a metric to report the number of traversed nodes along the path. It is also used as a constraint to indicate the maximum number of hops (i.e., hop limit) that a path may follow.

$$HP(X) = \textit{number of traversed nodes along a path } p \textit{ from } X \textit{ to root node}. \tag{2.5}$$

The control system considers this metric as a mean of time delay when a node desires to reach destination node rapidly. By minimizing the number of traversed nodes, the number of transmissions (but not re-transmission) is also reduced with equally expected link quality. As

a result, the total energy consumption or aggregation delay may be minimized. To formally represent HP metric, the quadruplet PWS $(\mathscr{P}, \oplus, c, \preceq)$ (see Definition 2.3.1) is used in the mapping of link cost c to 1 for any link. The path HP is equal to the number of links along the path. For example, the *Path HP* of a path p comprising m nodes (excluding source node) and also m links $l_i, i = \{1, \ldots, m\}$ is: $HP(p) = \sum_{i=1}^{m} c(l_i) = m$. The order relation $\preceq$ is "less than or equal", which is applied on the integer. The Objective Function can be described as $min\{HP(p)\}$, i.e., the best path is the one with minimum Path HP. Based on Lemma 2.4.2, this metric HP is monotonic and isotonic.

Remark 2.4.1. Three primary metrics (as quantified in Section 2.4.2) are strict monotonic and strict isotonic. So the Lemma 2.3.1 also holds.

Since the PWS left-isotonicity and left-monotonicity properties (here, strict isotonicity and monotonicity) of three primary metrics, above quantified, are guaranteed, the RPL routing protocol using separately one of these primary metrics will achieve the consistency, loop-freeness and path-optimality (by Lemma 2.4.1). These primary metrics with different properties (i.e., domains, aggregation rules, order relation) need to be transformed into derived metrics holding the same properties before combining them into an additive composite metric. The Table 2.3 shows the derived metrics suitable to be used for dynamic routing in the NCS hybrid network.

Table 2.3 Derived routing metrics used in NCS hybrid network.

Metric	Derived metric	Domain	Aggr. rule	Order rel.
Link ETX	(1 - 1/ETX)	[0,1]	additive	min.
Node energy	(1 - 1/NE)	[0,1]	additive	min.
Hop count	(1 - 1/HP)	[0,1]	additive	min.

Since monotonicity and isotonicity properties have been demonstrated with the use of primary metrics (as mentioned in Section 2.4.2), it is easy to deduce the same properties for their derived metrics in Table 2.3. Indeed, they are all additive, corresponding costs are positive, and order relations are "less than or equal", so they are all monotonic and isotonic by Lemma 2.4.2. Then, these derived metrics are used for the design of a composite metric.

2.4.3 Metric composition

Proposition 2.4.1. *A composite metric for the considered NCS hybrid network.*

Considering the NCS hybrid network as shown in Fig. 2.4, the composite metric m_h (see Eq(s). (2.1)) can be defined by combining three routing metrics in Table 2.3 as follows:

$$m_h = \alpha_1 * (1 - \frac{1}{ETX}) + \alpha_2 * (1 - \frac{1}{NE}) + \alpha_3 * (1 - \frac{1}{HP}), \tag{2.6}$$

where: $\alpha_i \in \mathscr{R}, i \in \{1,2,3\}$ such that: $\alpha_i \in [0,1]$ and $\sum_{i=1}^{3} \alpha_i = 1$.

For any path p of m links (and m nodes except the source node), the path cost $c_h(p)$ (see Eq(s). (2.2)) is calculated as follows:

$$c_h(p) = \alpha_1 * c_1(p) + \alpha_2 * c_2(p) + \alpha_3 * c_3(p), \tag{2.7}$$

where:

$$\begin{aligned} c_1(p) &= \sum_{i=1}^{m} c_1(l_i) = \sum_{i=1}^{m} (1 - \frac{1}{ETX(l_i)}), \\ c_2(p) &= \sum_{i=1}^{m} c_2(X_i) = \sum_{i=1}^{m} (1 - \frac{1}{NE(X_i)}), \\ c_3(p) &= \sum_{i=1}^{m} c_3(X_i) = \sum_{i=1}^{m} (1 - \frac{1}{HP(X_i)}). \end{aligned} \tag{2.8}$$

By Lemma 2.4.1, the RPL protocol using the composite metric m_h can achieve consistency, loop-freeness, and path-optimality (as defined in Definition 2.3.2).

The weight parameters (i.e., α_i) in Eq(s). (2.6) can be chosen to enable the relative importance of three metrics or to tune for the best performance criteria corresponding to the target network. For simulation, the following section presents a particular network benchmark using different (primary and composite) metrics with RPL protocol, which implements the distributed Bellman-Ford algorithm and hop-by-hop forwarding scheme.

2.5 Simulation results

2.5.1 Considered network topology

For the control of irrigation channels (see Fig. 2.1), the network topology is assumed to contain 144 nodes covering all possible communicating devices (e.g., water level or pressure meters, actuators, controllers) for a considered section of the BC irrigated field. These nodes are assumed homogeneous with the same power consumption scheme and transmission capacity (except unconstrained root nodes). They are scattered in the field of 2D-grid $1200mX1200m$ along channel section (including a part of mesh pressurized network). For simplicity, the topology is set up so that all nodes are horizontally and vertically aligned and equally distributed with a hop distance of $100m$. Their data exchange using wireless links operates in the range of $125m$ without obstruction. The channel capacity is set to maximum 255 bi-directional flows. Each node, assumed stationary in this example, is assigned the same integer for its identifier (ID) and network address.

A modeling and simulation framework, called J-Sim simulator (presented in [125]) is used in network simulations. An extension for RPL support in J-Sim (introduced in [51]) is based on the IETF specifications [RFC6550, version 17] and it operates on top of IEEE 802.11 standard as a link layer (MAC). Moreover, the integrated simulator also offers the capability of evaluating

some performance criteria while using a composite metric. The basic parameters for network simulation are summarized in Table 2.4.

Table 2.4 Basic network simulation parameters of the hybrid network.

Parameters	Setting value
Nodes	144 nodes on grid 1200m X 1200m
Communication range	125m in Tx/Rx, interference excluded
Layered protocols	FSP/UDP/RPL/802.11/PHY
Data packets/Size	620p/30B, 620p/50B, 1600p/30B
Energy model	1.6W Tx, 1.2W Rx, 1.15W Idle
Simulation time	6000s

2.5.2 Simulation scenarios

Simulations are performed with three root nodes (e.g., $n10$, $n5$, $n0$) representing the controller nodes equipped with Internet connection and power line. They receive data files comprising of 620 packets and 1600 packets (30 bytes/packet, and 50 bytes/packet) from 6 sensor nodes (e.g., $n122$, $n112$, $n104$, $n84$, $n75$, $n70$) by using File Service Protocol (FSP) in the application layer. This simple application protocol uses User Datagram Protocol (UDP) as the transport layer. The same network topology is used through all three scenarios in which the RPL protocol uses three instances with only one metric among ETX, NE, and HP at a time. Other scenarios are simulated with the designed composite metrics in different variations of weight parameters. In addition, another scenario with three different RPL instances, each uses a metric among ETX, NE, and HP, is investigated for performance comparison. The simulation lasts $6000s$ totally. The data flow from $n122$ to $n10$ were mainly observed as the reference flow in all scenarios to see what has been improved in terms of achieved performance while comparing different metrics (see Table 2.5).

Table 2.5 Some simulation scenarios for the dynamic routing with different metrics.

Controllers	n0	n5	n5	n5	n5	n10
Sensors/Actuators	n122	n112	n104	n84	n75	n70
Reference information flow	n122-n10					

2.5.3 Performance evaluation

The *percentage of packet loss* $(\%)$*, average latency* (ms)*, and network lifetime* (s) are considered as the performance criteria in this example. The packet loss ratio is computed from the number of packets that were dropped by lossy links (or buffer overflow) and a total number of emitted packets. The average latency is computed by the average of delays for a number of packets transmitted from the reference flow. Concerning power consumption, a node which is heavily traversed by data traffic (e.g., $n16$) is monitored. It is also the first node depleted from its

energy. Network lifetime is considered as network duration until 5% of nodes (i.e., about 8 nodes in this network topology) which get their energy depleted and therefore the network cannot fully guarantee its functionality. During the simulation of all scenarios above, three performance criteria have been evaluated and recorded (see Table 2.6). These results are then compared as illustrated in Fig. 2.6. They show that a composite metric can improve several performance criteria while primary metrics when used separately can only improve, but better, the corresponding performance criterion. For example, routing with only HP metric (first points $1.0HP$ in Fig. 2.6) gives the smallest latency ($21.79ms$), a consequent network lifetime ($2320.68s$), but increases in the packet loss ratio (about 60%) compared to other scenarios. The use of ETX metric in different compositions (e.g., $0.5HP+0.5ETX$,$0.2HP+0.3ETX+0.5NE$) can reduce the packet loss ratio to about 0% with a short latency and network lifetime. The presence of NE metric in composite metrics (e.g., $0.2HP+0.8NE$, $0.2HP+0.3ETX+0.5NE$) of different scenarios has distinctly improved the network lifetime to about 50% ($6000s$). As a result, by tuning around the weight parameters, the desired performance can be achieved for the designed hybrid network.

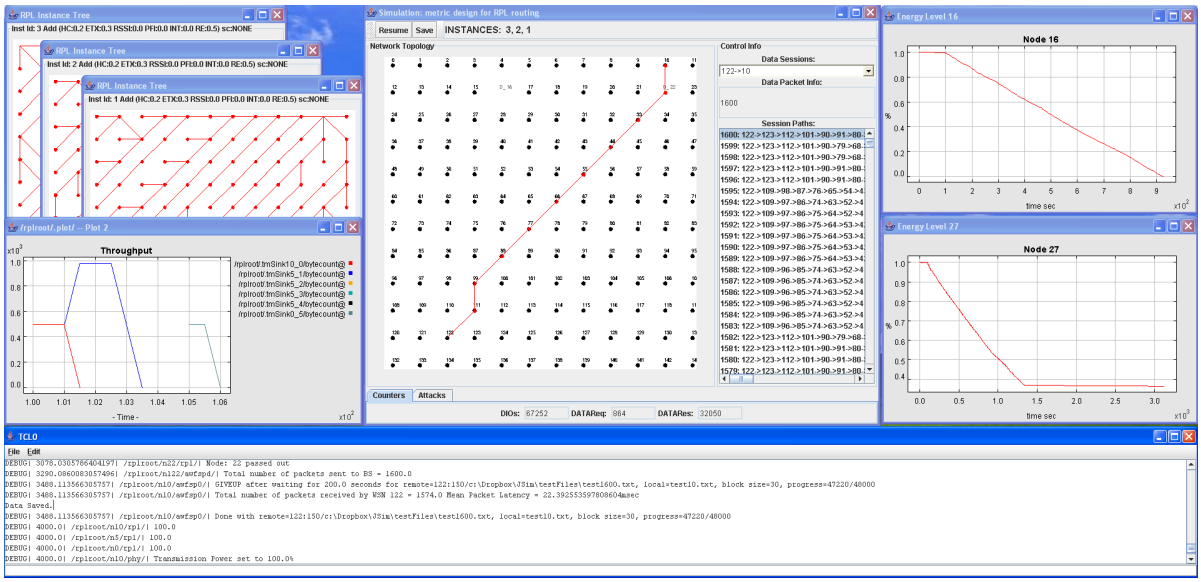

Fig. 2.5 Simulations using JSIM framework - Three RPL instances are used in network routing with mesh network topology.

Table 2.6 Simulation results of a hybrid network using a composite metric.

Metric	Packet loss (%)	Latency (ms)	Net. lifetime (s)
1.0HP	1060/1600=66.25	21.793497981029844	2320.6778962369626
1.0ETX	24/1600=1.50	21.719895608480915	2025.1918250257256
0.2HP+0.8NE	116/1600=7.25	24.184583240256114	6000
0.5HP+0.5ETX	24/1600=1.50	21.719895608480915	2025.1918250257256
0.2HP+0.3ETX+0.5NE	26/1600=1.63	22.392553597808604	6000
3 separate instances	1076/1600=67.25	21.88401692824656	2254.934818305747

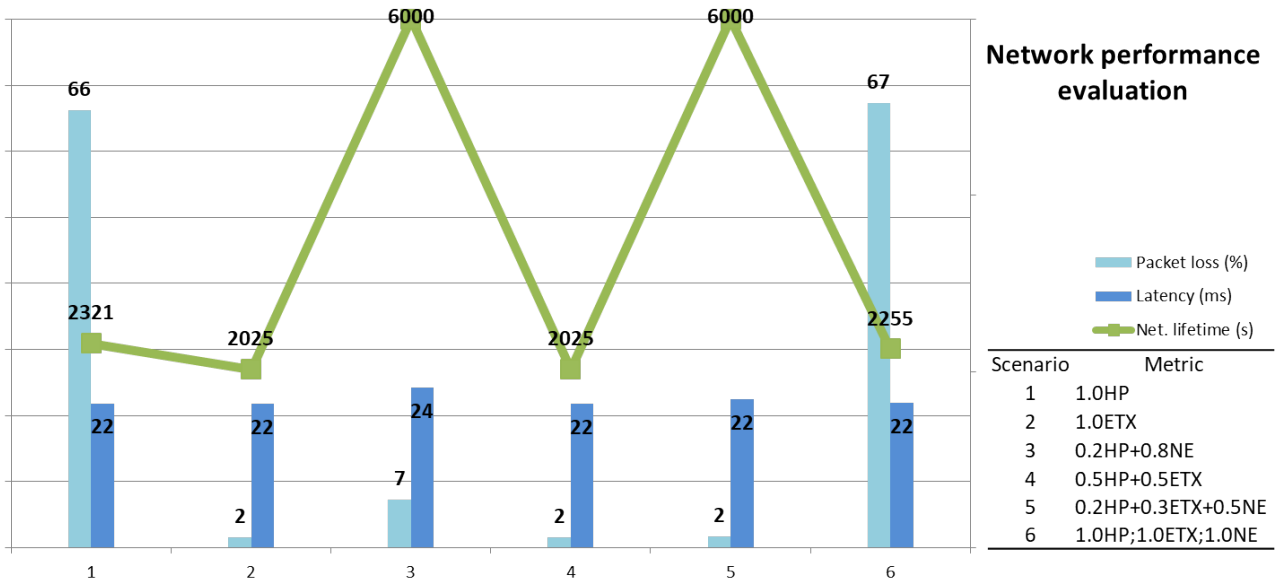

Fig. 2.6 Comparison of network performance criteria such as Packet Loss (%), Average Latency (ms), Network Lifetime (s) when using different metrics in RPL. Composite metrics are considered in different variations of weight parameters.

2.5.4 Results of other approaches

This section introduces some results of research works considering similar primary metrics (i.e., NE, HP, and ETX) or composite metrics in the RPL routing protocol. The work [16] defined a novel metric, namely "Lifetime and Latency Aggregateable Metric" (L2AM) for RPL routing protocol. It allows the RPL protocol to compute minimum path cost, based on a combination of both data reliability (defined by ETX) and node residual energy, thus to prolong the network lifetime. In the simulation scenario shown in [16], Fig. 3, RPL routing with L2AM metric reaches a network lifetime gain of 21% over RPL with ETX metric. Given the same overall degree of network reliability, the results from a wide variety of simulation scenarios show that L2AM clearly outperforms the standard ETX metric in terms of network lifetime. Whereas the work [17] proposed an energy-oriented routing mechanism to improve RPL routing protocol by incorporating ETX and residual energy metrics for path selection in LLN networks. The simulation result of the given scenario (see [17], Fig. 11) showed that the overall network lifetime for proposed routing algorithm increases about 12% compared to the standard RPL mechanism. The work [51] showed that by combining the Hop count metric and the node remaining energy with the additive composition approach, a significant energy savings (up to 16% for nodes participating in forwarding data from multiple data sections) can be reached without heavily compromising other performance criteria such as latency or packet loss. Interestingly, the work [49] designed and implemented a new objective function for RPL to optimize more than one network performance aspect using fuzzy-based routing metric combination. The example scenario used fuzzy inference system to combine ETX, delay, and node remaining power into one unique value. Experimental results of this work show that by using the composite metric with objective function, RPL routing obtains better results. These are for both network energy

distribution and packet reception rates (6.06% at throughput 12 packets/min), compared to the ETX scenario (9.40%). Another work [69] studied network lifetime maximization of wireless sensor networks through joint routing and sleep schedule. The proposed Iterative Geometric Programming (IGP) algorithm drastically outperforms the performance of optimal iterative separate routing and sleep scheduling method by an average of 29% over a large range of traffic rates. Compared to the design with optimal routing, but fixed sleep scheduling, the proposed IGP algorithm prolongs the lifetime by an average of 284%.

2.6 Conclusion

Through analytical demonstration and simulation results, this chapter has shown that several performance criteria related to QoS requirements of control applications, can be optimized for dynamic routing by using a metric composition approach. The additive combination method uses and derives some standard metrics characterizing the LLNs in order to preserve their routing properties. The designed composite metric also verifies the PWS properties guaranteeing the consistency, loop-freeness, and path optimality of the considered routing protocol. As a result, the design of a hybrid network for wide-area NCSs while taking into account the QoS requirements of control applications can be helped. Besides, it is necessary to emphasize that the QoS requirements in this chapter seem mild due to the context of control applications and the results are only shown by simulations. The practical networks with more complex characteristics, possibly produce different results. Nevertheless, the approach outlined in this chapter can be extended or replicated in other applications. The perspectives of this work aim to show the implementation of the designed composite metric in a practical network and obtain experimental results in order to validate the benefits of composition approach.

Chapter 3

Asynchronous information consensus in the distributed control of irrigation channels

In distributed model predictive control (DMPC), the global performance of the control system is improved by taking into account the interactions of subsystems, the coordination and/or the cooperation of controllers. For these tasks, the controllers need to exchange the information. However, the shared information may encounter some divergence due to time-varying topologies and communication issues. This chapter presents an approach to the challenges due to loss of the synchronization or imperfection in communication among controllers, by introducing an information consensus problem and an asynchronous consensus protocol. By exploring the information exchange topologies under proposed communication assumptions (e.g., directed graphs, connectivity, and asynchronism), we find the necessary and sufficient conditions for the information consensus to be reached asymptotically using the defined asynchronous protocol. The asynchronous consensus can then be integrated into the DMPC scheme so that the shared information among controllers asymptotically converges to the newest values after applying an action. The aim of this chapter is to (1) establish conditions for a class of "leader-followers" systems using an asynchronous linear protocol to asymptotically reach the consensus under fixed or time-varying directed communication topologies; (2) propose a global topology for "leader-switching" systems to satisfy the generalized consensus problems. For this purpose, the following sections present: (1) the definition of interaction variables incorporated into subsystem models and the information shared by controllers for coordination and cooperation (Section 3.2.2); (2) the formulation of a consensus problem with communication assumptions for the distributed control of irrigation channels (Section 3.3); (3) the design of an asynchronous protocol solving the consensus problem (Section 3.3.1); (4) the convergence analysis of the consensus processes (Section 3.3.3); (5) generalized consensus problems for a leader-switching system (Section 3.3.4). Through extensive simulation results, Section 3.4 demonstrates the benefits of the information consensus approach for the convergence problems of information states of all controllers once a controller applies an action to the subsystem.

3.1 Introduction

A fundamental concern in distributed model predictive control (DMPC) of large-scale systems is the coordination and/or the cooperation of groups of controllers to achieve better global performance [91, 96, 103, 86]. Some challenges of DMPC stem from the fact that the MPC method continuously uses the dynamic models of systems for the prediction of system outputs [9, 108]. An observation in such distributed control is that the interactions among subsystems influence not only local control decisions, but also the overall system optimality [130, 46, 86]. Therefore, in order to get better results for the global optimization, interaction variables involved in the prediction models need to be updated. The values of these variables are deduced from the neighbor states that are known only by exchanging information among controllers. For improving the control performance by neighboring cooperation, controllers might also share their objectives and/or constraints [88, 86]. In addition, controllers need to use some shared knowledge about state variables in order to coordinate their behaviors [86]. As a result, the efficient distributed control of a large-scale system requires that *all controllers have a consistent view of the shared information for the coordination, the cooperation or the consideration of subsystems' interactions* [114, 93]. The instantaneous values of shared information recorded by a controller are defined as its *information state*. Due to time-varying topology and communication issues (e.g., time delays, data packet dropouts, non-uniform sampling and quantization errors, missing and/or noisy measurements), controllers may lose the synchronization or may encounter updating problems for the shared information [43, 29]. Our approach to these problems is the so-called *information consensus problem* [106, 15, 112]. By integrating a consensus process into a control scheme, all controllers try to asymptotically reach a common knowledge on certain values of interest after executing an action that changes these variables. Even when neighboring controllers loss the direct communication, the interaction/coordination variables are still able to be updated with the benefit of consensus convergence. A *consensus protocol* comprises interaction rules specifying the information exchange among controllers over communication networks [111]. Moreover, it is impossible to fully synchronize all controllers in a large-scale control system. They cannot update their information states at the same time. Therefore, we focus on the information consensus in asynchronous mode [161, 59, 105, 34, 149, 82, 28]. First investigated in the field of computer science, especially in Multi-Agent Systems (MASs), consensus problems have recently attracted much attention in a large range of application areas in automatic control. Motivated by some pioneering works such as the simplified model of flocking [140], the coordination of mobile autonomous agents using nearest neighbor rules [47], and the theoretical framework for the analysis of consensus algorithms in multi-agent networked systems [93], many interesting works have been done for control applications (as surveyed in [142, 15, 114]). For instance, consensus problems can be found in two categories (classified by [111]): (1) formation control with application to multi-vehicle systems [109] or networked multiple mobile robot systems [123], or multi-unmanned aerial vehicle (UAV) systems [57]; and (2) non-formation cooperative control with application to role/task assignment, cooperative timing, cooperative search, payload transport and air traffic control [146, 135]. Whereas this

approach brings along numerous advantages over traditional control schemes, especially in networked control systems (NCSs) [72], challenges arise in the information exchange due to the imperfection in communication. For dealing with communication issues in a distributed NCS, many works have been investigated in system stabilization that sets some limitations in control performance when introducing communication constraints (see [61, 115, 116, 10] and references therein). The survey of recent progress in NCS, [153] have discussed various network conditions required for different control purposes (such as the minimum rate coding for stabilizability of linear systems in the presence of time-varying channel capacity, the critical packet loss condition for stability of the Kalman filter with intermittent observations, network topology for coordination of networked MASs, as well as event-based sampling for energy and communication efficiency). Another interesting overview on the theoretical development of NCSs under some challenging issues induced from communication networks is discussed in [157]. In recent years, there has been a renewed interest in consensus problems introduced in NCSs with communication constraints (see [76, 151, 141, 60, 74, 143, 114]). The consensus protocols presented in these works usually operate in a synchronous way. Although being relatively sparse, the asynchronous consensus of MASs has been discussed in some related works (e.g., [35, 105, 149, 28, 82, 5]). However, the updating problem of shared information (e.g., interaction among subsystems, coordination variables) among controllers considered as a consensus problem has been rarely discussed in the literature. As an example, the following sections will introduce a case study presenting DMPC scheme for irrigation channels and details of the associated consensus problem.

3.2 Distributed model predictive control of irrigation channels

We consider now an irrigation channel with multiple reaches interconnected through hydraulic control structures such as submerged gates, mixed gates and spillways (see Fig. 1.2). The irrigation channel is provided some local controllers implemented for the control of water flow at some points by adjusting the settings of control structures. In decentralized control schemes, these local controllers operate without being conscious of the presence of other controllers or subsystems. They compute the control action based only on local information without taking into account the information exchanged with other controllers. An observable drawback of such a decentralized control scheme is the reduced performance at a system-wide level due to unexpected and unanticipated interactions among subsystems by local controllers. For improving the global system performance, a distributed control is adequate in which controllers consider a negotiation, a coordination or a cooperation among them by exchanging the necessary information. An example of the DMPC scheme for the control of irrigation channels is given in Fig. 3.1. For the distributed control scheme, we observe that the computational complexity and theoretical properties (e.g., feasibility, stability and robustness) depend closely on the choice of the prediction model, control objectives, and constraints.

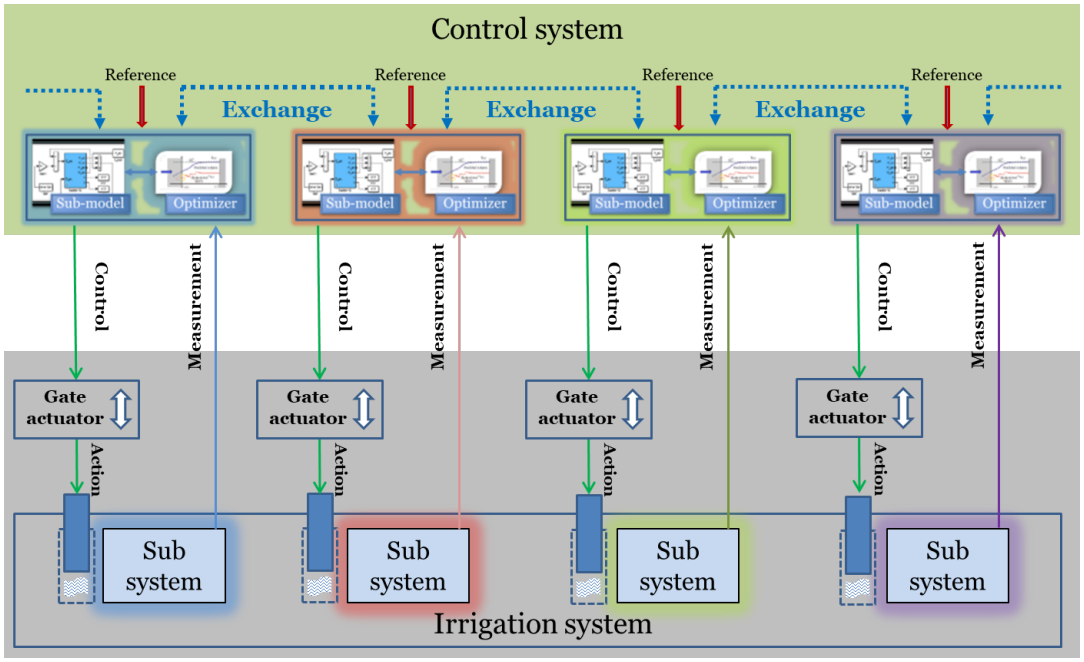

Fig. 3.1 A DMPC scheme for the control of irrigation channels.

3.2.1 Prediction model

The modeling of an irrigation channel using the LB method is introduced in Section 1.3.1. The dynamics of LB model are represented by Eq(s). (1.13) and rewritten as follows:

$$\begin{aligned} f_1(l,t+\Delta t) &= f_1(l,t)+\tfrac{1}{\tau}(f_1^e-f_1(l,t)) \\ f_2(l,t+\Delta t) &= f_2(l-v\Delta t,t)+\tfrac{1}{\tau}(f_2^e-f_2(l,t))-\tfrac{\Delta t}{2v}F \\ f_3(l,t+\Delta t) &= f_3(l+v\Delta t,t)+\tfrac{1}{\tau}(f_3^e-f_3(l,t))+\tfrac{\Delta t}{2v}F \end{aligned} \tag{3.1}$$

Accounting for the interactions of subsystems, the coordination or the cooperation of controllers requires the consideration of interaction variables or coordination variables from subsystem models. The following sections consider these variables suitable to be used for the coordination of controllers.

3.2.2 Definition and management of shared information

We consider here an irrigation channel comprising n reaches interconnected by the submerged gates (as shown in Fig. 3.2). The DMPC control of this system is divided over n controllers, $\{C_1, C_2, \ldots, C_i, \ldots, C_n\}$. The information shared by controllers is chosen depending on the control setting and system modeling. For example, as [86] adopted deterministic discrete-time linear integral delay models for channel control, the exchange of the flow rate at the downstream of each reach is sufficient for neighbor local controllers to compute actions because the inflow of downstream reach is equal to the outflow of upstream one. For our case study, we assume to use *the downstream configuration* (see Fig. 3.2) in which the control actions apply on the upstream gate of each reach $\textcircled{i}$, $i \in \{1,2,\ldots,n\}$ to adjust the gate opening, $\theta^{\textcircled{i}}$ (manipulated input), in order to regulate the downstream flow rate, $Q^{\textcircled{i}}$ (controlled variables). Some measurements are

assumed to be available such as the water heights at upstream, ($h_{us}^{\textcircled{i}}$), and downstream, ($h_{ds}^{\textcircled{i}}$), of each gate, the flow rate of water through a gate, $Q_g^{\textcircled{i}}$. To take into account the interactions among subsystems and the coordination of controllers, they need to share interaction variables. Using the prediction model Eq(s). (3.1) and the DMPC scheme shown in Fig. 3.3, we can easily identify that the necessary information exchanged by the neighbors of the controller $\textcircled{i}$ at control step k, denoted by $\chi_{in}^{\textcircled{i}}(\tau), \tau \in [k, k+1]$, contains: $\{f_1^{\textcircled{i-1}}(l_{L_{i-1}}, k), f_2^{\textcircled{i-1}}(l_{L_{i-1}}, k), f_3^{\textcircled{i+1}}(l_{us}, k)\}$. Thus, the management of the shared information needs to separate neighbor set $\mathcal{M}_i$ for each controller, C_i: $\mathcal{M}_i = \{C_{i_1}, C_{i_2}, \ldots, C_{i_{mi}}\}$ into upstream neighbor sub-set, $\mathcal{U}_i$, and downstream neighbor sub-set, $\mathcal{D}_i$. For simplicity, the information shared by controller C_i to its neighbors at time τ is chosen as: $\chi_{out}^{\textcircled{i}}(\tau) = [f_3^{\textcircled{i}}(l_{us}, \tau) \;\; f_1^{\textcircled{i}}(l_{L_i}, \tau) \;\; f_2^{\textcircled{i}}(l_{L_i}, \tau)]^T$. In inputs, the controller C_i receives the information shared by its neighbors at time τ as follows: $\chi_{in}^{\textcircled{i}}(\tau) = [\chi_{in|C_{i_1}}^{\textcircled{i}}(\tau) \;\; \chi_{in|C_{i_2}}^{\textcircled{i}}(\tau) \ldots \chi_{in|C_{i_{mi}}}^{\textcircled{i}}(\tau)]^T$. We observe that the gate equations (Eq(s). (4.4)) permit the computation of these interaction variables, once the neighbor controllers share the flow rate through the gate at their position. Therefore, the flow rate through each gate ($Q_g^{\textcircled{i}}$) is an appropriate variable to be used for coordination among controllers. The coordination variables, $Q_g^{\textcircled{i}}$, are considered in this chapter as the shared information for the consensus problem (see Fig. 3.4). In a control system of n controllers, $\{C_1, C_2, \ldots, C_i, \ldots, C_n\}$, the information vector of the controller C_i is defined by: $\chi^{\textcircled{i}} = [\chi_1^{\textcircled{i}} \;\; \chi_2^{\textcircled{i}} \;\; \ldots \;\; \chi_n^{\textcircled{i}}]^T$, where: $\chi_j^{\textcircled{i}} = Q_{g_j}^{\textcircled{i}} \in \mathbb{R}$ is the flow rate through gate j recorded by the controller C_i (see the example in Fig. 3.6). Other variables can appropriately be used as coordination or cooperation variables depending on distributed control schemes (an example of the cooperation of controllers is given in Chapter 4), but the corresponding consensus problems can be solved in the same manner. Timing for sharing information depends on the synchronization mechanism and the coordination method. The following section investigates the consensus while controllers exchange the information for coordination in an asynchronous way.

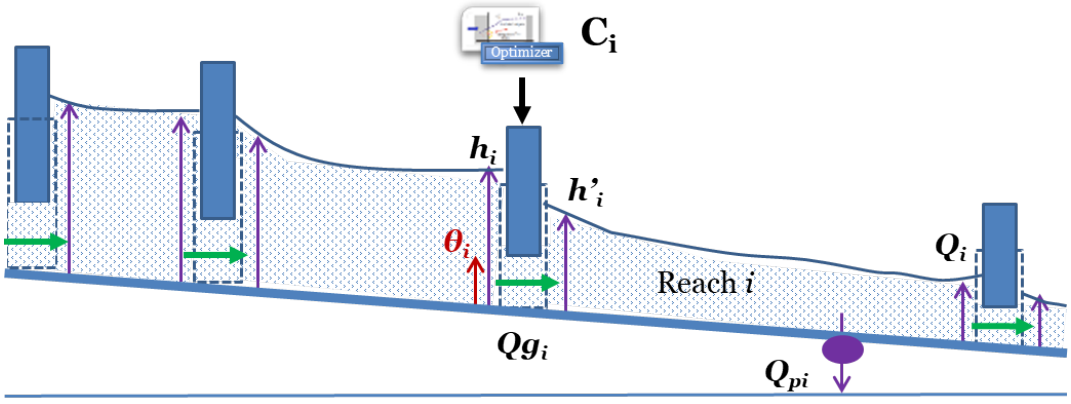

Fig. 3.2 A downstream configuration for the distributed control of an irrigation channel. The controller C_i is implemented for the control of water flow Q_i at the downstream end of a reach i by adjusting the opening θ_i of the gate at the upstream end.

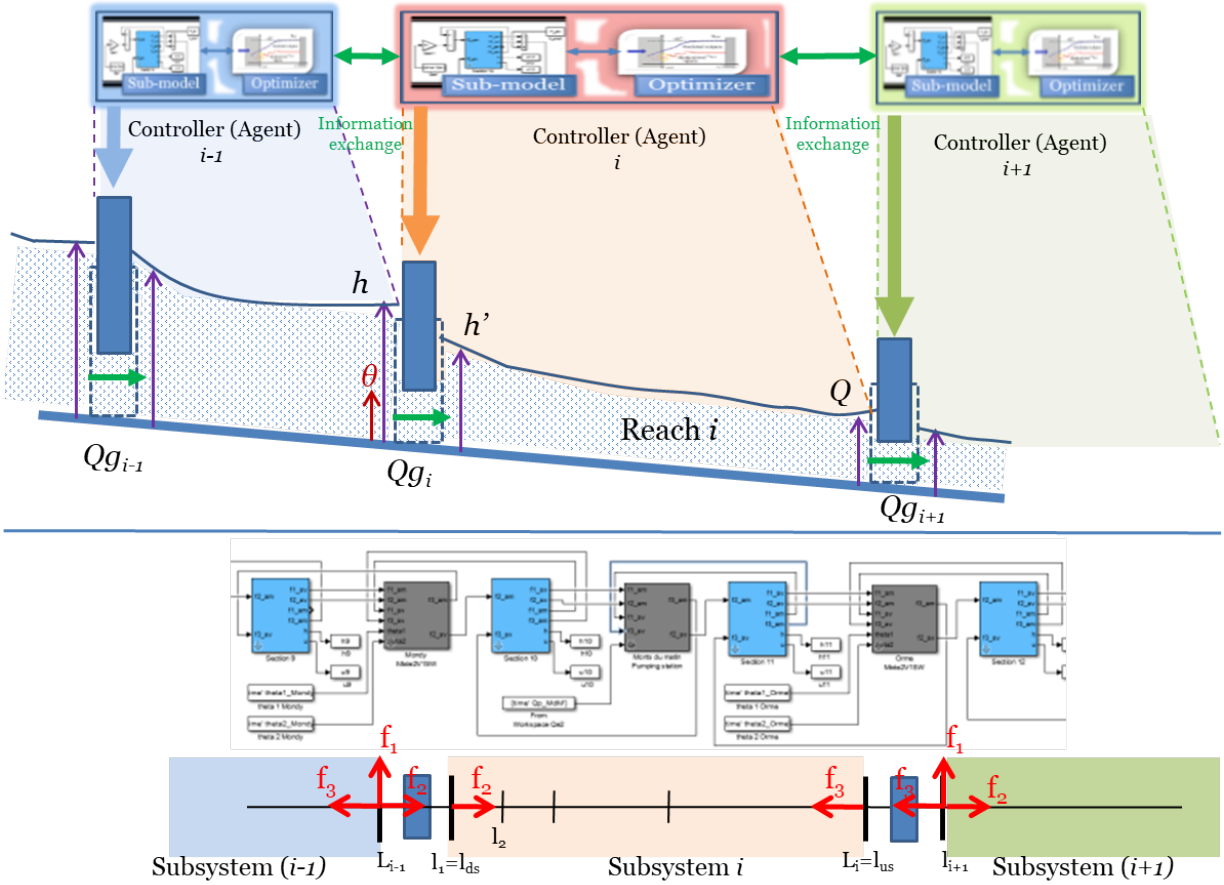

Fig. 3.3 An example of DMPC scheme in which the controllers share interaction variables ($\{f_1(l_{L_{i-1}},k), f_2(l_{L_{i-1}},k), f_3(l_{us},k)\}$) at time k for action computation.

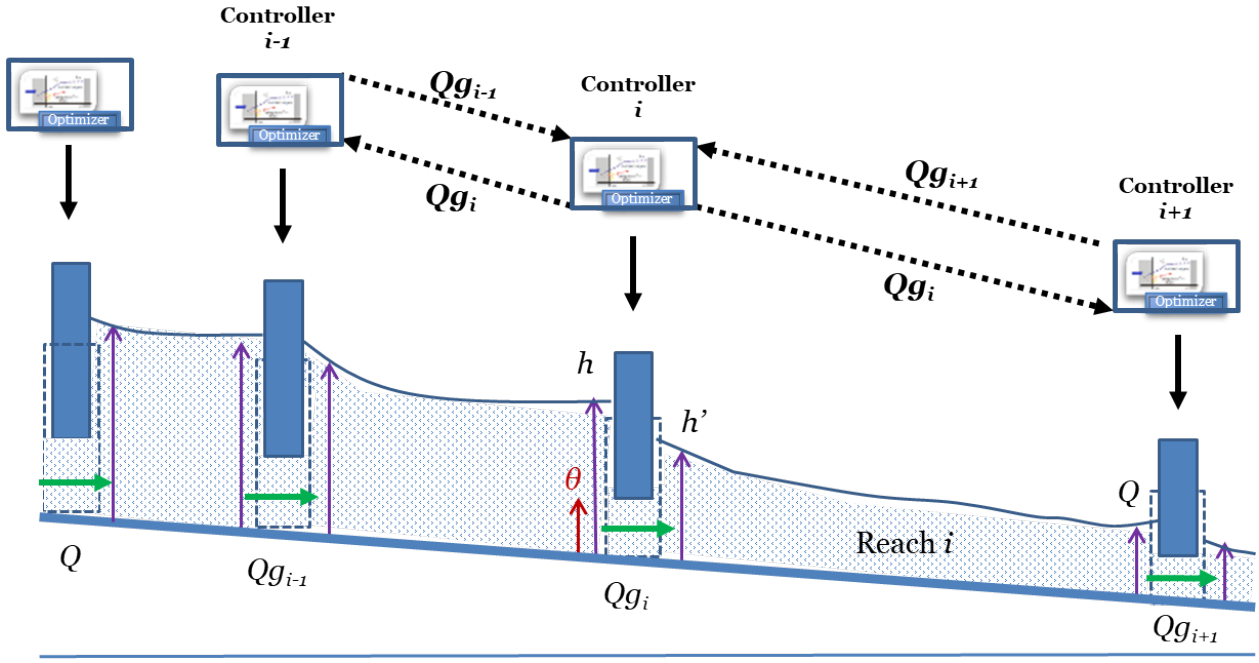

Fig. 3.4 An example of DMPC scheme in which the controllers share flow rates through their gates (Q_g) for coordination.

3.3 Asynchronous information consensus in distributed control of irrigation channels

The efficient distributed control of irrigation channels requires that all controllers have to exchange, coordinate and cooperate towards optimizing global objectives. In our distributed control scheme, each controller proceeds with (1) collecting the information from its neighbors; (2) updating the information state; (3) computing control actions according to control laws; (4) applying the control actions; (5) sharing and performing the consensus process for the convergence of the shared information among all controllers (as illustrated in Fig. 3.5). The controllers designed in this manner, are very close to the concept of agents [147]. Indeed, they possess limited capabilities of information gathering, processing skills, and actions. They also have communication capability and perform the coordination and/or the cooperation based on the information exchanged among them [99, 86]. Due to communication issues, controllers may encounter a divergence in the shared information, which can result in unexpected actions. We approach the problem of divergent information shared by controllers (i.e., agents) by *an information consensus problem* [43, 113, 28]. The information consensus guarantees that controllers sharing information over an unreliable and dynamically changing network topology, have a consistent view of critical information for coordination and cooperation tasks [113]. This problem is then solved by using *a consensus protocol* designed to achieve the convergence of *information states of controllers*. In DMPC scheme, the consensus process can be integrated into the control algorithms in a receding fashion in order to provide most updated values needed for adequate action computation. In addition, our MAS-like control system is characterized by some *asynchronism features* (as listed in [28]) such as:

1. each controller operates according to its own clock;
2. no guarantee on delivery time or successful delivery;
3. the exchange topology is time-dependent.

Therefore, the consensus problem is investigated in this chapter using an asynchronous framework. An overview of basic concepts of consensus problems in MASs and asynchronous consensus protocols for maintaining system stability property is presented in [58, 105, 34, 149, 28]. Under proposed asynchronism assumptions, [28] introduced a theoretical mapping in which models of synchronous and asynchronous MASs with various communication patterns (such as directed and delayed communication) can be addressed in the same framework. The work [105] is concerned with the asynchronous consensus problem of discrete-time second-order MAS under dynamically changing communication topology, in which the asynchrony means that each controller detects the neighbors' state information to update its information state by its own clock. Under a fixed topology, [58] studied the convergence conditions for asynchronous consensus problems in multi-agent systems such that the asynchronous consensus value converges to the synchronous consensus value. In recent years, there has been a tremendous amount of renewed interest in leader-follower configurations [31, 71, 121, 2, 151, 160, 33]. Based on the standard topologies (graphs) of information flow, these systems can be viewed as single-

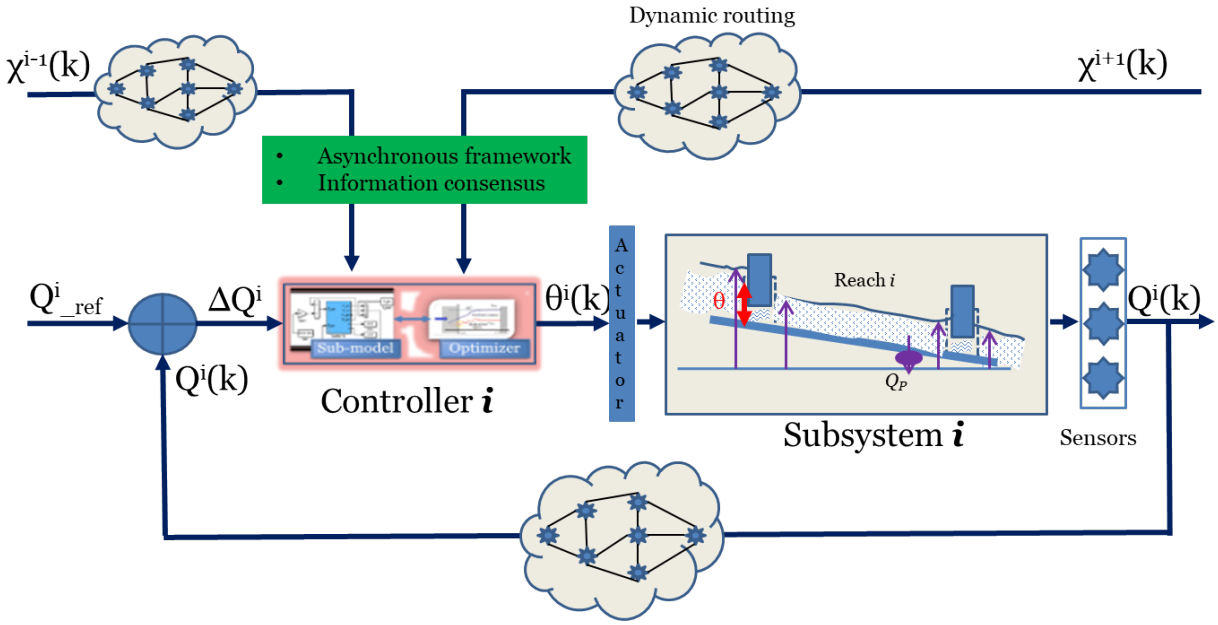

Fig. 3.5 Approach to the problem of divergent information shared among controllers by an information consensus problem. This problem is then solved by an asynchronous consensus protocol designed to achieve the convergence of information states of controllers.

leader–multiple-followers systems [149]. This chapter follows a rather different approach, called *the asynchronous information consensus for a leader-switching system*. In this system, the leader role of a controller is not fixed and chosen depending on the instant of an event in the system provoking a change in information states of the controllers. Solving this problem requires the design of an asynchronous consensus protocol such that the information states of all controllers eventually converge to the newest values once a controller (which becomes a leader) applies an action that changes the values of these variables. For example, the control system of irrigation channels switches the leader when a controller applies an action on a gate that changes the system inputs and consequently, the output, Q_g, is also changed. In consequence, the information states of all controllers need to be updated (an example is shown in Fig. 3.6). Henceforth, we use an asynchronous framework for the design and the performance analysis of consensus protocol possibly implemented in coordinated controllers.

3.3.1 Problem statements for asynchronous discrete-time system

From MAS point of view, our control system is characterized as a discrete-time system, in which the information flow among controllers is directed and the communication topology may be time-dependent (also called *switching topology*) [94]. As the subsystem states change over time, each controller attempts to reach an agreement with others on some values deduced from their states. We formulate a consensus problem for the agreement of all controllers by introducing the information states of controllers. *The information state vector of a controller records the instantaneous values of the information shared by all controllers and itself.* The asynchronous consensus protocol is eventually investigated to solve the convergence of information states to the newest values as shared by its neighbors (an example is presented in Fig. 3.6). By

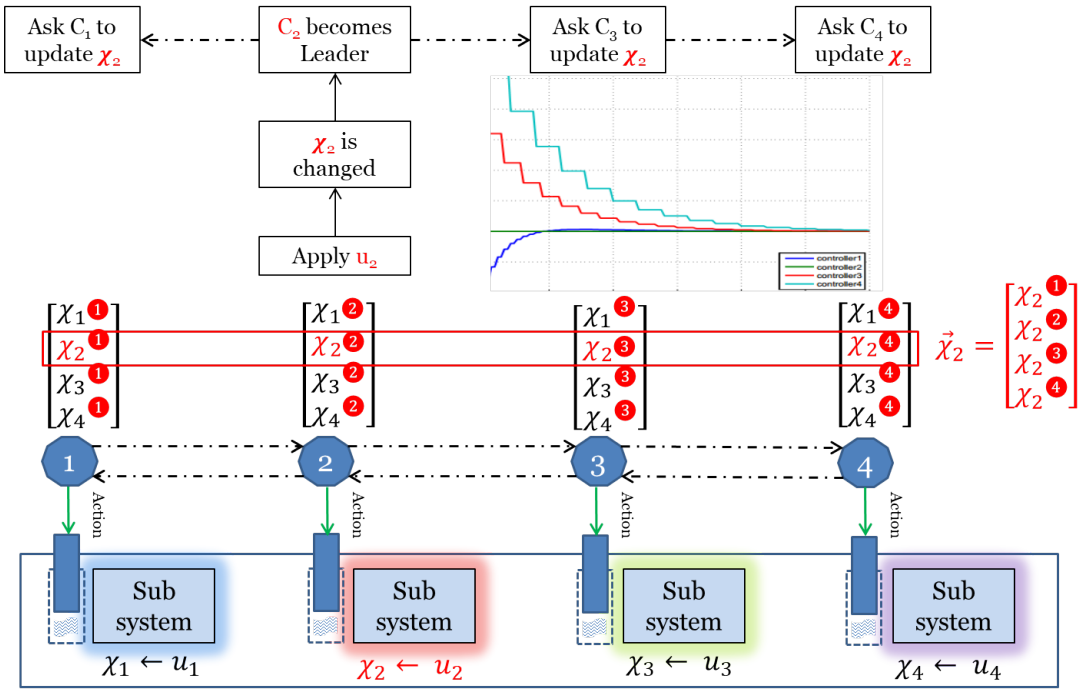

Fig. 3.6 An example of consensus problem in distributed control of irrigation channels is used to illustrate the asynchronous information consensus of the leader-switching system. In this example, the controller, C_2, applies a computed action, u_2, to the subsystem, which changes the value of its information state, χ_2. C_2 actually becomes the leader. The consensus process is started by C_2 for providing the convergence of information element χ_2 of all controllers.

accomplishing the consensus processes, the information state vectors of all controllers must contain the same values asymptotically. In this chapter, we are interested in the consensus problem of an asynchronous discrete-time MAS-like system under fixed or time-varying topology in the presence of communication issues such as time delays [15, 111].

Assumptions 3.3.1. *Regularity assumptions* [28].

The convergence analysis of asynchronous consensus process requires making some communication assumptions (introduced in [28], Section II as regularity assumptions) such as:

1. any delay is bounded (see [94], section X.A for quantitatively bounded delay), only a finite number of updating instants can occur within any finite time interval;

2. a controller does not fail to be updated or is updated infinitely often;

3. all controllers can access their own states and at least one of these controllers can achieve it without delay.

The basic idea for a consensus protocol design is to impose similar dynamics for updating information states of all controllers [113]. Solving a consensus problem consists in designing an update law so that the information states of all controllers converge to common values.

We consider a control system of n controllers, $\mathcal{C} = \{C_1, C_2, \ldots, C_i, \ldots, C_n\}$, indexed using an index set $\mathcal{N} = \{1, 2, \ldots, n\}$. The information state of controller C_i, $i \in \mathcal{N}$, is defined as: $\chi^{ⓘ} = [\chi_1^{ⓘ} \ \chi_2^{ⓘ} \ \ldots \ \chi_n^{ⓘ}]^T$. All controllers share a common state space $\chi^{ⓘ} \in \mathbb{R}_{n\times 1}$. Let $t_0 <$

$t_1 < \cdots < t_a < \ldots$ be event-based discrete-time instants [151, 60] when an event (e.g., applying an action) occurs in the control system provoking a change in information states of controllers. We assume that, at the time instant t_a, the controller C_i applies the control action which changes the information state: $\chi^{\textcircled{i}}(t_a)$. The controller C_i becomes then the actual leader and starts the consensus processes executed on other controllers (i.e., followers) so that the change is updated in their information states. The updating instants for asynchronous information exchanged among controllers are denoted by $\tau_0 < \tau_1 < \cdots < \tau_u < \ldots$. By accomplishing the consensus process, the consensus vector defined as:

$$\chi(\tau) = [\chi^{\textcircled{1}}(\tau) \ \ldots \ \chi^{\textcircled{i}}(\tau) \ \ldots \ \chi^{\textcircled{n}}(\tau)]^T = [\chi_i^{\textcircled{1}}(\tau) \ \ldots \ \chi_i^{\textcircled{i}}(\tau) \ \ldots \ \chi_i^{\textcircled{n}}(\tau)]^T \tag{3.2}$$

converges to the same value $\chi^{\textcircled{i}}(\tau_0) = \chi_i^{\textcircled{i}}(t_a)$ for all elements. An example of the asynchronous framework used for the convergence of the information exchanged among controllers is illustrated in Fig. 4.5, which shows different time instants and intervals.

For the control system, we consider a *localized consensus protocol* [28], in which each controller updates its information state using latest-known state values of its neighbors and itself such that [94]:

$$\chi^{\textcircled{i}}(\tau_{u+1}) = \chi^{\textcircled{i}}(\tau_u) + \lambda u^{\textcircled{i}}(\tau_u) \tag{3.3}$$

where: $\lambda > 0$ is step-size and $u^{\textcircled{i}}(\tau_u)$ is a linear consensus protocol defined by:

$$u^{\textcircled{i}}(\tau_u) = \sum_{j=1}^{n} A_{ij}(\chi^{\textcircled{j}}(\tau_u) - \chi^{\textcircled{i}}(\tau_u)) \tag{3.4}$$

in which $A_{ij},\ i,j \in \mathcal{N}$ represents neighboring information flow (i.e., the magnitude of $A_{ij}(\tau)$ can represent time-varying relative confidence of the controller C_i in the information shared by the controller C_j at time τ or the relative reliability of information exchange links between them).

Using the protocol Eq(s). (3.4), the dynamics of discrete-time consensus process Eq(s). (3.3) while $\lambda = 1$ can be described by:

$$\begin{aligned}
\chi^{\textcircled{i}}(\tau_{u+1}) &= \chi^{\textcircled{i}}(\tau_u) + \sum_{j=1}^{n} A_{ij}(\chi^{\textcircled{j}}(\tau_u) - \chi^{\textcircled{i}}(\tau_u)) \\
&= (1 - \sum_{j=1, j\neq i}^{n} A_{ij})\chi^{\textcircled{i}}(\tau_u) + \sum_{j=1, j\neq i}^{n} A_{ij}\chi^{\textcircled{j}}(\tau_u) \\
&= A_{ii}\chi^{\textcircled{i}}(\tau_u) + \sum_{j=1, j\neq i}^{n} A_{ij}\chi^{\textcircled{j}}(\tau_u) = \sum_{j=1}^{n} A_{ij}\chi^{\textcircled{j}}(\tau_u)
\end{aligned} \tag{3.5}$$

where, we set $A_{ii} = (1 - \sum_{j=1, j\neq i}^{n} A_{ij})$.

Whereas numerous asynchronous models have been proposed and successfully applied to some practical problems [53, 32, 8], the asynchronous model proposed in [129] is one of the prevalent models in asynchronous theory [28]. According to [129, 28], the time-varying topology and communication delays can be integrated into the asynchronous consensus protocol 3.4, for

updating information states of a controller C_i, as follows:

$$\chi^{\textcircled{i}}(\tau_{u+1}) = \begin{cases} \sum_{j=1}^{n} A_{ij}(\tau_u)\chi^{\textcircled{j}}(\tau_u - d_{ij}(\tau_u)), & i \in S(\tau_u) \\ \chi^{\textcircled{i}}(\tau_u), & otherwise \end{cases} \tag{3.6}$$

where: for $i, j \in \mathcal{N}$, $\chi^{\textcircled{i}}(\tau_0)$ is initial information state of controller C_i; $A_{ij}(\tau)$ is neighboring information flow between controllers C_i and C_j and $A_{ii} = (1 - \sum_{j=1, j\neq i}^{n} A_{ij})$; $d_{ij}(\tau)$ are time-varying communication delays; $S(\tau)$ is the set of already updated controllers at the instant τ. The Eq(s). (3.6) is also called the asynchronous consensus protocol in the literature [28].

The matrices $\mathcal{A}(\tau) = [A_{ij}(\tau)]$ are *non-negative stochastic matrices*, which have an eigenvalue equal to 1 and a corresponding eigenvector equal to $1_n = [1\ 1\ \ldots\ 1]^T$, that is: $\mathcal{A}(\tau)1_n = 1_n, \forall\tau$. The matrices $\mathcal{A}(\tau)$ represent the *time-varying communication topologies* of the control system and are principally explored in the convergence analysis of the asynchronous consensus problem.

The global information consensus is asymptotically achieved for all controllers when the information states of all controllers tend to the initial value of the actual leader. Assuming that the leader is C_i: $\chi^{\textcircled{i}}(\tau_0) = \chi_i^{\textcircled{i}}(t_a)$ and for any initial values of followers: $\chi^{\textcircled{j}}(\tau_0), (j \neq i)$, the asymptotic achievement of the consensus means:

$$\forall j \in \mathcal{N}, \qquad ||\chi^{\textcircled{i}}(\tau) - \chi^{\textcircled{j}}(\tau_0)|| \to 0, \quad \text{as } \tau \to \tau_{+\infty}. \tag{3.7}$$

Formally, the Assumptions 3.3.1 used in the convergence analysis of asynchronous consensus can be formulated as follows:

Assumptions 3.3.2. *Communication assumptions* [129, 28].

1. $0 \leq d_{ij}(\tau) \leq D_{max} \leq +\infty, \forall i, j \in \mathcal{N}, \forall\tau$, where: D_{max} is a constant (regulated delays);
2. $\bigcup_{\tau=\tau_c}^{+\infty} S(\tau) = \mathcal{C}, \forall\tau_c$ (admissible updating sets);
3. $A_{ii} > 0, \forall i \in \mathcal{N}$, and $\exists i \in \mathcal{N} : d_{ii}(\tau) = 0, \forall\tau$;
4. $\chi^{\textcircled{i}}(\tau_0) > 0, \forall i \in \mathcal{N}$ to avoid considering the trivial consensus point $[0\,0\ldots0]$.

Under the Assumptions 3.3.2, we investigate the reachability of a consensus while the information exchange among controllers is in asynchronous mode. Concretely, we search the conditions for information states of controllers to converge to the consensus point, depending on the initial state of the root node. Normally, asynchronous consensus points are determined depending on the set of updated controllers, delays, and initial states of controllers [28]. The convergence analysis is based on the properties of the matrix $\mathcal{A}$ representing the communication topologies of the control system.

3.3.2 Preliminaries

Communication topology of MAS-like systems can be represented by a directed graph (called *digraph*). In a digraph, each node corresponds to an agent (i.e., a controller) and each edge

represents an available communication channel. Based on algebraic graph theory, matrix theory, and control theory, we discuss the convergence of asynchronous consensus protocol in networks of dynamic agents with fixed and time-varying topology. Following definitions and results are useful for solving the asynchronous consensus problem.

Definition 3.3.1. *Background on graph theory* (see more detail in [113, 94])

The information exchange among agents in MAS is modeled by a weighted directed graph, $\mathcal{G}(\mathcal{C},\mathcal{E},\mathcal{A})$, of order n, where:

- $\mathcal{C} = \{C_1, C_2, \ldots, C_n\}$ is a finite non-empty set of n nodes (i.e., agents), indexed using an index set $\mathcal{N} = \{1, 2, \ldots, n\}$;
- $\mathcal{E} \subseteq \mathcal{C}\mathrm{x}\mathcal{C}$ is a set of edges (e.g., ordered pairs of nodes $e_{ij} = (C_i, C_j), i, j \in \mathcal{N}$, representing a unidirectional information exchange link from C_i to C_j);
- $\mathcal{A} = [A_{ij}]$ is an adjacency matrix defined with non-negative elements $A_{ij} \geq 0, \forall i, j \in \mathcal{N}$ and $A_{ij} > 0$ if and only if $e_{ji} = (C_j, C_i) \in \mathcal{E}$;
- the neighbor set $\mathcal{M}_i$ of a node $C_i \in \mathcal{C}$ is defined by $\mathcal{M}_i = \{C_j \in \mathcal{C} \mid e_{ji} = (C_j, C_i) \in \mathcal{E}\}$.

Due to dynamic information flow among agents, the time-varying digraph, $\mathcal{G}(\tau)$, represents the communication pattern at a time τ. All possible graphs defined for a group of n agents can be denoted by: $\tilde{\mathcal{G}} = \{\mathcal{G}_1, \mathcal{G}_2, \ldots, \mathcal{G}_m\}$, where: m, the cardinality of $\tilde{\mathcal{G}}$, is a finite number. The union of a set of p graphs, $\{\mathcal{G}_{g_1}, \mathcal{G}_{g_2}, \ldots, \mathcal{G}_{g_p}\}$, each graph has a node set $\mathcal{C}$ of n elements, is a graph $\breve{\mathcal{G}}$ comprising the same node set $\mathcal{C}$ and the edge set equal to the union of edge sets of p graphs. Some graph properties involved in the convergence analysis of asynchronous consensus, are defined in [44, 15, 93, 113, 28] as follows:

- A digraph, $\mathcal{G}$, is *strongly connected* if there is a directed path from C_i to C_j and also a directed path from C_j to C_i for any pair of distinct nodes $C_i, C_j \in \mathcal{C}$;
- *A spanning tree* of a digraph is a tree formed by graph edges connecting all nodes of the graph. The digraph $\mathcal{G}$ has *a rooted directed spanning tree* if and only if $\mathcal{G}$ has at least one node (called root node) with a directed path to all of the other nodes;
- The *graph associated with a matrix* $\mathcal{A} \in \mathbb{R}_{n\times n}$, denoted by $\mathcal{G}_A$, is a digraph on n nodes C_i, $i \in \mathcal{N}$, such that there is a directed edge in $\mathcal{G}_A$ from C_j to C_i if and only if $A_{ij} > 0$ for any pair of nodes $C_i, C_j \in \mathcal{C}$.

Definition 3.3.2. *Background on non-negative matrix theory* (see more detail in [44, 83])

Let $\mathbb{R}_{n\times n}$ $(n > 1)$ be a set of all $(n \times n)$ real matrices and $\mathcal{N} = \{1, 2, \ldots, n\}$ be an index set. A matrix $\mathcal{A} = [A_{ij}] \in \mathbb{R}_{n\times n}$ is:

- *non-negative*, denoted by $\mathcal{A} \geq 0$, if all of its components are non-negative real numbers, that is: $A_{ij} \in \mathbb{R}, A_{ij} \geq 0, \forall i, j \in \mathcal{N}$ ([44], Definition 6.2.17);
- *(row) stochastic* if sum of elements of each row is unity, that is: $\sum_{j=1}^{n} A_{ij} = 1$, $\forall i \in \mathcal{N}$ ([44], Definition 8.7);

- *irreducible* or *indecomposable* if $\mathcal{A}$ cannot be conjugated into block upper triangular form by a permutation matrix ([44], Definition 6.2.22). By [44], Theorem 6.2.24, the matrix $\mathcal{A}$ is irreducible if and only if $(I_n + |\mathcal{A}|)^{n-1} > 0$ or its associated graph $\mathcal{G}_A$ is strongly connected;

- *primitive* if $\mathcal{A}$ is irreducible and $\mathcal{A}$ has a unique nonzero eigenvalue of maximum modulus ([44], Definition 8.5.0). By [44], Theorem 8.5.2, the matrix $\mathcal{A}$ is primitive if and only if $\mathcal{A}^k > 0$, for some natural number $k \in \mathbb{N}^+$. By [44], Corollary 8.5.8 (Wielandt), the non-negative matrix $\mathcal{A}$ is primitive if and only if $\mathcal{A}^{n^2-2n+2} > 0$.

The eigenvalues of a real square matrix $\mathcal{A}$ are complex numbers that make up the spectrum of the matrix. The exponential growth rate of the matrix powers $\mathcal{A}^k$ as $k \to +\infty$ is controlled by the eigenvalue of $\mathcal{A}$ with the largest absolute value (spectral radius $\rho(\mathcal{A})$).

The Perron–Frobenius (P-F) theorem describes the properties of the leading eigenvalue and the corresponding eigenvectors when $\mathcal{A}$ is a non-negative irreducible matrix as follows:

Theorem 3.3.1. *Perron–Frobenius theorem for non-negative irreducible matrices* ([44], Theorem 8.4.4 and [83], Chapter 8)

Let $\mathcal{A} \in \mathbb{R}_{n\times n}$ be a non-negative irreducible matrix with spectral radius $\rho(\mathcal{A}) = f$, also called *P-F eigenvalue*. The following statements hold:

- f is a *positive, real* number, algebraically *simple* eigenvalue of $\mathcal{A}$.

- There is a unique positive real vector $\mathbf{r} = [r_i] \in \mathbb{R}_{n\times 1}$ such that: $\mathcal{A}\mathbf{r} = f\mathbf{r}$ (i.e., $\mathbf{r}$ is *right P-F eigenvector* corresponding to P-F eigenvalue f).

- There is a unique positive real vector $\ell = [l_i] \in \mathbb{R}_{n\times 1}$ such that: $\ell^T\mathcal{A} = \ell^T f$ (i.e., ℓ is *left P-F eigenvector* corresponding to P-F eigenvalue f).

- Cesàro averages ([44], Theorem 8.6.1)

$$\lim_{k\to+\infty} \frac{1}{k} \sum_{i=0}^{k} \frac{\mathcal{A}^i}{f^i} = \mathbf{r}\ell^T \tag{3.8}$$

  where: ℓ and $\mathbf{r}$ are the left and right P-F eigenvectors of $\mathcal{A}$ corresponding to the P-F eigenvalue f (i.e., $\mathcal{A}\mathbf{r} = f\mathbf{r}$ and $\ell^T\mathcal{A} = \ell^T f$) and are normalized so that $\ell^T\mathbf{r} = 1$.

- If $\mathcal{A}$ has exactly p distinct eigenvalues of maximum modulus, then $\mathcal{A}$ is similar to $e^{2\pi ik/p}\mathcal{A}$ for each $k = 0, 1, \ldots, (p-1)$ and the maximum-modulus eigenvalues of $\mathcal{A}$ are $e^{2\pi ik/p} f$, each has algebraic multiplicity 1 ([44], Theorem 8.4.6).

Based on Theorem 3.3.1, the following results state the convergence of a primitive matrix.

Lemma 3.3.1. ([44], Lemma 8.5.4) If $\mathcal{A} \in \mathbb{R}_{n\times n}$ is a non-negative irreducible matrix and all its main diagonal elements are positive, then $\mathcal{A}^{n-1} > 0$, and by definition, $\mathcal{A}$ is primitive.

Lemma 3.3.2. ([44], Theorem 8.5.1 and Lemma 8.5.5) If $\mathcal{A} \in \mathbb{R}_{n\times n}$ is a non-negative and primitive matrix with spectral radius $\rho(\mathcal{A}) = f$, the vectors $\mathbf{r}$ and ℓ are respectively right and left P-F eigenvectors corresponding to P-F eigenvalue f, then:

- $\mathcal{A}^k$ is non-negative and primitive for every integer $k \geq 1$
- $$\lim_{k \to +\infty} (\frac{\mathcal{A}}{f})^k = \mathbf{r}\ell^T \tag{3.9}$$

  where the matrix $\mathbf{r}\ell^T$ is spectral projection, called *P-F projection*, corresponding to P-F eigenvalue f.

Corollary 3.3.1. ([44], Theorem 8.5.1) If $\mathcal{A} \in \mathbb{R}_{n \times n}$ is a non-negative, stochastic and primitive matrix (NSP) with spectral radius $\rho(\mathcal{A}) = f = 1$, the vectors $\mathbf{r} = 1_n$ and ℓ are respectively right and left P-F eigenvectors corresponding to P-F eigenvalue $f = 1$, then:

$$\lim_{k \to +\infty} \mathcal{A}^k = 1_n \ell^T \tag{3.10}$$

Based on these fundamental results of the graph and matrix theories, we discuss in the next section the convergence conditions for asynchronous systems presented in Section 3.3.1.

3.3.3 Convergence analysis of the asynchronous information consensus

The communication topologies play a key role in consensus problems [71]. This section explores the communication topologies to derive appropriate conditions for the convergence of an asynchronous consensus process. Considering an asynchronous consensus protocol in the information exchange among controllers may break down the convergence properties obtained with the synchronous communication [58, 28]. By introducing the Assumptions 3.3.2, we demonstrate that the asynchronous consensus protocol guarantees the stability property (i.e., the convergence of information states). The results about the consensus problems of synchronous and asynchronous systems may be found in the literature (e.g., [15, 114, 93, 111, 28, 110, 128]). These results are related to the distributed coordination, distributed optimization, formation control, cooperative control and consensus problems of MAS-like systems (e.g., multiple mobile robotic systems, unmanned aerial vehicles, automated highway systems, satellite clusters) in which all agents reach a consensus asymptotically when their states converge to a common value. As stated in Section 3.3.1, we are henceforth interested in the communication topologies represented by non-negative stochastic matrices.

For the stability of asynchronous systems, the following results are fundamental to give a direction for the convergence analysis of asynchronous consensus process.

Lemma 3.3.3. *Fixed point of asynchronous system* ([28], Lemma 1, [129], Theorem 1 and [75]).

Let the communication topology is fixed for the asynchronous system represented by Eq(s). (3.6), that is: $\mathcal{A}(\tau) = [A_{ij}(\tau)] = \mathcal{A}$, $\forall \tau$. The fixed point of asynchronous system Eq(s). (3.6) is asymptotically stable under the class of regular asynchronism (Assumptions 3.3.2) if the spectral radius, $\rho(\mathcal{A})$, of non-negative matrix $\mathcal{A} = [A_{ij}]$, is less than unity.

Remark 3.3.1. Based on Lemma 3.3.3, if $\mathcal{A}$ does not have an eigenvalue equal to 1 and $\rho(\mathcal{A}) > 1$, there exists an initial state $\chi^{\textcircled{i}}(\tau_0)$ and a sequence $d_{ij}(\tau) \leq 1,\ i, j \in \mathcal{N}$, such that the Eq(s). (3.6) does not converge ([129], Theorem 2).

Therefore, the necessary conditions for the convergence of asynchronous iterations are $\rho(\mathcal{A}) < 1$ [129] and $\rho(\mathcal{A}) = 1$ for specific cases [101, 75, 28]. The following lemmas provide further results.

Lemma 3.3.4. *The convergence for a non-negative irreducible matrix* ([28], Lemma 2 and [129]).

Let consider the asynchronous system Eq(s). (3.6) characterized by the non-negative irreducible matrix $\mathcal{A}$, which has the spectral radius, $\rho(\mathcal{A}) = 1$ and the corresponding right eigenvector, $\mathbf{r}$, that is: $\mathcal{A}\mathbf{r} = \mathbf{r}$. Under the Assumptions 3.3.2, there exists a bounded positive constant $C \in \mathbb{R}$ such that: $\chi(\tau) \to Cr$, as $\tau \to \tau_{+\infty}$, where the value of C depends on $\mathcal{A}$, $\chi(\tau_0)$, $S(\tau)$, $d_{ij}(\tau)$.

Following the Lemma 3.3.4, the information states $\chi(\tau)$ converge to $C1_n$ when $\mathbf{r}$ is similar to 1_n. Tight lower and upper bounds for the constant C are given in [75]. Assuming that there is a link from each node to itself (as mentioned in Assumptions 3.3.2), the diagonal elements of $\mathcal{A}$ are positive, the following lemma approaches the convergence based on the properties of the matrix $\mathcal{A}$ with positive diagonal elements, the associated graph $\mathcal{G}_A$ and Perron–Frobenius theorem (see Theorem 3.3.1).

Lemma 3.3.5. *Unique eigenvalue with a maximum modulus of a matrix and the associated graph has a spanning tree* ([110], Lemma 3.4).

- If a non-negative matrix $\mathcal{A} = [A_{ij}] \in \mathbb{R}_{n\times n}$ has the sum of each row equal to the same positive constant $f > 0$, then f is an eigenvalue of $\mathcal{A}$ with a corresponding right eigenvector 1_n, such that: $\mathcal{A}1_n = f1_n$ and the spectral radius $\rho(\mathcal{A}) = f$.
- The eigenvalue f of $\mathcal{A}$ has algebraic multiplicity equal to 1, if and only if the graph associated with $\mathcal{A}$, $\mathcal{G}_A$, has a spanning tree.
- If the graph $\mathcal{G}_A$ associated with $\mathcal{A}$, has a spanning tree and $A_{ii} > 0$, then f is the unique eigenvalue with maximum modulus.

The Lemma 3.3.5 can derive the following results for an NSP matrix.

Corollary 3.3.2. *Unique eigenvalue equal to* 1 *of a non-negative stochastic matrix with positive diagonal elements* (see Lemma 3.3.1, Lemma 3.3.2, and [28], Lemma 3).

Let $\mathcal{A} = [A_{ij}] \in \mathbb{R}_{n\times n}$ be a non-negative stochastic matrix with positive diagonal elements. The following statements hold:

- $\mathcal{A}$ is primitive, so $\mathcal{A}$ is NSP.
- $\lim_{k\to+\infty} \mathcal{A}^k = 1_n\ell^T$, where: $k \in \mathbb{N}^+$, 1_n and ℓ are right and left P-F eigenvectors corresponding to P-F eigenvalue 1, that is: $\ell^T\mathcal{A} = \ell^T$, and are normalized such that: $\ell^T 1_n = 1$.

- The graph $\mathcal{G}_A$ associated with $\mathcal{A}$, has a spanning tree, if and only if 1 is the unique eigenvalue of $\mathcal{A}$ with maximum modulus.

The results in Corollary 3.3.2 summarize the conditions for the convergence of asynchronous systems based on the communication topology represented by an adjacency matrix. We distinguish two cases of the communication topology.

3.3.3.1 The consensus of asynchronous one-leader-multiple-followers systems under fixed communication topology

We consider now the first case in which the topology is fixed, and consequently, the matrix $\mathcal{A}(\tau) = [A_{ij}(\tau)] = \mathcal{A}$, $\forall\tau$. Based on the convergence results of synchronous systems [15, 113, 93, 110], and Corollary 3.3.2, we derive the conditions for the convergence of asynchronous consensus process as follows:

Theorem 3.3.2. *The consensus of asynchronous systems under fixed communication topology* ([28], Theorem 2, [129], Theorem 11, and [101], Section 4).

For the asynchronous system Eq(s). (3.6) with fixed communication topology represented by a non-negative stochastic matrix $\mathcal{A}$ and under the Assumptions 3.3.2, the global consensus Eq(s). (3.7) is asymptotically reachable if and only if the graph $\mathcal{G}_A$ associated to $\mathcal{A}$, has *a unique spanning tree rooted by the specified root node*.

Proof. ($\Leftarrow$) Based on Lemma 3.3.4 and the Assumptions 3.3.2, demonstrating that the asynchronous system Eq(s). (3.6) can achieve global consensus asymptotically, is equivalent to show that:

- $\chi(\tau) \to C1_n$, as $\tau \to \tau_{+\infty}$
- $C = \chi_i^{\textcircled{i}}(\tau_0) = \chi_i^{\textcircled{i}}(t_a)$

Indeed, $\mathcal{A}$ is a non-negative stochastic matrix with positive diagonal elements, the Corollary 3.3.2 shows that the matrix $\mathcal{A}$ is NSP and $\lim_{p\to+\infty}\mathcal{A}^p = 1_n l^T$, where: 1_n and ℓ are the right and left eigenvectors corresponding to the eigenvalue 1. By Lemma 3.3.4 and the Assumptions 3.3.2, the information states converge $\chi(\tau) \to C1_n$, as $\tau \to \tau_{+\infty}$. In other words, the asynchronous system Eq(s). (3.6) asymptotically achieves the global consensus. The graph $\mathcal{G}_A$ associated with $\mathcal{A}$, has a unique spanning tree rooted by the specified root node (i.e., C_i in this case), so the information states of all nodes asymptotically converge to the initial state of the root node, that is: $C = \chi_i^{\textcircled{i}}(\tau_0) = \chi_i^{\textcircled{i}}(t_a)$.

($\Rightarrow$) When the asynchronous system Eq(s). (3.6) asymptotically achieves the global consensus, we suppose that the graph associated with the matrix $\mathcal{A}$ does not have a spanning tree. By Corollary 3.3.2, the algebraic multiplicity of eigenvalue 1 of $\mathcal{A}$ is $m_1 > 1$. The Perron–Frobenius theorem (see Theorem 3.3.1) ensures that $\mathcal{A}^p$ is similar to $e^{2\pi ik/m_1}\mathcal{A}$ and $tr\mathcal{A}^p = e^{2\pi ik/m_1} tr\mathcal{A}^p$. Since $e^{2\pi ik/m_1}$ is real and positive only if k is an integer multiple of m_1, this is impossible if $\mathcal{A}$ has any positive main diagonal entry and k is not divisible by m_1. Therefore, the graph associated with the matrix $\mathcal{A}$ has a spanning tree. If the spanning tree is not unique and rooted by the specified root node, the information state $\chi(\tau)$ converges to a

consensus point, depending on the computation (i.e., depending on initial states of controllers, the delays, and update sets). A counterexample is given in [28], Example 1. □

With regards to the synchronous case, the consensus points of the asynchronous system are normally different depending on the computation (i.e., depending on the set of updated controllers, delays, and initial states) [28]. Especially, information states of all the nodes asymptotically converge to the initial state of the root node when the interaction graph has a unique rooted spanning tree.

3.3.3.2 The consensus of asynchronous one-leader-multiple-followers system under time-varying communication topologies

The following theorem provides the convergence results in the second case where the communication topologies are time-varying. The topologies change in a control system while communication links between controllers may be unreliable due to disturbances, loss and/or subject to communication range limitations.

Theorem 3.3.3. *The consensus of asynchronous systems under time-varying communication topologies* ([27], Theorem 2.3, [85], Proposition 1, and [110], Theorem 3.3).

Consider a dynamic graph $\mathcal{G}(\tau) \in \breve{\mathcal{G}}$, representing the information exchange among n controllers at the time τ. The time-varying weight $A_{ij}(\tau)$ of each edge belongs to a finite set of arbitrary positive numbers $\breve{b}$. The asynchronous discrete-time consensus protocol defined in Eq(s). (3.6) achieves the convergence (Eq(s). (3.7)) asymptotically if and only if there exists an infinite sequence of uniformly bounded, non-overlapping time intervals $[\tau_u, \tau_{u+1}), u \geq 0$, starting at $\tau_0 = 0$, and across each such interval, the union of interaction graphs has a spanning tree rooted at the specified root node.

Proof. The Theorem 3.3.3 is a particular case of [27], Theorem 2.3, [85], Proposition 1, or [110], Theorem 3.3 with one spanning tree routed by the specified root node. Different proof techniques are proposed in these works. See more detail in [27], Theorem 2.3 □

In brief, the Theorem 3.3.3 shows that asynchronous information consensus under time-varying communication topologies can be asymptotically achieved if the union of directed interaction graphs has a spanning tree frequently enough in the evolution of consensus process. From the asynchronous point of view, the same synchronous system under the time-varying topologies may be mapped to different asynchronous systems with different spanning trees [28]. Therefore, the consensus point depends on the sequence of the spanning trees in the course of the computations (e.g., as stated in Lemma 3.3.4, the constant C is computationally dependent).

3.3.4 Generalized consensus problems in a leader-switching system

In this section, we study the consensus problems of discrete-time leader-switching systems with fixed topologies representing a distributed control system. The notions of “leader” and “follower” roles are extensively used in broad applications related to MAS, such as leader–follower control,

leader-following consensus, leader-follower synchronization and leaderless coordination [160, 71, 121, 2]. In the asynchronous control system, a controller can play two roles alternatively, that is a leader or a follower, or both simultaneously in different consensus processes. The actual leaders are the controllers that determine the ultimate information state of the control system. For the structural decomposition of MAS-like systems, [150] proposed leaders-followers configurations and established the necessary and sufficient conditions for an agent to be a leader and for the convergence of consensus problems. The global system performance is commonly related to the interactions among controllers ([94], Theorem 8).

In previous sections, we have proposed an asynchronous consensus protocol Eq(s). (3.4) and established the necessary and sufficient conditions for this protocol to solve a consensus problem (Theorem 3.3.2) in the single-leader–multiple-follower configuration [150]. The convergence results are based on the communication topologies considered as standard topologies. To accomplish the updating of the information vector of a controller defined in Section 3.2.2, different consensus processes are involved in the control system characterized as a leader-switching system. Therefore, we need the global topology so that different consensus processes of the whole control system converge (evidently, to different consensus points). Based on common characteristics of these consensus processes and the combination of standard topologies, the global topology can be designed for the convergence of all consensus processes.

Consider a control system of n controllers, $\mathcal{C} = \{C_1, C_2, \ldots, C_i, \ldots, C_n\}$, indexed using an index set $\mathcal{N} = \{1, 2, \ldots, n\}$. The information state of a controller C_i, $i \in \mathcal{N}$, is defined as: $\chi^{ⓘ} = [\chi_1^{ⓘ} \ \chi_2^{ⓘ} \ \ldots \ \chi_n^{ⓘ}]^T$. All controllers share a common state space $\chi^{ⓘ} \in \mathbb{R}_{n\times 1}$. An elementary consensus problem is described as follows:

Definition 3.3.3. *Elementary consensus problem P_i*

Let $t_0 < t_1 < \cdots < t_a < \ldots$ be event-based discrete-time instants. Assuming that, at time instant t_a, a controller C_i applies a control action which changes its output: $\chi_i^{ⓘ}(t_a)$, and so the information state: $\chi^{ⓘ}(\tau)$. The controller C_i becomes the actual leader and starts the consensus process applied on other controllers (i.e., followers) so that the change is updated in their information states. The updating instants for asynchronous information exchange among controllers are denoted by $\tau_0 < \tau_1 < \cdots < \tau_u < \ldots$. By accomplishing the consensus process, the consensus vector defined as:

$$\chi(\tau) = [\chi^{①}(\tau)\, \chi^{②}(\tau)\, \ldots\, \chi^{ⓝ}(\tau)]^T \tag{3.11}$$

converges to the same value $\chi^{ⓘ}(\tau_0) = \chi_i^{ⓘ}(t_a)$ for all elements.

The elementary consensus problem (denoted by P_i), is solved by the asynchronous protocol (denoted by F_i), defined by Eq(s). (3.4). The conditions for the convergence of asynchronous consensus protocol, F_i, are related to the standard topology (denoted by T_i) or the corresponding adjacency matrix (denoted by A_i). As stated in Theorem 3.3.2, the convergence conditions are one of following statements:

- Graph associated with A_i (denoted by G_i) has a unique spanning tree rooted by the root node C_i.
- Or, the non-negative stochastic matrix A_i is primitive.

- Or, by Corollary 3.3.2, $\lim_{k\to+\infty} A_i^k = 1_n \ell_i^T$, where: $k \in \mathbb{N}^+$, 1_n and ℓ_i are right and left positive P-F eigenvectors corresponding to P-F eigenvalue 1, that is: $\ell_i > 0$, $\ell_i^T A_i = \ell_i^T$, and are normalized such that: $\ell_i^T 1_n = 1$.

We introduce the concept of consensus function for the consensus problems of discrete-time leader-switching systems with fixed topologies.

Definition 3.3.4. *Consensus function* $\mathcal{F}$ [150] *and* $\mathcal{F}$*-consensus problem* [150, 93].

A consensus function, $\mathcal{F}$, corresponding to the consensus protocol F, that solves a consensus problem P (also called $\mathcal{F}$-consensus problem), can be expressed by:

$$\begin{array}{rcl} \mathcal{F} : \mathbb{R}_{n\times 1} & \longrightarrow & \mathbb{R} \\ \mathcal{F}(\chi(\tau)) & \longrightarrow & \underline{C}, \end{array} \tag{3.12}$$

where: $\underline{C} = \chi^{\textcircled{i}}(\tau_0)$ is the initial state of controller C.

For simplicity, in the case of an asynchronous system with the complete updating set $S(\tau) = \{1,\ldots,n\}, \forall\tau$ and zero delays (see the mapping between asynchronous and synchronous systems in [28]), the Eq(s). (3.6) can be presented by:

$$\begin{array}{l} \chi(\tau_{u+1}) = A\chi(\tau_u) \\ \chi(\tau_{u+1}) = A^k\chi(\tau_0) \end{array} \tag{3.13}$$

Based on Corollary 3.3.2 and Lemma 3.3.4, $\lim_{k\to+\infty} A^k = 1_n \ell^T$ and $\chi(\tau_u) \to \underline{C} 1_n$, as $\tau \to \tau_{+\infty}$, the consensus function, $\mathcal{F}$, is defined for this specific asynchronous system as:

$$\mathcal{F}(\chi(\tau)) = \ell^T \chi(\tau) \tag{3.14}$$

where: 1_n and ℓ are right and left positive P-F eigenvectors corresponding to P-F eigenvalue 1, that is: $\ell^T A = \ell^T$, and are normalized such that: $\ell^T 1_n = 1$.

For an asynchronous system mapped into a synchronous system, the consensus process can be illustrated using the consensus function as follows:

$$\begin{array}{rl} \mathcal{F}(\chi(\tau_1)) = \mathcal{F}(A\chi(\tau_0)) & = \mathcal{F}(\chi(\tau_0)) \\ \mathcal{F}(\chi(\tau_2)) = \mathcal{F}(A\chi(\tau_1)) & = \mathcal{F}(\chi(\tau_0)) \\ \mathcal{F}(\chi(\tau_3)) = \mathcal{F}(A\chi(\tau_2)) & = \mathcal{F}(\chi(\tau_0)) \\ \vdots & \vdots \\ \mathcal{F}(\chi(\tau_{u+1})) = \mathcal{F}(A\chi(\tau_u)) & = \mathcal{F}(\chi(\tau_0)) \end{array} \tag{3.15}$$

For the complete control system, n standard topologies (or single-leader–multi-follower configuration), $\{T_1,\ldots,T_i,\ldots,T_n\}$, represented by adjacency matrices $\{A_1,\ldots,A_i,\ldots,A_n\}$, are involved.

Assumptions 3.3.3. *Elementary* $\mathcal{F}_i$*-consensus problem*

Assuming that all standard topologies, $T_i,\ i \in \mathcal{N}$, represented by NSP matrices, $A_i,\ i \in \mathcal{N}$, consensus functions $\mathcal{F}_i,,\ i \in \mathcal{N}$ solve $\mathcal{F}_i$-consensus problem. That is:

$$\forall i \in \mathcal{N}, \lim_{k \to +\infty} A_i^k = 1_n \ell_i^T \tag{3.16}$$

where: $k \in \mathbb{N}^+$, 1_n and ℓ_i are right and left positive P-F eigenvectors corresponding to P-F eigenvalue 1, that is: $\ell_i > 0$, $\ell_i^T A_i = \ell_i^T$, and are normalized such that: $\ell_i^T 1_n = 1$.

A priori, the following convex combination of these standard topologies [150] can create a solution that solves the consensus problems for a class of "leader-switching" systems:

$$\left.\begin{array}{ll} \chi_1(\tau_{u+1}) & = A_1 \chi_1(\tau_u) \\ \chi_2(\tau_{u+1}) & = A_2 \chi_2(\tau_u) \\ & \vdots \\ \chi_n(\tau_{u+1}) & = A_n \chi_n(\tau_u) \end{array}\right\} \Longrightarrow \chi(\tau_{u+1}) = \overline{A}\chi(\tau_u) \tag{3.17}$$

Let $e_i = [0 \ \ \ldots 1_{(row\ i)} \ldots \ \ 0]^T \in \mathbb{R}_{n\times 1}$ and $\alpha_i \in [0,1]$, such that: $\sum_{i=1}^n \alpha_i = 1$.

Proposition 3.3.1. *Consensus function $\overline{\mathcal{F}}$ for a $\overline{\mathcal{F}}$-consensus problem.*

Based on the matrix $\overline{A}$ defined as follows:

$$\overline{A} = \sum_{i=1}^{n} \alpha_i A_i \tag{3.18}$$

the consensus protocol Eq(s). (3.17) can solve the global consensus problem of leader-switching system (called $\overline{\mathcal{F}}$-consensus problem) using the following consensus function:

$$\overline{\mathcal{F}}(\chi(\tau)) = \overline{\ell}^T \chi(\tau) \tag{3.19}$$

where: $\overline{\ell} = \sum_{i=1}^n \alpha_i \ell_i$.

Proof. Obviously, the matrix $\overline{A}$ defined in Proposition 3.3.1, has following properties:

- non-negative: $\forall i \in \mathcal{N}, A_i \geq 0$, and $\alpha_i \in [0,1] \Rightarrow \overline{A} = \sum_{i=1}^n \alpha_i A_i \geq 0$
- stochastic: $\forall i \in \mathcal{N}, A_i 1_n = 1_n$ and $\sum_{i=1}^n \alpha_i = 1$, $\alpha_i \in [0,1] \Rightarrow \overline{A} 1_n = (\sum_{i=1}^n \alpha_i A_i) 1_n = 1_n$
- $\lim_{k\to+\infty} \overline{A}^k = 1_n \overline{\ell}^T$:
  By Eq(s). (3.16): $\forall i \in \mathcal{N}$, $\lim_{k\to+\infty} A_i^k = 1_n \ell_i^T$, $\ell_i^T 1_n = 1$ and $\alpha_i \in [0,1]$, we obtain:

$$\lim_{k\to+\infty} \overline{A}^k = \lim_{k\to+\infty} \sum_{i=1}^{n} (\alpha_i A_i)^k = \sum_{i=1}^{n} \alpha_i 1_n \ell_i^T = \sum_{i=1}^{n} 1_n \alpha_i \ell_i^T = 1_n \overline{\ell}^T$$

  and:

$$\overline{\ell}^T \overline{A} = (\sum_{i=1}^{n} \alpha_i \ell_i)^T (\sum_{i=1}^{n} \alpha_i A_i) = \sum_{i=1,j=1}^{n} \alpha_i \alpha_j \ell_i^T A_i$$

$$= \sum_{i=1}^{n} \alpha_i^2 \ell_i^T + \sum_{i=1, j=1, i\neq j}^{n} \alpha_i \alpha_j \ell_i^T A_j = \sum_{i=1}^{n} (\alpha_i^2 \ell_i^T + \alpha_i \ell_i^T \sum_{i\neq j}^{n} \alpha_j)$$
$$= \sum_{i=1}^{n} (\alpha_i^2 \ell_i^T + (\alpha_i - \alpha_i^2) \ell_i^T) = \sum_{i=1}^{n} \alpha_i \ell_i = \overline{\ell}^T$$

Therefore, the consensus protocol defined by Eq(s). (3.17) solves the $\overline{\mathcal{F}}$-consensus problem. □

Remark 3.3.2. By selecting α_i, $i \in \mathcal{N}$ appropriately, the proposed protocol Eq(s). (3.17) can solve any $\overline{\mathcal{F}}$-consensus problem. However, due to the complexity of a considered system, not all protocols that solve a consensus problem can be expressed by the form Eq(s). (3.17).

Example 3.3.1. *An example of a simple leader-switching system.*

- A standard topology represented by the following matrix A_i:

$$A_i = \begin{bmatrix} (1-\alpha_{i1}) & 0 & \dots & \alpha_{i1} & \dots & 0 \\ 0 & (1-\alpha_{i2}) & \dots & \alpha_{i2} & \dots & 0 \\ \vdots & \vdots & \ddots & \vdots & \dots & \vdots \\ 0 & 0 & \dots & 1_{(row\ i)} & \dots & 0 \\ \vdots & \vdots & \dots & \vdots & \ddots & \vdots \\ 0 & 0 & \dots & \alpha_{in} & \dots & (1-\alpha_{in}) \end{bmatrix} \in \mathbb{R}_{n\times n} \tag{3.20}$$

  where: $\alpha_{ij} \in (0,1]$, $\forall i, j \in \mathcal{N} = \{1, 2, \dots, n\}$, such that: $\alpha_{ij} = \alpha_{ji}$.

- Consensus protocol: $\chi_i(\tau_{u+1}) = A_i \chi_i(\tau_u)$, $i \in \mathcal{N}$ solves $\mathcal{F}_i$-consensus problem.

- Consensus function: $\mathcal{F}_i(\chi) = \ell_i^T \chi$, where: $\ell_i = [0\, 0 \dots 1_{row\ i} \dots 0]^T$ and $\ell_i^T A_i = \ell_i^T$.

The global topology for a leader-switching system is given in summary form as follows:

$$\overline{A} = \begin{bmatrix} (1 - \sum_{i\neq 1} \alpha_i \alpha_{i1}) & \alpha_2 \alpha_{21} & \dots & \alpha_n \alpha_{n1} \\ \alpha_1 \alpha_{12} & (1 - \sum_{i\neq 2} \alpha_i \alpha_{i2}) & \dots & \alpha_n \alpha_{n2} \\ \vdots & \vdots & \ddots & \vdots \\ \alpha_1 \alpha_{1n} & \alpha_2 \alpha_{2n} & \dots & (1 - \sum_{i\neq n} \alpha_i \alpha_{in}) \end{bmatrix} \tag{3.21}$$

where: $\alpha_i \in [0,1]$, $\alpha_{ij} \in (0,1]$, $\forall i, j \in \mathcal{N}$, such that: $\sum_{i=1}^{n} \alpha_i = 1$. By Proposition 3.3.1, the protocol Eq(s). (3.17) solves the $\overline{\mathcal{F}}$-consensus problem with the consensus function Eq(s). (3.19). An example of the global topology for the system with five controllers is given in Fig. 3.7.

In this section, we have discussed the feasibility and the stability of asynchronous consensus protocol in achieving the convergence of information states of controllers. Based on the stability theory of asynchronous system and proposed communication assumptions, we have established the necessary and sufficient conditions for the information consensus to be reached asymptotically using the asynchronous protocol defined in Section 3.3.1. The results are obtained for an asynchronous system under the fixed and time-varying communication topologies and bounded time-varying communication delays. The consensus points of information states are different

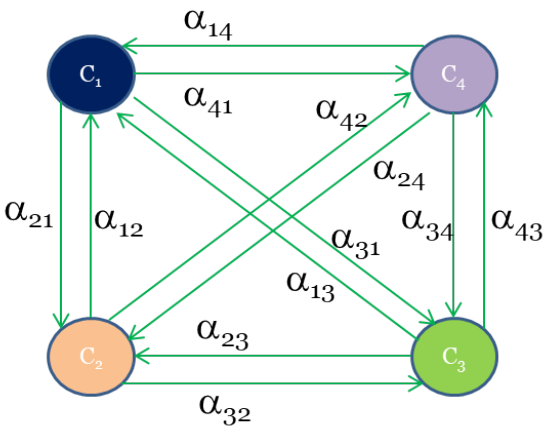

Fig. 3.7 An example of the global topology for the system with four controllers illustrates the parameterizable adjacency matrix $\overline{A}$.

depending on the initial state of the actual root node. Furthermore, the consensus protocol added to control algorithm will be demonstrated to still guarantee the control performance, but with robustness to changes in exchange topology due to link/node failures and time delays (see Section 4.2.3).

3.4 Simulation results

We have performed simulations of the consensus problems for one controller (when it becomes a leader) of one-leader DMPC control system to show the convergence of designed asynchronous consensus protocol such that the information states of all controllers update the newest value from the leader. Simulations of the leader-switching system, when different consensus processes are executed in the control system, are also performed to illustrate the possibility of switching the leader using the parameterizable global topologies.

Based on the example shown in Fig. 3.6, we consider a control system of $n = 4$ controllers, $\mathcal{C} = \{C_1, C_2, C_3, C_4\}$, indexed using an index set $\mathcal{N} = \{1, 2, 3, 4\}$. The communication topologies are constructed from the Eq(s). (3.21), where: if C_i is a root, $\alpha_i = \alpha_r = 0.9$, otherwise, $\alpha_i = (1 - \alpha_r)/n$, $\alpha_{ij} = 1/n$, $\forall i, j \in \mathcal{N}$, such that: $\sum_{i=1}^{n} \alpha_i = 1$. The information state of controller C_i, $i \in \mathcal{N}$, is defined as: $\chi^{\textcircled{i}} = [\chi_1^{\textcircled{i}} \ \chi_2^{\textcircled{i}} \ \chi_3^{\textcircled{i}} \ \chi_4^{\textcircled{i}}]^T$. All controllers share a common state space: $\chi^{\textcircled{i}} \in \mathbb{R}_{4\times 1}$, $\forall i \in \mathcal{N}$. The initial information states of all controllers (except the leader) are assumed to be random values between 0 and 5 (m^3/s). Let $t_0 < t_1 < \cdots < t_a < \ldots$ be event-based discrete-time instants when a controller applies an action provoking a change in information states of controllers. Assuming that, at time instant t_{i_a}, the controller C_i applies the control action which changes the information state: $\chi^{\textcircled{i}}(t_{i_a})$. The controller C_i becomes the actual leader and starts the consensus process executed on other controllers (i.e., followers) so that the change is updated in their information states. The sampling time in simulations is chosen as: $dt = 0.05$ (s). The updating instants of the controller C_i are assumed to be every $\tau = 2 * i * dt$ (s) in order to illustrate the asynchronism. By Proposition 3.3.1, the protocol Eq(s). (3.17) solves the

consensus problem of the system characterized by the matrix Eq(s). (3.21), in other words, the consensus vector defined as: $\chi(\tau) = [\chi^{①}(\tau)\ \chi^{②}(\tau)\ \chi^{③}(\tau)\ \chi^{④}(\tau)]^T$ converges to the same value $\chi^{①}(\tau_0) = \chi_i^{①}(t_{i_a})$ for all elements. The simulation parameters are summarized in Table 3.1. The simulations were done in Matlab R2016b on a computer Intel®Core™i5-4310U CPU 2.0GHz.

Table 3.1 Simulation parameters for the asynchronous consensus.

Parameters	Setting value
Nodes (n)	4
Time sampling (dt)	0.05s
Updating instants of controllers i	2*i*dt
Time delay (d_{ij})	2*i*j*0.01s
Simulation time ($Tsim$)	6s, 10s, and 40s

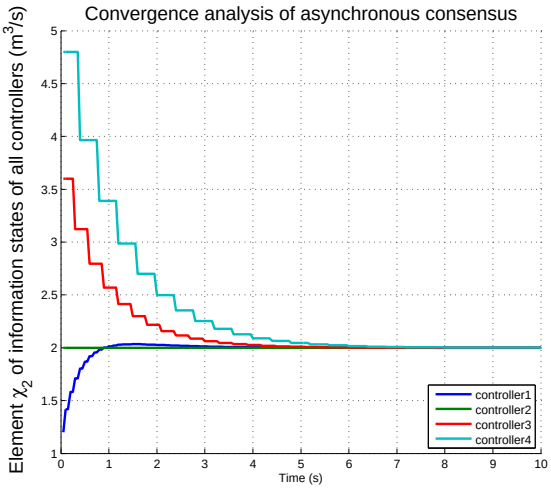

Fig. 3.8 Simulation results of the asynchronous consensus protocol used in the one-leader control system (see Fig. 3.6).

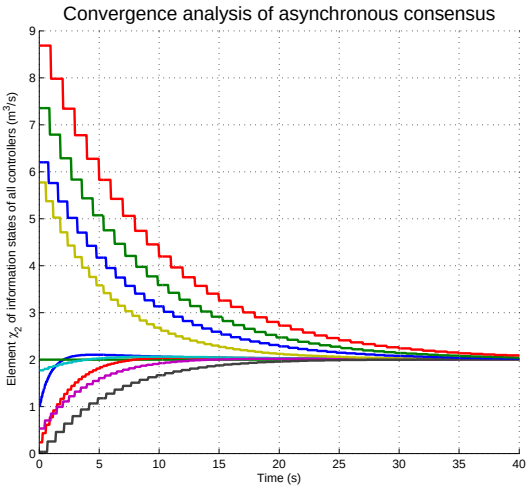

Fig. 3.9 Simulation results of asynchronous consensus protocol used in the one-leader control system with 10 controllers.

The first simulation scenario uses the example presented in Fig. 3.6. In this scenario, the controller C_2 applies a computed action u_2 to the subsystem, which changes the value of its information state χ_2. C_2 actually becomes the leader. The consensus process is started by C_2 for providing the convergence of information states of all controllers. The simulation results are shown in Fig. 3.8. We see that the information states of four controllers, which start from different initial values, can reach asymptotically a common value after 6 (s). The updating instants are chosen to be different for every controller. For more complex control system with 10 controllers using the designed asynchronous consensus protocol, the simulation results presented in Fig. 3.9, show the convergence of their information states, which is achieved after 40 (s).

The second scenario explores the first scenario for testing the losses of direct communication. Assuming that the controller C_4 loses the communication in two directions with the controller C_1 at $\tau = 2$ (s). Through simulation, the Fig. 3.10 shows a divergence of the information states over the simulation time $Tsim = 10$ (s). In the other hand, in the case the controller C_4 loses

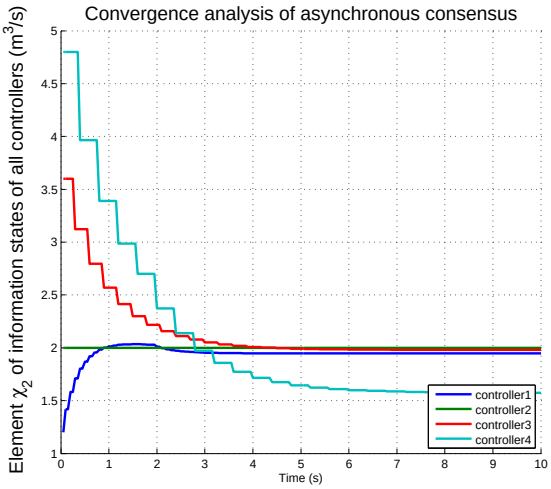

Fig. 3.10 Simulation results of asynchronous consensus protocol used in one-leader control system in a scenario in which the controller 4 loses the direct communication with the controller 1 at $\tau = 2\ (s)$.

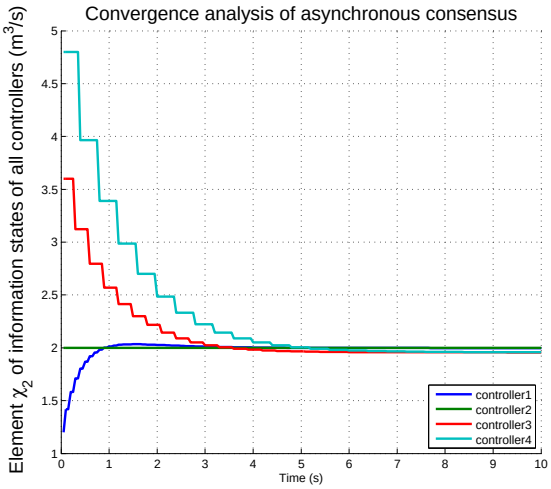

Fig. 3.11 Simulation results of asynchronous consensus protocol used in one-leader control system in a scenario in which the controller 4 loses the direct communication with the controller 3 at $\tau = 2\ (s)$.

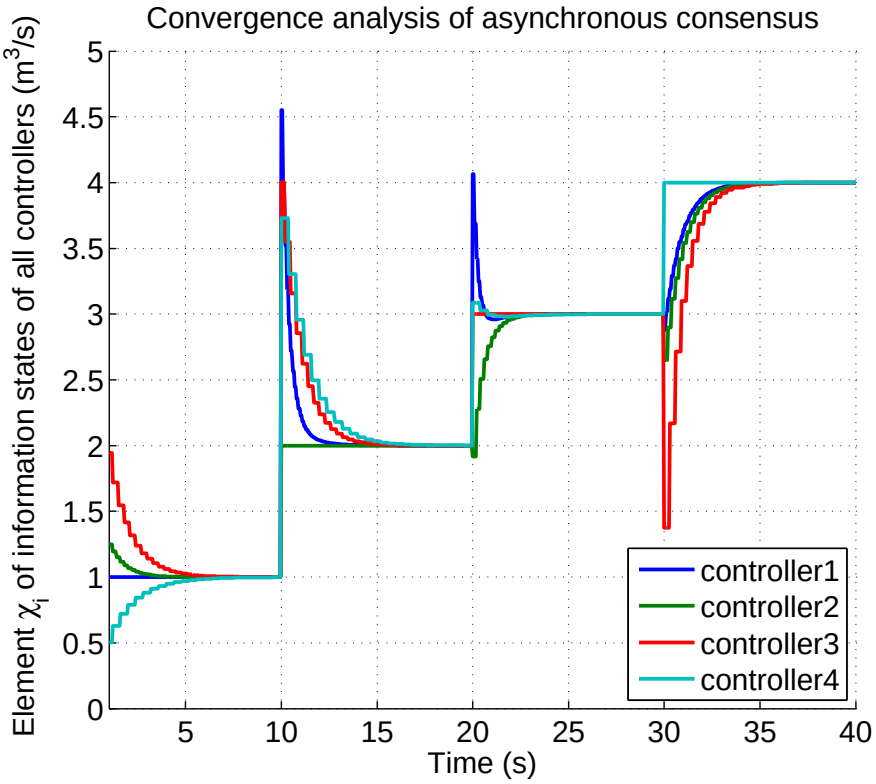

Fig. 3.12 Simulation results of the asynchronous consensus protocol used in the leader-switching system. Four controllers C_i are involved. As an example, the initial state of the leader C_i is $\chi_i = i$. The controller C_i is assumed to apply a control action at time instant $(i-1)*Tsim/4$. For τ between $(i-1)*Tsim/4$ and $i*Tsim/4$, the controller C_i becomes the leader which updates all elements χ_i of all controllers.

the communication in two directions with the controller C_3 at $\tau = 2\ (s)$, the convergence of the information states still is achieved. Indeed, the loss of direct communication between C_4 and C_3 infers the elements $\alpha_{34} = \alpha_{43} = 0$ in the matrix Eq(s). (3.21). However, the adjacency matrix still has a unique eigenvalue with maximum modulus $\rho(\overline{A}) = 1$. By Corollary 3.3.2, the controllers can reach the consensus asymptotically. These examples demonstrate that the change in topology of control system can cause a divergence or keep the convergence property. In terms of communication aspects, these results help the control system design for considering the robustness of link/node failures.

The third simulation scenario analyzes the convergence of different consensus processes with different actual leaders in a control system. In this scheme, four controllers are involved in four different consensus processes. Assuming that at time instant $t_{i_a} = (i-1) * Tsim/4$, the controller C_i applies the control action which changes the information state: $\chi^{\textcircled{i}}(t_{i_a})$. The simulation results shown in Fig. 3.12 demonstrate that the system using the global communication topology can switch the leader by changing the values of α_i, $i \in \mathcal{N}$. The consensus is asymptotically reached with the random initial values of the information states and the controllers use the asynchronous consensus protocol.

3.5 Conclusion

The coordinated controllers in distributed control encounter some challenging problems in the presence of time-varying topology and communication issues such as loss of synchronization or the updating problem of interaction variables and coordination variables. We have approached these problems by formulating them as an asynchronous information consensus problem. In this chapter, we have determined the characteristics and properties of information exchange topologies for solving the asynchronous consensus problem with communication constraints such as communication delays. Under certain communication assumptions, the analytical demonstration shows that information consensus of asynchronous systems under fixed communication topologies can be achieved asymptotically if the associated graph has a spanning tree. For the systems with time-varying communication topologies, the asynchronous information consensus is asymptotically achieved if the union of directed interaction graphs across some intervals has a spanning tree frequently enough during the evolution of consensus processes. Based on these conditions, the asynchronous consensus protocol is then designed to achieve the convergence of information states of controllers. Integrating the consensus protocol in DMPC scheme results in the most updated values of interaction variables and coordination variables that the controllers can use for the action computation. Therefore, the computed actions are more appropriate to apply to subsystems than other cases with outdated values of coordination variables. The implementation of a consensus-based control algorithm in distributed controllers improves the control performance when compared to decentralized control. In addition, when the synchronization among controllers in distributed control strategy is not guaranteed, this asynchronous framework can be used to provide the control performance close to those of the synchronous case. The consensus algorithm has been applied to the example of a distributed control of irrigation

channels modeled by using the Lattice Boltzmann method. The simulation results demonstrate the effectiveness and usefulness of the asynchronous consensus approach to distributed control.

Chapter 4

Distributed Model Predictive Control of irrigation channels using cooperative controllers

This chapter investigates the regulatory control of large-scale irrigation channels under a Distributed Cooperative Model Predictive Control (DCMPC) framework. Operationally, the regulatory control involves the regulation of water levels and/or flow rates at some points in the channel by manipulating available hydraulic structures (e.g., submerged gates, movable weirs, etc.) in order to satisfy real-time performance requirements. For this purpose, we firstly provide a discrete-time linearized model of the large-scale system suitable for adequately capturing its dynamics and the interactions among subsystems using the Lattice Boltzmann (LB) method. Next, we discuss different control implementation strategies (i.e., centralized, decentralized and distributed strategies) and how the cooperative communication among local controllers can be included to improve the performance of the overall system. For simulations, a particular benchmark of an irrigation channel is considered. Comparisons through simulations among the proposed control approaches validate the benefits of the distributed cooperative control approach. The rest of this chapter is organized as follows. Section 4.1 explores the methods and tools needed to address this problem. Section 4.2 introduces the distributed cooperative control approach for irrigation channels. Section 4.3 provides the simulation results under different scenarios, details comparison results and discussions. Finally, Section 4.4 draws with some conclusions and presents future perspectives.

4.1 Model predictive control of irrigation channels

Our approach to control irrigation channels is based on the optimization of an objective function to compute the best actions and the dynamic models to predict the system behaviors. The DMPC method has its roots in such optimal control while explicitly taking into account the constraints and the predictions [9, 108]. MPC is a well-known technique for handling control and state constraints while offering good performance specifications (the basic notions about MPC are

presented in [108]). In principle, MPC allows a uniformity, that is, the same technique can be successfully applied for a wide range of control problems [9]. The delay compensation is also one interesting characteristic that makes MPC particularly suitable for delay-varying systems such as irrigation channels. There are many works which employ different control strategies within an MPC framework for the control of irrigation channels (as surveyed in [45]). For example, [91] presents a methodology for the optimal management of combined water supply and navigability/sustainability in river systems based on the MPC. [96] presents a decentralized MPC scheme for large-scale systems whose components can exchange information through a network. [130] proposes a scheme to determine the weighting values that are proportional to the control load for each subsystem. This weighting scheme is then applied to control the irrigation channel using Feasible-Cooperation MPC and Nash-bargaining MPC. [46] proposes a distributed MPC algorithm for a water delivery channel using linearized and discretized Saint-Venant model. A methodology for the optimal management of a combined irrigation and water supply system based on MPC is proposed in [102, 103]. [87] focuses on distributed MPC strategy in which a discrete-time linear integral delay model is used for prediction. Their distributed control algorithm is based on the augmented Lagrangian duality method. [96, 137] address a MPC methodology configured for water quantity control on open water systems modeled by the classical Integrator Delay model and the Saint-Venant model. [13] proposed a scheme to achieve some degree of coordination among agents (i.e., controllers) that solve MPC problems with locally relevant variables, costs, and constraints, but without solving a centralized MPC problem. In this scheme [13], agents within each neighborhood work sequentially. Each agent uses the same interior-point method (i.e., barrier method [9]) with the same Lagrange multipliers to generate its iterations. The predictive control theory is also used in [119] to formulate a set of local controllers for the automatic operation of gates of each reach. The distributed control scheme presented in the work [119] takes into account explicitly the interactions among subsystems using Saint-Venant models. In MPC, the computational complexity and theoretical properties (e.g., feasibility, stability and robustness) depend closely on the choice of the prediction model, the control objectives and the constraints [108].

One of the Arrowhead project demonstrators (focusing on the automation of Bourne channel (BC) irrigation network in Drôme - France) introduces the distributed control of a large-scale irrigation system as a case study (for more details, see [89]). The structural diagram of BC irrigation system is shown in Fig. 1.2. This system is equipped with only local controllers developed to guarantee the water level at some points within a specified range by adjusting control structures such as submerged gates or mixed gates and spillway. Their action decisions are only based on local information (e.g., measured water level at gate location), without taking into account the potential coordination/cooperation with other controllers. To determine the acceptable ranges, a centralized coordinator is involved and proceeds with a course of actions: collecting measurements from the whole irrigation channel, optimizing, choosing values in a pre-defined way and pushing reference values to local controllers. Controlling a such system in a centralized way [84] would give rise to a large computational charge and set up a single point of failure. The important delays may occur in information gathering, from level sensors to

the centralized coordinator, due to communication issues. The decentralized approach [26, 91] will scale better for the large-scale system. In the decentralized scheme, the objective of each controller is to locally determine the actions that optimize the behavior of the subsystem (i.e., by minimizing the specified local cost function). The drawback of decentralized control is that these local control actions are computed regardless of the effects on the overall system performance. The controllers do not consider a cooperation, a coordination or a negotiation among them. As a consequence, the global performance may be degraded due to the unexpected and unanticipated interactions among the subsystems. The distributed approach [20, 133, 12, 118, 87] combines the optimality of centralized approach and the less complexity of decentralized approach to provide a good compromise.

Motivated by the above-mentioned observations, the aims of this chapter is to implement and compare realistic and flexible control schemes in which:

- costs, constraints, profiles are taken into account in decentralized and distributed constrained optimization problems via an MPC design;
- the cooperation among local MPC controllers can be included in order to improve the performance of the overall system.

Next, we employ the LB method for providing a prediction model of the irrigation channel suitable for capturing its dynamics and the interactions among the subsystems.

4.1.1 Prediction model

As already presented in Section 1.3.1, the modeling of a dynamic flow with D1Q3 LB method in the presence of a simple external force F, results in the Eq(s). (1.13), which are rewritten as follows:

$$\begin{array}{rcl} f_1(l,t+\Delta t) & = & f_1(l,t)+\frac{1}{\tau}(f_1^e-f_1(l,t)) \\ f_2(l,t+\Delta t) & = & f_2(l-v\Delta t,t)+\frac{1}{\tau}(f_2^e-f_2(l,t))-\frac{\Delta t}{2v}F \\ f_3(l,t+\Delta t) & = & f_3(l+v\Delta t,t)+\frac{1}{\tau}(f_3^e-f_3(l,t))+\frac{\Delta t}{2v}F \end{array} \tag{4.1}$$

The macroscopic variables h and u are determined by Eq(s). (1.18) and rewritten as follows:

$$\begin{aligned} h &= \sum_{i=1}^{3} f_i = f_1+f_2+f_3 \\ q &= hu = \sum_{i=1}^{3} v_i f_i = v(f_2-f_3) \end{aligned} \tag{4.2}$$

In distributed scheme, we also consider the coupling of two reaches modeled by D1Q3 LB method with a gate in a submerged regime. The flow rate through gate Q_g depends on the difference between the water heights at upstream h and downstream h' around the gate, as expressed in Eq(s). (1.23):

$$Q_g = B_g \alpha \theta \sqrt{2g(h-h')} \tag{4.3}$$

where: B_g is the gate width, α is the gate coefficient and θ is the gate opening. In addition, the outflow Q of upstream reach is equal to the inflow Q' of downstream reach, that is: $Q = Q' = Q_g$. The manipulated variable θ is deduced from following gate equations:

$$vB(f_2 - f_3) = vB'(f_2' - f_3') = B_g \alpha \theta \sqrt{2g(h - h')} \tag{4.4}$$

4.1.1.1 Linearization of a nonlinear LB model

For use in MPC method, we need a good model that is both descriptive enough to capture the most significant dynamics of the real irrigation channel and simple enough for solving the optimization problem [102, 96, 87, 108]. The linearized D1Q3 LB model offers a good compromise. For further use, we consider the linearization of the LB dynamics (Eq(s). (4.1)) around an equilibrium height, $h = h_0$, and an equilibrium velocity, $u = u_0$, which can deduce an equilibrium flow rate: $Q_0 = Bh_0u_0$. The small derivations ε_i, $i = \{1,2,3\}$, around the equilibrium points are expressed by: $\varepsilon_i = f_i - f_i^e(h_0, u_0)$, where: $f_i, i = \{1,2,3\}$, are the solution of the Eq(s). (4.1).

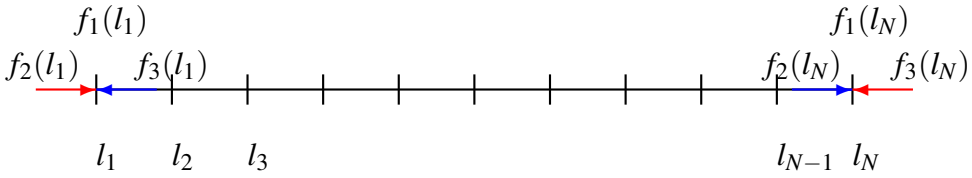

Fig. 4.1 The discretized points of a reach in D1Q3 LB model.

For a reach of length L (corresponding to N discretized points l_j, $j = 1, \ldots, N$), the state-space representation of discrete-time system described by Eq(s). (1.14) is rewritten as follows:

$$\begin{bmatrix} f_2(l_j, t+\Delta t) \\ f_1(l_j, t+\Delta t) \\ f_3(l_j, t+\Delta t) \end{bmatrix} = \begin{bmatrix} f_2(l_{j-1}, t) \\ f_1(l, t) \\ f_3(l_{j+1}, t) \end{bmatrix} + \frac{1}{\tau} \begin{bmatrix} f_2^e(l_{j-1}, t) - f_2(l_{j-1}, t) \\ f_1^e(l_j, t) - f_1(l_j, t) \\ f_3^e(l_{j+1}, t) - f_3(l_{j+1}, t) \end{bmatrix} + \frac{\Delta t}{2v} \begin{bmatrix} F \\ 0 \\ -F \end{bmatrix} \tag{4.5}$$

The simple force term, F, is calculated by Eq(s). (1.3):

$$F = gh \left(I - \frac{n^2 u^2}{\left(\frac{Bh}{B+2h}\right)^{4/3}} \right) \tag{4.6}$$

The equilibrium density distributions, f_i^e, follow the conditions of mass and momentum conservation such that:

$$\begin{aligned} \sum_i f_i &= h = h_0 + \sum_i \varepsilon_i, \\ \sum_i v_i f_i &= hu = h_0 u_0 + (\varepsilon_2 - \varepsilon_3) v, \\ \sum_i v_i^2 f_i &= \frac{1}{2} g h^2 + h u^2 = \frac{1}{2} g (h_0 + \sum_i \varepsilon_i)^2 + (h_0 u_0^2 - u_0^2 \sum_i \varepsilon_i + 2(\varepsilon_2 - \varepsilon_3) v u_0). \end{aligned} \tag{4.7}$$

These condition gives the following results for $f_i^e(h,u)$:

$$\begin{aligned}
f_1^e(h,u) &= f_1^e(h_0,u_0) + \left(1 - \frac{gh_0}{v^2} + \frac{u_0^2}{v^2}\right)\sum_i \varepsilon_i - \frac{2u_0}{v}(\varepsilon_2 - \varepsilon_3),\\
f_2^e(h,u) &= f_2^e(h_0,u_0) + \frac{1}{2}\left(\frac{(}{gh_0}v^2 - \frac{u_0^2}{v^2}\right)\sum_i \varepsilon_i + \left(\frac{1}{2} + \frac{u_0}{v}\right)(\varepsilon_2 - \varepsilon_3)\\
f_3^e(h,u) &= f_3^e(h_0,u_0) + \frac{1}{2}\left(\frac{gh_0}{v^2} - \frac{u_0^2}{v^2}\right)\sum_i \varepsilon_i - \left(\frac{1}{2} - \frac{u_0}{v}\right)(\varepsilon_2 - \varepsilon_3)
\end{aligned} \tag{4.8}$$

By combining Eq(s). (4.5) and Eq(s). (4.8), the linearization of the Eq(s). (4.5) provides the following equations (as detailed in [98]):

$$\begin{bmatrix} \varepsilon_2(l_{j+1},t+\Delta t) \\ \varepsilon_1(l_j,t+\Delta t) \\ \varepsilon_3(l_{j-1},t+\Delta t) \end{bmatrix} = M \begin{bmatrix} \varepsilon_2(l_j,t) \\ \varepsilon_1(l_j,t) \\ \varepsilon_3(l_j,t) \end{bmatrix} + N \begin{bmatrix} \varepsilon_2(l_j,t) \\ \varepsilon_1(l_j,t) \\ \varepsilon_3(l_j,t) \end{bmatrix} \tag{4.9}$$

where:

$$\begin{aligned}
M &= \frac{1}{\tau}\begin{bmatrix} \tau - \frac{1}{\Psi_e^2}(1-Fr_e^2) & 1 - \frac{1}{\Psi_e^2}(1-Fr_e^2) - 2\frac{Fr_e}{\Psi_e} & 1 - \frac{1}{\Psi_e^2}(1-Fr_e^2) + 2\frac{Fr_e}{\Psi_e} \\ \frac{1}{2\Psi_e^2}(1-Fr_e^2) & \tau - \frac{1}{2} + \frac{1}{2\Psi_e^2}(1-Fr_e^2) + \frac{Fr_e}{\Psi_e} & \frac{1}{2\Psi_e^2}(1-Fr_e^2) - \frac{1}{2} - \frac{Fr_e}{\Psi_e} \\ \frac{1}{2\Psi_e^2}(1-Fr_e^2) & \frac{1}{2\Psi_e^2}(1-Fr_e^2) - \frac{1}{2} + \frac{Fr_e}{\Psi_e} & \tau - \frac{1}{2} + \frac{1}{2\Psi_e^2}(1-Fr_e^2) - \frac{Fr_e}{\Psi_e} \end{bmatrix}\\
N &= \frac{\Delta t}{2v}\begin{bmatrix} 1 & 1 & 1 \\ 0 & 0 & 0 \\ -1 & -1 & -1 \end{bmatrix}\begin{bmatrix} g(I + J_e + \frac{4J_eR_e}{3h_0} - 2vJ_e) \\ g(I + J_e + \frac{4J_eR_e}{3h_0}) \\ g(I + J_e + \frac{4J_eR_e}{3h_0} + 2vJ_e) \end{bmatrix}
\end{aligned} \tag{4.10}$$

and

$$Fr_e = \frac{u_0}{\sqrt{gh_0}}, \quad \Psi_e = \frac{v}{\sqrt{gh_0}}, \quad R_e = \frac{Bh_0}{B+2h_0}, \quad J_e = \frac{n^2u_e^2}{R_e^{4/3}}. \tag{4.11}$$

Then, we immediately obtain $(M+N)$, represented by:

$$M+N = \begin{bmatrix} a_{11} & a_{12} & a_{13} \\ a_{21} & a_{22} & a_{23} \\ a_{31} & a_{32} & a_{33} \end{bmatrix} \tag{4.12}$$

By normalizing the time step Δt, $t-\Delta t = (k-1)$, $(t=k)$, $t+\Delta t = (k+1)$, the dynamics of free-surface flow can be represented as a linearized discrete-time systems using state-space representation as follows:

$$x(k+1) = \mathrm{A}x(k) + \mathrm{B}u(k) \tag{4.13}$$

where:

$$x(k) = \begin{bmatrix} \varepsilon_1(l_1,k) & \varepsilon_3(l_1,k) & \dots & \varepsilon_2(l_j,k) & \varepsilon_1(l_j,k) & \varepsilon_3(l_j,k) & \dots & \varepsilon_2(l_N,k) & \varepsilon_1(l_N,k) \end{bmatrix}^T, \tag{4.14}$$

$$u(t) = \begin{bmatrix} \varepsilon_1(l_1,k) \\ \varepsilon_2(l_N,k) \end{bmatrix} \tag{4.15}$$

$$A = \begin{bmatrix} a_{22} & a_{23} & 0 & 0 & 0 & \cdots & 0 & 0 & 0 & 0 & 0 \\ 0 & 0 & a_{31} & a_{32} & a_{33} & \cdots & 0 & 0 & 0 & 0 & 0 \\ a_{12} & a_{13} & 0 & 0 & 0 & \cdots & 0 & 0 & 0 & 0 & 0 \\ 0 & 0 & a_{21} & a_{22} & a_{23} & \cdots & 0 & 0 & 0 & 0 & 0 \\ & & & & & \vdots & & & & & \\ 0 & 0 & 0 & 0 & 0 & \cdots & a_{21} & a_{22} & a_{23} & 0 & 0 \\ 0 & 0 & 0 & 0 & 0 & \cdots & 0 & 0 & 0 & a_{31} & a_{32} \\ 0 & 0 & 0 & 0 & 0 & \cdots & a_{11} & a_{12} & a_{13} & 0 & 0 \\ 0 & 0 & 0 & 0 & 0 & \cdots & 0 & 0 & 0 & a_{21} & a_{22} \end{bmatrix}, B = \begin{bmatrix} a_{21} & 0 \\ 0 & 0 \\ a_{11} & 0 \\ 0 & 0 \\ \vdots & \\ 0 & 0 \\ 0 & a_{33} \\ 0 & 0 \\ 0 & a_{23} \end{bmatrix}, \tag{4.16}$$

4.1.1.2 Dynamics of a subsystem

We consider here an irrigation channel comprising n reaches interconnected by the submerged gates. Each reach (i.e., a subsystem), ⓘ, $i \in \{1,2,\ldots,n\}$ has the length L_i. The DMPC control of this system is divided over n controllers. Assuming that we use the downstream configuration (as shown in Fig. 4.2) in which the control actions apply on the upstream gate of each reach, ⓘ, to adjust the gate opening, $\theta^{ⓘ}$ (manipulated input), in order to regulate the downstream flow rate, $Q^{ⓘ}$ (controlled variables). Each controller, C_i, obtains the measurement available from sensors such as the water height at upstream, $h_{us}^{ⓘ}$, and at downstream, $h_{ds}^{ⓘ}$, of each gate and the flow rate, $Q^{ⓘ}$, at the downstream of each reach. We also consider a lateral pumping discharge, $Q_p^{ⓘ}$, at point

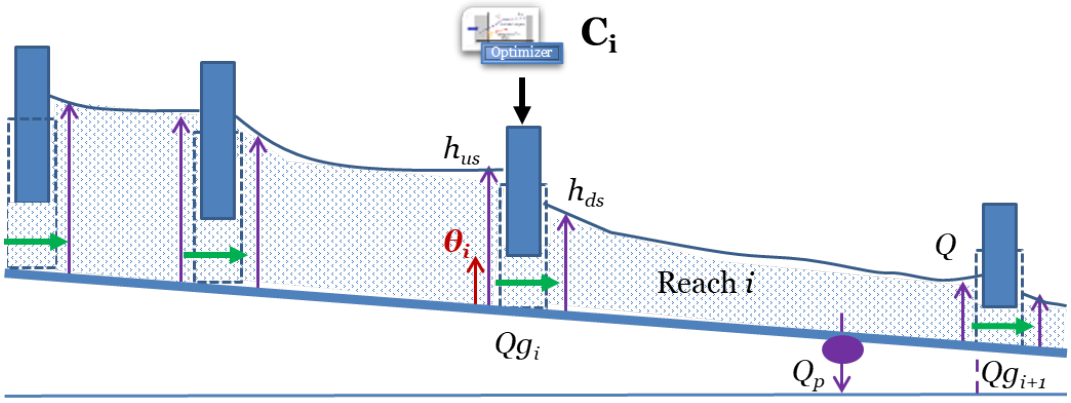

Fig. 4.2 Schematic of the flow rate control in downstream configuration.

L_{p_i} of each reach as a perturbation. The dynamics of a subsystem are modeled by a linearized discrete-time model as presented above (Eq(s). (4.13)). For a reach ⓘ, $i \in \{1,\ldots,n\}$ of length L_i (corresponding to N discretized points l_j, $j = 1,\ldots,N$), when integrating the interaction variables

among subsystems into this model, we obtain:

$$\begin{aligned} x^{\textcircled{i}}(k+1) =& \mathrm{A}^{\textcircled{i}} x^{\textcircled{i}}(k) + \mathrm{B}^{\textcircled{i}} u^{\textcircled{i}}(k) + \mathrm{B_p}^{\textcircled{i}} p^{\textcircled{i}}(k) + \mathrm{B_d}^{\textcircled{i}} d^{\textcircled{i}}(k) \\ y^{\textcircled{i}}(k) =& \mathrm{C_y}^{\textcircled{i}} x^{\textcircled{i}}(k) + \mathrm{D_y}^{\textcircled{i}} u^{\textcircled{i}}(k) + \mathrm{D_{yd}}^{\textcircled{i}} d^{\textcircled{i}}(k) \\ z^{\textcircled{i}}(k) =& \mathrm{C_z}^{\textcircled{i}} x^{\textcircled{i}}(k) + \mathrm{D_z}^{\textcircled{i}} u^{\textcircled{i}}(k) + \mathrm{D_{zd}}^{\textcircled{i}} d^{\textcircled{i}}(k) \\ q^{\textcircled{i}}(k) =& \mathrm{C_q}^{\textcircled{i}} x^{\textcircled{i}}(k) + \mathrm{D_q}^{\textcircled{i}} u^{\textcircled{i}}(k) + \mathrm{D_{qd}}^{\textcircled{i}} d^{\textcircled{i}}(k) \\ h^{\textcircled{i}}(k) =& \mathrm{C_h}^{\textcircled{i}} x^{\textcircled{i}}(k) + \mathrm{D_h}^{\textcircled{i}} u^{\textcircled{i}}(k) + \mathrm{D_{hd}}^{\textcircled{i}} d^{\textcircled{i}}(k) \end{aligned} \tag{4.17}$$

where, as illustrated in Fig. 4.3, we define:

- the discrete-time local states of each reach as:

$$x^{\textcircled{i}}(k) = [\varepsilon_1^{\textcircled{i}}(l_1,k)\ \ \varepsilon_3^{\textcircled{i}}(l_1,k)\ldots\varepsilon_2^{\textcircled{i}}(l_j,k)\ \ \varepsilon_1^{\textcircled{i}}(l_j,k)\ \ \varepsilon_3^{\textcircled{i}}(l_j,k)\ldots\varepsilon_2^{\textcircled{i}}(l_N,k)\ \ \varepsilon_1^{\textcircled{i}}(l_N,k)]^T, \tag{4.18}$$

  $x^{\textcircled{i}}(k) \in \mathbb{R}^{(N-2)\times 1}$,

- the inputs as: $u^{\textcircled{i}}(k) = \varepsilon_2^{\textcircled{i}}(l_1,k) \in \mathbb{R}$,
- the perturbations as: $p^{\textcircled{i}}(k) \in \mathbb{R}$,
- the interaction variables among subsystems as: $d^{\textcircled{i}}(k) = \varepsilon_3^{\textcircled{i}}(l_N,k) \in \mathbb{R}$,
- the controlled variable as: $z^{\textcircled{i}}(k) = \tilde{Q}^{\textcircled{i}}(l_N,k) \in \mathbb{R}$, (where: $\tilde{Q}^{\textcircled{i}}(k) = Q^{\textcircled{i}}(k) - Q_0$),
- the measured output as: $y^{\textcircled{i}}(k) = [\tilde{h}^{\textcircled{i}}(l_1,k)\ \ \tilde{h}^{\textcircled{i}}(l_N,k)]$, (where: $\tilde{h}^{\textcircled{i}}(l,k) = h^{\textcircled{i}}(l,k) - h_0$),
- the estimated flow rate through controlled gate as: $q^{\textcircled{i}}(k) = \tilde{Q}^{\textcircled{i}}(l_1,k) \in \mathbb{R}$,
- the water heights along the channel as: $h^{\textcircled{i}}(k) = [h^{\textcircled{i}}(l_1,k),\ldots,h^{\textcircled{i}}(L_i,k)]$
- the corresponding matrices as: $A^{\textcircled{i}} \in \mathbb{R}^{(N-2)\times(N-2)}$, $B^{\textcircled{i}} \in \mathbb{R}^{(N-2)\times 1}$, $B_p^{\textcircled{i}} \in \mathbb{R}^{(N-2)\times 1}$, $B_d^{\textcircled{i}} \in \mathbb{R}^{(N-2)\times 1}$, $C_y^{\textcircled{i}} \in \mathbb{R}^{2\times(N-2)}$, $D_y^{\textcircled{i}} \in \mathbb{R}^{2\times 1}$, $D_{yd}^{\textcircled{i}} \in \mathbb{R}^{2\times 1}$, $C_z^{\textcircled{i}} \in \mathbb{R}^{1\times(N-2)}$, $D_z^{\textcircled{i}} \in \mathbb{R}^{1\times 1}$, $D_{zd}^{\textcircled{i}} \in \mathbb{R}^{1\times 1}$, $C_q^{\textcircled{i}} \in \mathbb{R}^{1\times(N-2)}$, $D_q^{\textcircled{i}} \in \mathbb{R}^{1\times 1}$, $D_{qd}^{\textcircled{i}} \in \mathbb{R}^{1\times 1}$.

For distributed control scheme, we also consider the interaction/coordination variables, $\chi^{\textcircled{i}}$, in the information exchange among controllers (see Section 4.2.1).

4.1.2 Structural and operational constraints

The operational management of irrigation channels is subject to constraints on the channel structure (e.g., limits of the gate opening, reliability, and robustness of equipment, limits of reservoir capacity) as well as on channel operations (e.g., overflow risks, bank stability, minimum off-take levels). Assuming that the solutions for the control of the considered irrigation channel illustrated in Figs. 4.2 and 4.3 and modeled by the discrete-time systems in Eq(s). (4.17) must

satisfy constraints on water height, gate opening, and on variation of gate opening as follows [86]:

$$\begin{aligned} h_{min} \leq h^{\textcircled{i}} \leq h_{max} \\ \theta_{min} \leq \theta^{\textcircled{i}} \leq \theta_{max} \\ \Delta\theta_{min} \leq \Delta\theta^{\textcircled{i}} \leq \Delta\theta_{max} \end{aligned} \tag{4.19}$$

where the water height is given by: $h^{\textcircled{i}}(l,k) = \tilde{h}^{\textcircled{i}}(l,k) + h_0$ with $\tilde{h}^{\textcircled{i}}(l,k) = \varepsilon_1^{\textcircled{i}}(l,k) + \varepsilon_2^{\textcircled{i}}(l,k) + \varepsilon_3^{\textcircled{i}}(l,k)$ and the gate opening is deduced from gate equations Eq(s). (4.4) with $\varepsilon_i = f_i - f_i^e(h_0,u_0)$, $i = \{1,2,3\}$, that is:

$$\theta^{\textcircled{i}}(k) = \frac{vB(\varepsilon_2^{\textcircled{i}}(l_1,k) - \varepsilon_3^{\textcircled{i}}(l_1,k) + f_2^e - f_3^e)}{B_g \alpha \sqrt{2g(h_{us}^{\textcircled{i}}(k) - h_{ds}^{\textcircled{i}}(k))}} \tag{4.20}$$

where: $h_{us}^{\textcircled{i}}(k), h_{ds}^{\textcircled{i}}(k)$ are the water heights at upstream and downstream ends of the considered gate (given by water level sensors).

These structural constraints, Eqs. (4.19) and (4.20), imply the constraints on the states (described by Eq(s). (4.17)) as follows:

$$\begin{aligned} x_{min} \leq x^{\textcircled{i}} \leq x_{max} \\ \Delta x_{min} \leq \Delta x^{\textcircled{i}} \leq \Delta x_{max} \end{aligned} \tag{4.21}$$

The computation of control action has to take into account of these constraints, Eqs. (4.19) and (4.21).

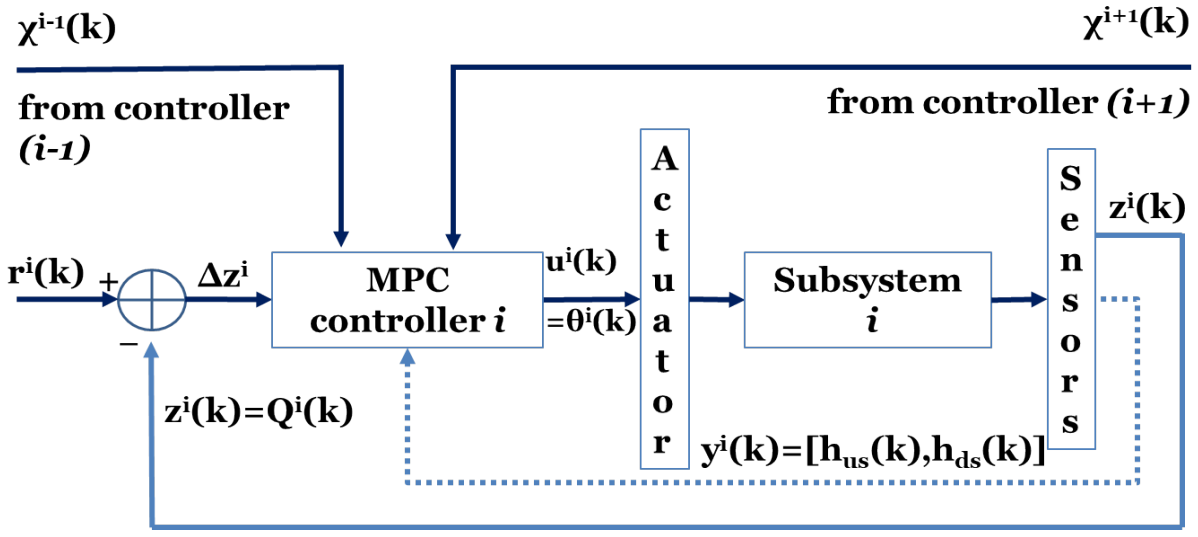

Fig. 4.3 Variables are involved in the flow rate control of a reach using the MPC method.

4.1.3 Cost function

The regulatory control of irrigation channels expects an automatic adjustment of controlled structures with reliability and durability. For example, a gate will move up and down permanently to regulate the flow rate at the end of a reach close to reference values (set-points). In other words, a local controller seeks to achieve the objectives as follows (see [87, 103]):

- Minimize the deviation of controlled variable from the set-points in order to perform the regularization (first term of Eq(s). (4.22)),
- Minimize the sudden change in deviation of controlled variable (e.g., flow rate) from one control step to the next in order to encourage smooth change of this variable (second term of Eq(s). (4.22)),
- Minimize the change in sequence of computed actions in order to avoid the oscillation (third term of Eq(s). (4.22)).

Therefore, we adopt the following cost function for each controller $^{\textcircled{i}}$:

$$\begin{aligned} J^{\textcircled{i}}(k) = \sum_{n=0}^{(N_p-1)} & (||z^{\textcircled{i}}(k+n|k) - r^{\textcircled{i}}(k)||^2_{Z_1} \\ & + ||\Delta z^{\textcircled{i}}(k+n|k)||^2_{Z_2} \\ & + ||\Delta u^{\textcircled{i}}(k+n|k)||^2_{U_1}) \end{aligned} \tag{4.22}$$

where: $z^{\textcircled{i}}$ is the controlled variable over the prediction horizon N_p, $r^{\textcircled{i}}(k)$ is the set-points, $u^{\textcircled{i}}$ is system input over prediction horizon N_p, and Z_1, Z_2, U_1 are weighting matrices of appropriate dimensions.

In the forthcoming sections, we make use of the optimization problem formulated by Eq(s). (4.22) to discuss different implementation strategies (i.e., decentralized and distributed) and how the cooperative communication among local MPC controllers can be included to improve the performance of the overall system.

4.1.4 Decentralized control algorithm

For a centralized control scheme (as surveyed in [77, 163]), the centralized MPC controller can obtain the measurements from available sensors (e.g., flow meters at downstream of each reach, water level meters around gates), makes the prediction based on the complete system model and determines actions for all controlled structures by optimizing a global cost function [137]. Because the controller has a global view of the system, this implementation can provide good overall performances, but with a high computational complexity and computation delay due to communication issues [144, 14, 137]. To overcome the computational burden, a first choice would be to implement a decentralized scheme [91, 26, 119]. A decentralized MPC approach can divide the control of the global system over multiple controllers. These local controllers operate without being conscious of the presence of other controllers or subsystems [119]. They compute the control action based only on local information without taking into account the

information exchanged with other controllers. For instance, [119] presented the design of a predictive controller for decentralized control of delivery channel and the control performance is tested on an open-canal flow nonlinear model in realistic conditions. In the decentralized predictive control scheme presented in [119], a set of local controllers based on predictive control theory, has been designed for manipulating each gate with the objective of ensuring the water level at the downstream end of each reach close to the set-points under external perturbation conditions, such as on-demand deliveries. [26] introduced a combination of decentralized control and networked control where control loops are closed through a network. In [26], two design methods of decentralized control for non-networked systems were chosen as a base for the design of a controller for the networked systems, the first being an observer-based decentralized control, while the second is the well-known Luenberger combined observer-controller design. For another example, a multi-layer decentralized MPC approach is proposed and designed in [91] for its application to large-scale networked systems. In this work [91], the topology of the controller is structured in two layers and a system partitioning allows to establish a hierarchical flow of information between a set of controllers designed based on the MPC. Therefore, the strategy proposed by [91] results in a centralized optimization problem for considering the global control objectives, followed of a decentralized scheme for reaching the local control objectives. For our case study, the details on the decentralized algorithm construction can be synthesized in Algorithm 4.1.

Algorithm 4.1 Decentralized MPC scheme for a controller C_i.

1: **Inputs**: Initial state $x^{\textcircled{i}}(1)$, initial input $u^{\textcircled{i}}(1)$, predicted perturbation $p^{\textcircled{i}}(k)$ and reference trajectory $r^{\textcircled{i}}(k)$
2: **for** $k = 1 : k_{max}$ **do**
3: **Inputs**: predicted perturbation $p^{\textcircled{i}}(k)$ and reference trajectory $r^{\textcircled{i}}(k)$
4: **measure** the flow rate $Q^{\textcircled{i}}$ at downstream of each reach
5: **estimate** the interaction variable $d^{\textcircled{i}}(k)$ from gate equations (Eq(s). (4.4))
6: **obtain** $U_k^{\textcircled{i}*}(x^{\textcircled{i}}(k))$ by solving optimization problems (Eq(s). (4.22)) for prediction horizon Np under the constraints (Eqs. (4.19) and (4.21))
7: **apply** the first element $u_k^{\textcircled{i}*}$ of $U_k^{\textcircled{i}*}$ to the subsystem
8: **determine** the state $x^{\textcircled{i}}(k+1)$ and outputs $z^{\textcircled{i}}(k), y^{\textcircled{i}}(k)$ at time instant k from (Eq(s). (4.17))
9: **go** to the next step $(k+1)$
10: **end for**

The local MPC controller for each subsystem can be separately designed using the Algorithm 4.1. However, a distributed strategy can improve the global performance by taking into account the interactions among subsystems and the cooperation among controllers.

4.2 Distributed model predictive control using cooperative controllers

We consider the channel comprising a cascade of n reaches interconnected by submerged gates (as shown in Fig. 4.2). To account for the interactions among subsystems, the information exchange among controllers is required (see more details in Section 4.2.1). Assuming that the reliable data exchange among system components are guaranteed (e.g., by an asynchronous consensus process presented in Chapter 3). The cooperation is considered in our DCMPC scheme in such a way that all local objectives of the controllers have to be coordinated towards optimizing global objective (e.g., all controlled variables rapidly reach their set-points). Therefore, a controller needs to know the interaction variables for action computation and the coordination variables (e.g., set-points) for the neighboring cooperation. In consequence, the definition and management of shared information are of great importance for DCMPC scheme.

4.2.1 Definition and management of shared information

The selection of the information shared among controllers depends on the channel setting and system modeling. We consider the downstream configuration of our case study as presented in Section 4.1.1.2. When we couple two reaches ⓘ-1 and ⓘ with a gate controlled by controller C_i, the upstream point $l_{us}^{\text{ⓘ}}$ of the gate also is the downstream point of the reach ⓘ-1, and the downstream point $l_{ds}^{\text{ⓘ}}$ of the gate is the upstream point of the reach ⓘ. The flow rate through the gate, $Q_g^{\text{ⓘ}}$, is computed from the gate equations (Eq(s). (4.4)). In order to determine interaction variable $d^{\text{ⓘ}}$ and to compute the gate opening $\theta^{\text{ⓘ}}$, we may identify from the linearized LB model (Eq(s). (4.17)) and the gate equations (Eq(s). (4.4)) that the necessary information for the exchange among the controllers contains: $\{\varepsilon_1^{\text{ⓘ-1}}(l_{L_{i-1}},k), \varepsilon_2^{\text{ⓘ-1}}(l_{L_{i-1}},k), \varepsilon_3^{\text{ⓘ+1}}(l_{us},k)\}$. The information shared by controller $C^{\text{ⓘ}}$ with its neighbors can be chosen as: $[\varepsilon_3^{\text{ⓘ}}(l_{us},\tau)\ \ \varepsilon_1^{\text{ⓘ}}(l_{L_i},\tau)\ \ \varepsilon_2^{\text{ⓘ}}(l_{L_i},\tau)]^T$. In addition, the gate equations (Eq(s). (4.4)) permit the computation of these interaction variables, once the neighbor controllers share the flow rate Q_g through the gate at their position. For improving the global performance by neighboring cooperation, a controller, C_i, also shares its set-points, $r^{\text{ⓘ}}$. Other variables (e.g., water heights) can appropriately be used as interaction/coordination variables depending on distributed control schemes. Timing for sharing information depends on asynchronization mechanism and also the coordination method for controllers. For example, the exchange of interaction/coordination variables among controllers is considered in Chapter 3 as an information consensus problem and solved by using an asynchronous consensus protocol.

4.2.2 Design of cooperative controllers

The cooperation among controllers can improve the global control performance. In DMPC scheme, accounting for the cooperation requires that all controllers have to compute actions towards optimizing local and global objectives. As an example, the designed controllers in [87, 86] are already cooperative in the way that they are subjected to common constraints. By using

an augmented Lagrangian duality approach, the interconnecting constraints are removed from the local constraint set. They are then added to the cost function under additional linear cost terms and additional quadratic terms using Lagrange multipliers. For our case study, we consider again the channel comprising a cascade of n reaches interconnected by submerged gates (as shown in Fig. 4.2). In order to improve the global performance (e.g., response time of the overall system) of our control application, we aim to minimize the time needed for the controlled variables of all controllers to reach their set-points. The global regularization objective can be expressed by:

$$J_{global}(k) = \sum_{i=1}^{n} |z^{\textcircled{i}}(k) - r^{\textcircled{i}}(k)| \tag{4.23}$$

In the downstream configuration (as shown in Fig. 4.2) and from the gate equations (Eq(s). (4.4)), we observe that the flow rate through the controlled gate, estimated by a controller may be involved in neighbor regularization objective (i.e., the first term of Eq(s). (4.22)). Thus, in the proposed DCMPC scheme, each controller, $\textcircled{i}$, shares the interaction variable, $Q_g^{\textcircled{i}}$, for action computation of upstream neighbor and a coordination variable, $r^{\textcircled{i-1}}$, for the cooperation with downstream neighbor (see Fig. 4.4). As a result, each controller C_i has to optimize local

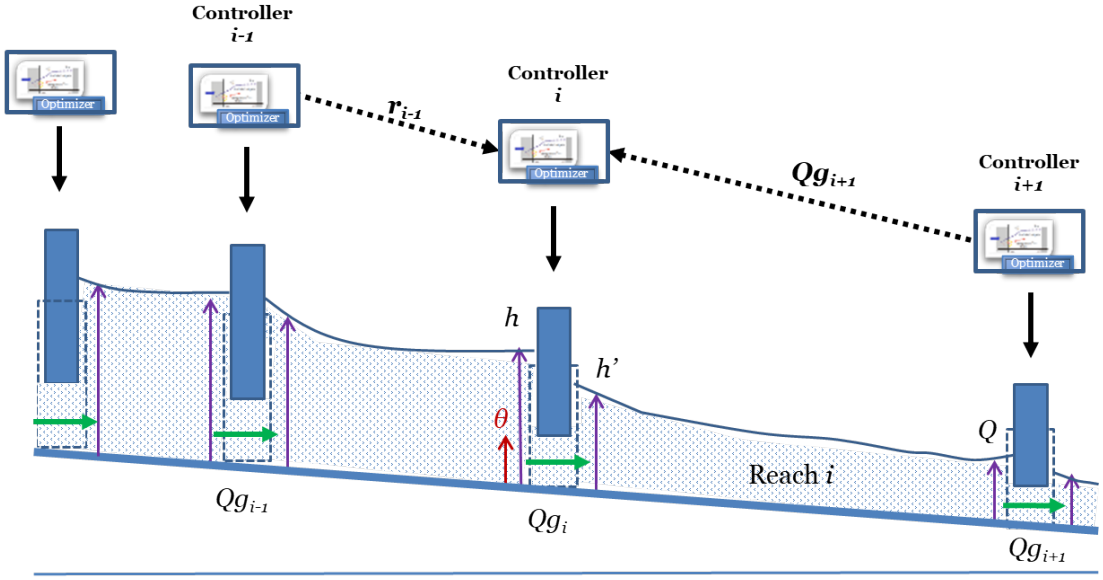

Fig. 4.4 An example of DCMPC scheme in which each controller, $\textcircled{i}$, shares the interaction variable, $Q_g^{\textcircled{i}}$, for action computation of upstream neighbor and a coordination variable, $r^{\textcircled{i-1}}$, for the cooperation with downstream neighbor.

objectives (Eq(s). (4.22)) and also minimize deviations of the estimated flow rate through gate $Q_g^{\textcircled{i}}$ and the upstream neighbor set-points $r^{\textcircled{i-1}}$ for helping the upstream controller to faster reach the regularization objective. Based on Eq(s). (4.22), the cost function of cooperative controller

C_i can be reformulated as follows:

$$\begin{aligned} J^{\textcircled{i}}_{coop}(k) = \sum_{n=0}^{(N_p-1)} & (||z^{\textcircled{i}}(k+n|k) - r^{\textcircled{i}}(k)||^2_{Z_1} \\ & + ||\Delta z^{\textcircled{i}}(k+n|k)||^2_{Z_2} \\ & + ||\Delta u^{\textcircled{i}}(k+n|k)||^2_{U_1} \\ & + ||q^{\textcircled{i}}(k+n|k) - r^{\textcircled{i-1}}(k)||^2_{Q1}) \end{aligned} \tag{4.24}$$

where: $r^{\textcircled{i-1}}(k)$ are the set-points of the reach $\textcircled{i-1}$, $q^{\textcircled{i}}(k)$ is the estimated flow rate through the controlled gate over the prediction horizon N_p, and Q_1 are weighting matrices of appropriate dimensions. The receding horizon control algorithm can be implemented in a distributed (and cooperative) control fashion as summarized in Algorithm 4.2.

Algorithm 4.2 Distributed MPC scheme for n controllers.

1: **for** $\textcircled{i} = 1, \ldots, n$ **do**
2: **Inputs**: Initial state $x^{\textcircled{i}}(1)$, initial input $u^{\textcircled{i}}(1)$
3: **for** $k = 1 : k_{max}$ **do**
4: **Inputs**: predicted perturbation $p^{\textcircled{i}}(k)$ and reference trajectory $r^{\textcircled{i}}(k)$
5: **receive** the flow rate $Q_g^{\textcircled{i+1}}$ through downstream gate from downstream controller $C^{\textcircled{i+1}}$ and the set-points $r^{\textcircled{i-1}}$ of upstream controller $C^{\textcircled{i-1}}$
6: **determine** the interaction variable $d^{\textcircled{i}}(k)$ from gate equations (Eq(s). (4.4))
7: **obtain** $U_k^{\textcircled{i}*}(x^{\textcircled{i}}(k))$ by solving optimization problems (Eq(s). (4.24)) for prediction horizon Np under constraints (Eqs. (4.19) and (4.21))
8: **apply** the first element $u_k^{\textcircled{i}*}$ of $U_k^{\textcircled{i}*}$ to the subsystem
9: **determine** the state $x^{\textcircled{i}}(k+1)$ and outputs $z^{\textcircled{i}}(k), y^{\textcircled{i}}(k)$ at time instant k from (Eq(s). (4.17))
10: **send** the estimated flow rate through gate $Q_g^{\textcircled{i}}(k) = q^{\textcircled{i}}(k) + Q_0$ and set-points $r^{\textcircled{i}}(k+1)$
11: **go** to the next step $(k+1)$
12: **end for**
13: **end for**

4.2.3 Distributed control scheme integrated consensus protocol for cooperative controllers

The asynchronous framework used for the convergence of the information exchanged among controllers is illustrated in Fig. 4.5. In this framework, each controller exchanges information asynchronously and updates its information states with the latest-known (possibly outdated) information from its local neighbors. The information exchange among controllers using the consensus protocol defined by Eq(s). (3.6) allows taking into account the dynamically changing communication topologies, bounded time-varying time delays, and asynchronous mode in the same framework. A controller starts the asynchronous consensus process after applying the

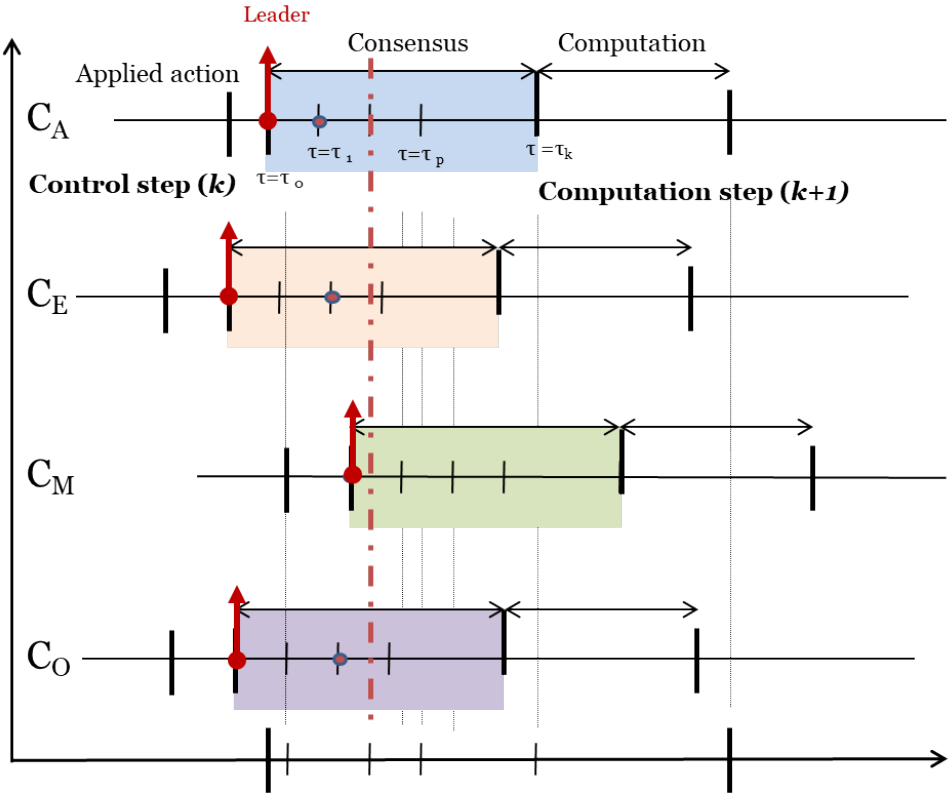

Fig. 4.5 Asynchronous framework for consensus problem in distributed control of irrigation channels. Four controllers C_A, C_E, C_M, C_O are involved in DCMPC scheme. After applying the computed optimal action to the subsystem, the corresponding controller becomes the actual leader and starts a consensus process.

control action to the subsystem, estimating the flow rate through the controlled gate and sending this estimated flow rate. The details of the DCMPC scheme with consensus process can be summarized in Algorithm 4.3. In this scheme, after computed action is applied to the subsystem, the controller becomes the actual leader, which starts a consensus process (see an example in Fig. 3.6). We define a new time scale $\tau \in [\tau_0, \tau_{max})$ for solving consensus problem. As presented in Chapter 3, the asynchronous consensus protocol is designed in order to obtain the convergence of information states of controllers. When the information consensus among controllers is achieved, the controller can wait for the next control step. The speed of reaching a consensus as well as the performance analysis of the consensus protocol are the key in the selection of different time sampling.

The next section provides the simulation of different scenarios and a particular benchmark for the considered irrigation channel.

4.3 Simulation results

This section presents some simulation results of various control schemes for the lab-scale micro-channel presented in Fig. 4.2 with $n = 3$ reaches. For simulations, we first consider *a centralized control scheme* (using a single controller controlling all of considered gates), then *a decentralized*

Algorithm 4.3 Distributed MPC scheme for n controllers with consensus process.

for $\textcircled{i} = 1, \ldots, n$ **do**
  Inputs: Initial state $x^{\textcircled{i}}(1)$, initial input $u^{\textcircled{i}}(1)$
  for $k = 1 : k_{max}$ **do**
    Inputs: predicted perturbation $p^{\textcircled{i}}(k)$ and reference trajectory $r^{\textcircled{i}}(k)$
    receive the flow rate $Q_g^{\textcircled{i+1}}$ through downstream gate from downstream controller $C^{\textcircled{i+1}}$ and the set-points $r^{\textcircled{i-1}}$ of upstream controller $C^{\textcircled{i-1}}$
    determine the interaction variable $d^{\textcircled{i}}(k)$ from gate equations (Eq(s). (4.4))
    obtain $U_k^{\textcircled{i}*}(x^{\textcircled{i}}(k))$ by solving optimization problems (Eq(s). (4.24)) for prediction horizon Np under constraints (Eqs. (4.19) and (4.21))
    apply the first element $u_k^{\textcircled{i}*}$ of $U_k^{\textcircled{i}*}$ to the subsystem (assumed at t_{i_a})
    determine the state $x^{\textcircled{i}}(k+1)$ and outputs $z^{\textcircled{i}}(k), y^{\textcircled{i}}(k)$ at time instant k from (Eq(s). (4.17))
    send estimated flow rate through gate $Q_g^{\textcircled{i}}(k) = q^{\textcircled{i}}(k) + Q_0$ and set-points $r^{\textcircled{i}}(k+1)$
    start *consensus process guaranteeing the estimated flow rate through gate received by other controllers converge to the same value* $Q_g^{\textcircled{i}}(k)$
    for $\tau = \tau_0 : \tau_{max}$ **do**
      $\chi^{\textcircled{i}}(\tau_0) = Q_g^{\textcircled{i}}(k)$
      apply the asynchronous consensus protocol Eq(s). (3.6)
      stop when the convergence conditions Eq(s). (3.7) are satisfied.
    end for
    go to the next step $(k+1)$
  end for
end for

control scheme (using several separate local controllers as presented in Section 4.1.4), *a distributed control scheme* (using several controllers exchanging the flow rates through controlled gate as presented in Section 4.2) and finally *a distributed cooperative control scheme* (using several cooperative controllers exchanging the flow rates through controlled gate and the set-points as detailed in Section 4.2.2). The simulation results of different control approaches are eventually compared according to performance criteria such as the response time, overshoot limit, and computational time. The response time for global performance is defined as the time needed for all reaches to attain $per^{\textcircled{i}} = 95\%, i = \{1,2,3\}$ of their set-points. The overshoot limit is defined as the maximum overshot of three reaches with regards to their set-points. For all simulations, we have used the same parameters (see Table 4.1, Table 4.2) and constraints (see Table 4.3). The simulations were done in Matlab R2016b on a computer Intel®Core™i5-4310U CPU 2.0GHz.

Table 4.1 Structural parameters of lab-scale micro-channel used in simulations.

Length of the reach (L_i)	$7m$
Length until the pumping station (Lp_i)	$4m$
Width of the reach (B_i)	$0.1m$
Bed slope (I_i)	2.6e$-$3
Manning coefficient (n_i)	$1/97$
Performance coefficient of the gate (α_i)	0.8

In order to properly analyze the entire evolution of our system, we have chosen the sampling period: $\Delta t = 0.05\ (s)$, prediction horizon: $N_p = 0.5\ (s)$, communication delay among the

Table 4.2 Simulation parameters of lab-scale micro-channel.

LB parameters	
Spacing step (Δx)	$1m$
Time step (Δt)	$0.05s$
Relaxation time (τ_i)	0.8
Linearization around equilibrium points	
Water height at equilibrium (h_0)	$0.16m$
Boundary conditions	
Upstream water height of the first gate (H_{us})	$0.20m$
Downstream water height of the final gate (H_{ds})	$0.10m$
Simulation parameters	
Simulation time (T)	$45s$
Prediction horizon (N_{pred})	$0.5s$
Weighting matrices (of appropriate dimensions)	$Z_i = Q_i = I,\ U_i = 1$
Set-points (r_i)(m^3/s)	$r_{r1} = 2.6e-3$
	$r_{r2} = 1.8e-3$
	$r_{r3} = 1.0e-3$

Table 4.3 Constraints in the control of lab-scale micro-channel.

Gate opening	$0m \leq \theta \leq 0.5m$
Variation of gate opening	$-0.02m \leq \Delta\theta \leq 0.02m$
Constraints on water heights	$0.10m \leq h \leq 0.25m$
Constraints on state variables	$-0.5 \leq x \leq 0.5$
	$-0.5 \leq \Delta x \leq 0.5$
Constraints on the inputs	$-0.002 \leq u \leq 0.002$
	$-0.004 \leq \Delta u \leq 0.004$

controllers: $Tc = 0.01\ (s)$ and simulation time: $T = 45\ (s)$. For each reach, we assume having constraints on the values of manipulated variable: $\theta_{min} = 0\ (m)$; $\theta_{max} = 0.5\ (m)$; $\Delta\theta_{min} = -0.02\ (m)$; $\Delta\theta_{max} = 0.02\ (m)$. These constraints infer the limits on the inputs and the local states as follows: $-0.002 \leq u \leq 0.002$; $-0.004 \leq \Delta u \leq 0.004$; $-0.5 \leq x \leq 0.5$; $-0.5 \leq \Delta x \leq 0.5$.

The control objective for the reach ⓘ, (denoted by the subscript $ri, i = \{1,2,3\}$) is to keep the downstream flow rate Q_{ri} (with $Q_{ri}(k) = z_{ri}(k) + Q_0$) to the set-points Q_{ri}^{ref} (with $Q_{ri}^{ref}(k) = r_{ri}(k) + Q_0$) by acting on the opening θ_{ri} of the upstream gate. In addition, we also tested the ability of MPC to reject a perturbation. We have considered, for example, a lateral withdrawing at the location $L_p = 4\ (m)$ of each reach with the constant discharge $Q_p = 0.8e-3\ (m^3/s)$, beginning at time instant $k = 5\ (s)$ to the end of the simulation.

As shown in Figs. 4.7 to 4.10, the controlled variables z_{ri}, starting from 0 ($Q_{ri} = Q_0$), have reached the set-points r_{ri} through the use of all four control settings and the computed values of the manipulated variables θ_{ri}, starting from θ_{max}, fully respect the specified constraints (see Fig. 4.11). The performance of each control approach given by the simulation results have been summarized in Table 4.4 and Fig. 4.6.

Table 4.4 Simulation results of different implementation strategies.

Perf. criterion	Resp. time (s)	Overshoot (m^3/s)	Comput. time (s)
Centralized	8.4000	5.3577e-05	31.644207
Decentralized	23.5500	1.2516e-04	26.846662
Distributed	16.6000	2.3128e-04	28.149515
Cooperative	11.6000	1.6854e-04	32.235586

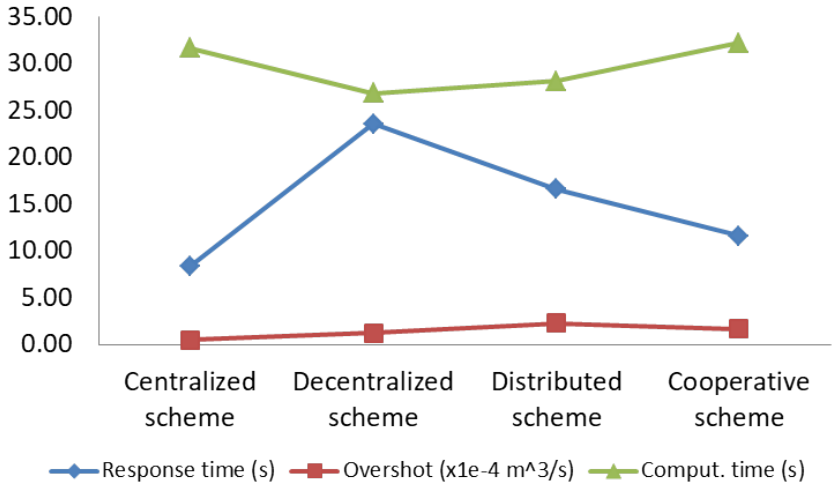

Fig. 4.6 Performance comparison of four MPC settings: centralized, decentralized, distributed and distributed cooperative control.

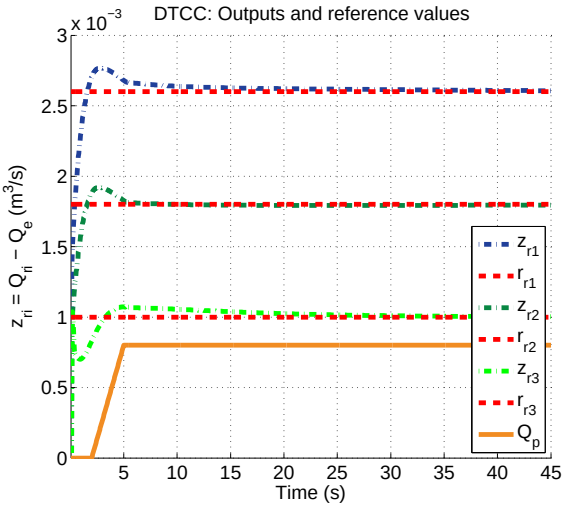

Fig. 4.7 Distributed cooperative control with perturbation Q_p - Variation of downstream flow rates ($z_{ri} = Q_{ri} - Q_0$) with regards to equilibrium points Q_0 of three reaches ($ri = \{r1, r2, r3\}$).

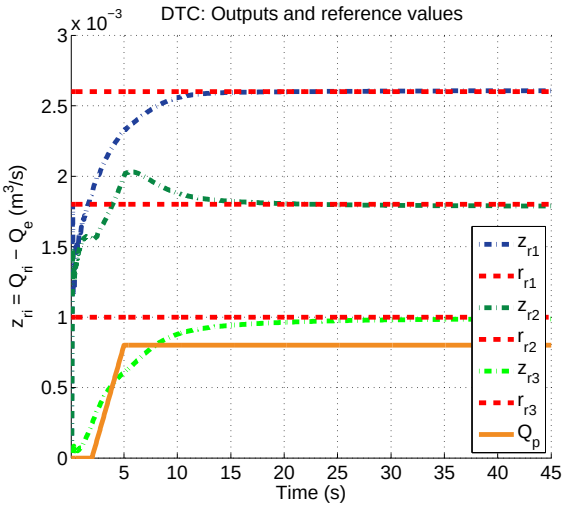

Fig. 4.8 Distributed control with perturbation Q_p - Variation of downstream flow rates ($z_{ri} = Q_{ri} - Q_0$) with regards to equilibrium points Q_0 of three reaches ($ri = \{r1, r2, r3\}$).

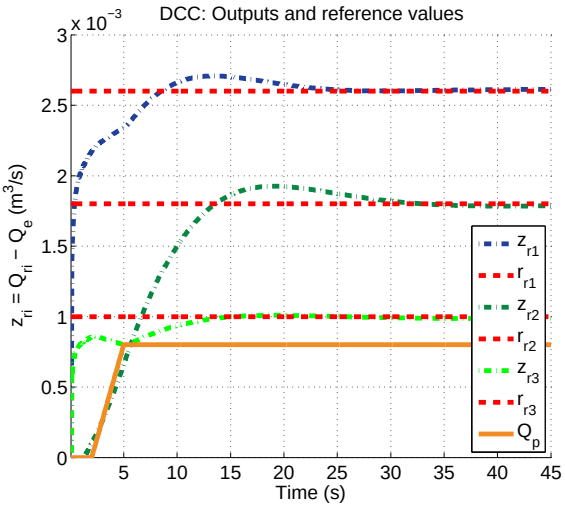

Fig. 4.9 Decentralized control with perturbation Q_p - Variation of downstream flow rates ($z_{ri} = Q_{ri} - Q_0$) with regards to equilibrium points Q_0 of three reaches ($ri = \{r1, r2, r3\}$).

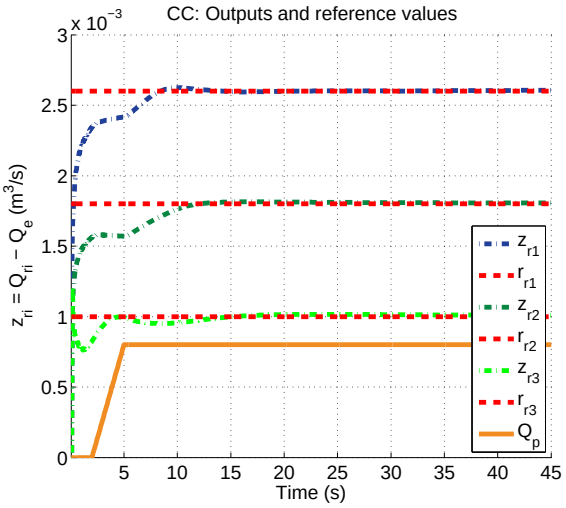

Fig. 4.10 Centralized control with perturbation Q_p - Variation of downstream flow rates ($z_{ri} = Q_{ri} - Q_0$) with regards to equilibrium points Q_0 of three reaches ($ri = \{r1, r2, r3\}$).

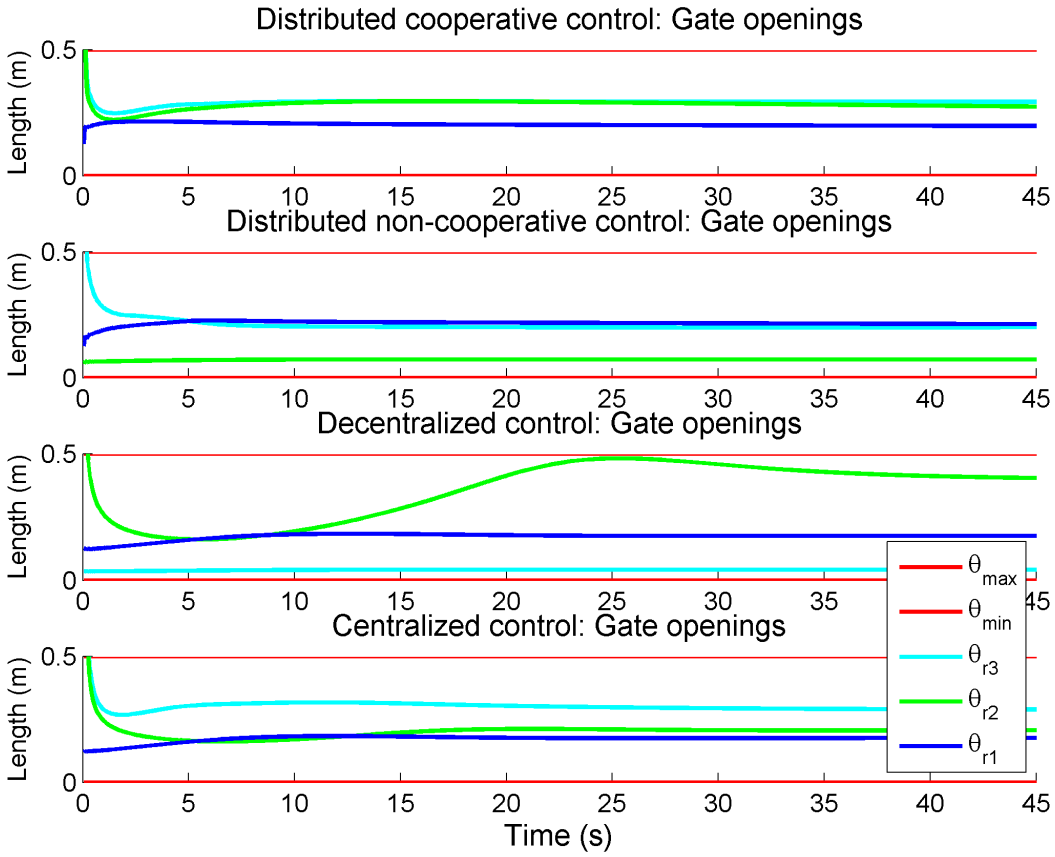

Fig. 4.11 Four control settings with perturbations - Evolution of gate openings (θ_{ri}) of three reaches ($ri = \{r1, r2, r3\}$) respecting the constraints specified in Table 4.3

For the chosen prediction horizon and weighting matrices, we see that:

- In terms of response time, the controlled variable has reached the set-points faster with the centralized and distributed/distributed cooperative schemes compared to the decentralized scheme. In the distributed cooperative scheme, each controller has to optimize local objectives (as in the decentralize scheme) and also minimize the deviations of the estimated flow rate through controlled gate and the set-points of upstream neighbor, so the response time of the overall system is faster than in the decentralized scheme.

- In terms of overshoot limits, the simulations of these schemes have shown that the overshot is more important for distributed and distributed cooperative schemes with regard to the centralized and decentralized schemes.

- For the comparison of the computational time, we have performed the simulations of four schemes in the same operational conditions. However, the distributed cooperative scheme does not provide a decisive advantage in terms of computational time due to the computation of cooperative terms during the prediction horizons (see Eq(s). (4.24) and Algorithm 4.2). In terms of computational time, we concluded that the computational time can be reduced by 16.72% using the decentralized approach, 12.68% using the distributed approach while using a distributed cooperative approach as a reference.

The centralized control presents interesting performances in terms of response time, and overshoot. The decentralized control needs more time for all reaches to attain their objectives. We can deduce that the distributed cooperative control is a good compromise between global control performance and computational speed. In addition, the cooperative strategy gives a shorter response time and smaller overshot with regards to the distributed non-cooperative control. It is also noted that four approaches have rejected external perturbations due to the common use of the MPC method.

Afterward, we have implemented the asynchronous consensus protocol for the distributed control using the DCMPC scheme. The details are presented in Section 4.2.3. For simulations, we re-use the same parameters and constraints as in previous simulations (see Table 4.1, Table 4.2, Table 4.3). To demonstrate the benefits of the consensus process added to DCMPC scheme, we consider two simulation scenarios: a DCMPC scheme with the loss of direct communication and a DCMPC scheme integrated an asynchronous consensus protocol. The first scenario assumes that at $t = 10\ (s)$, controller C_2 does not receive the information shared by controller C_3 during $25\ (s)$ and similarly, at $t = 20\ (s)$, controller C_1 does not receive the information shared by controller C_2 during $25\ (s)$. The second scenario implements the DCMPC scheme as presented in Algorithm 4.3. The simulations of the first scenario are illustrated in Fig. 4.12. For the second scenario, the simulation results are the same as in Fig. 4.7 but with longer computational time. The control performance obtained by simulations of these scenarios have been summarized in Table 4.5. Through the simulation results presented in Fig. 4.13, we see that the consensus process can help the coordination/interaction variables to be updated to the newest values and the controlled variables have reached the set-points. As a result, the control

objectives are still achieved in the distributed control scheme integrated the consensus protocol, but with the robustness of loss of communication.

Table 4.5 Simulation results of different scenarios.

Perf. criterion	Resp. time (s)	Overshoot (m^3/s)	Comput. time (s)
With loss of communication	23.3000	1.6854e-04	28.480434
With integrated consensus	11.6000	1.6854e-04	52.989587
With $N_p = 5s$	11.6500	1.6856e-04	183.914195

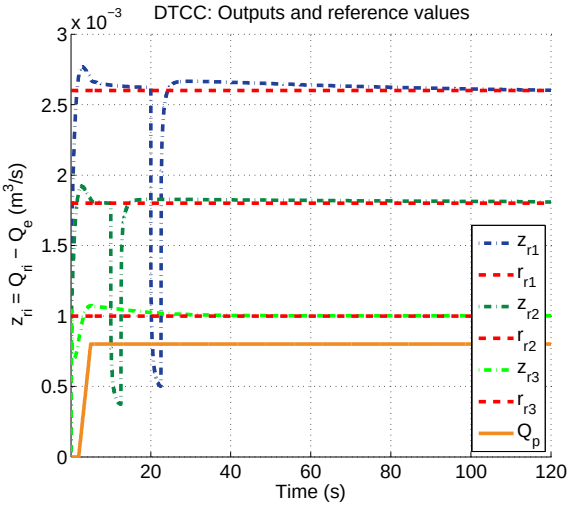

Fig. 4.12 Simulation results - the distributed control of micro-channel with loss of direct communication among controllers.

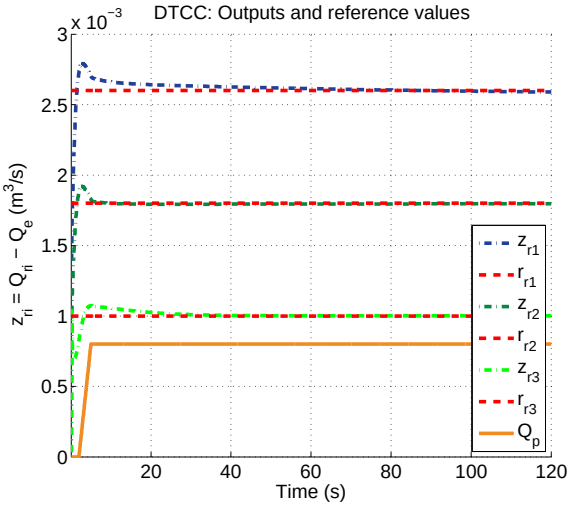

Fig. 4.13 Simulation results - the distributed control of micro-channel with the integrated consensus.

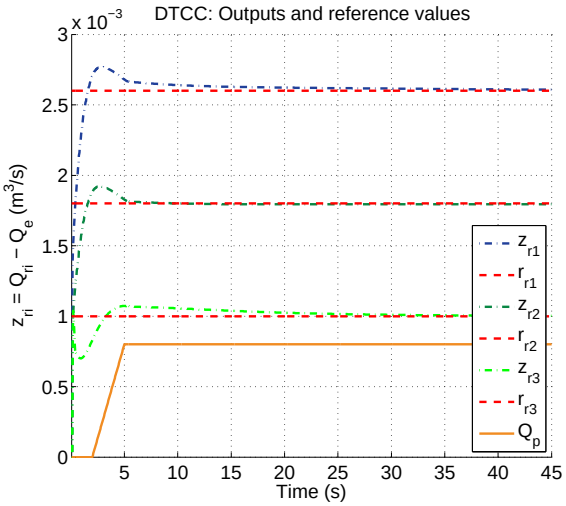

Fig. 4.14 Simulation results - the distributed control of micro-channel with the prediction horizon $N_p = 5s$.

In addition, we have tested the change of the prediction horizons $N_p = 5\ (s)$ in simulations in order to observe the system behaviors. The simulation results presented in Fig. 4.14 show the same behavior as with prediction horizon $N_p = 0.5\ (s)$ presented in Fig. 4.7.

Briefly, the proposed distributed cooperative control combines the optimality of centralized approach and the reduction in terms of computation charge of decentralized approach to provide a good compromise as shown in simulation results.

4.4 Conclusions

This chapter investigated the control of irrigation channels using a distributed cooperative MPC framework. Using the LB method, we have firstly provided a discrete-time linearized model of the irrigation channel that captures its dynamics and the interactions among the subsystems. Different control implementation strategies (e.g., decentralized and distributed strategies) were then discussed and compared. Several simulations over a particular benchmark of the irrigation channel have validated the proposed approaches. The MPC framework used within the four control strategies has demonstrated that: (1) it respects the constraints on the controlled and manipulated variables; (2) it avoids excessive variations on the manipulated variables allowing better use of actuators; and (3) it rejects external perturbations. Future work will concentrate on more comparisons with other linear/nonlinear optimization-based control approaches over different benchmarks available in the literature. Also, different cost criteria and economic MPC implementations will be thoroughly investigated.

Chapter 5

Conclusions and future research

Control applications for water systems are more and more complex due to the inherently distributed nature of these physical systems or due to the spatially integration of heterogeneous devices and communicators with their own control laws and autonomous behaviors. This thesis presents the distributed control of water transport systems such as irrigation channels or water drainage systems. The dynamics of the water transportation in these systems can be represented by shallow water free-surface models. The Lattice Boltzmann (LB) method is used for fluid simulation and mesoscopic description of dynamics. The distributed control of the system involves the exchange of information among the components of the control system (e.g., controllers, sensors, actuators, etc.) and creates certain communication problems. Solving communication problems requires the design of communication network including heterogeneous devices, thus based on a hybrid architecture. Our approach to different Quality of Service requirements of control applications (i.e., the information gathering from sensors, the cooperation of controllers, the transmission of the computed control decision to actuators) is based on the design of a composite metric used by a dynamic routing protocol. An asynchronous information consensus process has been added to the distributed control algorithm to reinforce the robustness to changes in communication topology due to link/node failures and time delays. For the distributed control, an optimization based control has been developed with a cost function accounting for the performance and the cooperation of controllers, while encouraging smooth change in the controlled variables and avoiding oscillations. The details of these points described throughout several chapters are briefly outlined as follows:

- **Discrete-time nonlinear LBM model of irrigation channels**: Chapter 1 was dedicated to the component-based modeling of the irrigation channels using the Lattice Boltzmann method and mathematical relations. Modularity in modeling involves the modularized and parameterized modeling technique and the creation of *Model Library*. The proposed modular approach can reduce the system design and review cycle and significantly improve the design consistency of a large-scale system. In simulation, it takes less time and enables a more efficient co-simulation. The model had a decisive role in the understanding, and diagnosis of irrigation channels.

- **Dynamic routing design for networked control systems using hybrid architecture**: Chapter 2 has investigated the design of a hybrid network to cope with the heterogeneity of wide-area networked control systems and a composite metric for the dynamic routing over this hybrid network in order to satisfy some QoS requirements. The resulting network model can be used to dynamically compute the QoS-related costs (or probabilities) of different paths among the components of networked control systems (NCSs). These are important concerns while considering the information exchange in NCSs.

- **Asynchronous information consensus for networked control systems**: Chapter 3 has focused on solving updating problems of the information shared by controllers in a networked control system with communication constraints. These problems are considered as a consensus problem. The design of a distributed cooperative MPC scheme and an appropriate asynchronous consensus protocol is presented such that the shared information among controllers asymptotically converges to the newest values.

- **Distributed cooperative MPC framework**: Chapter 4 has implemented and compared different control schemes in which costs, constraints, profiles are taken into account in decentralized and distributed constrained optimization problems (i.e., via an MPC design). The cooperation among local MPC controllers has been included in order to improve the performance of the overall system.

At some points, this thesis is considered to have following contributions:

- using the LB method for fluid simulation, we provide a Model Library for the hydraulic components in large-scale irrigation systems, suitably designed to capture the dynamics and interactions among the subsystems;

- to address challenging QoS requirements of control applications in network design, we show that several performance criteria related to the communication needs for control applications can be optimized by using the metric composition approach;

- for the convergence of shared information among controllers, we design an asynchronous consensus protocol and establish conditions for a class of "leader-followers" systems to asymptotically reach the consensus under fixed or time-varying directed communication topology;

- we propose a global topology for the "leader-switching" system (representing a more practical control system) to satisfy multiple consensus problems;

- we integrate the consensus process into the DCMPC algorithm

- we propose a decentralized implementation of control system where the local MPC controller for each subsystem is separately designed. They compute the action using only the local information;

- the distributed cooperative controllers are designed by taking into account the information of neighboring controllers (e.g., the output and reference value) to compute the action.

They cooperate with their neighbors by minimizing the influence of the applied action with regularization objective of their neighbors;

- extensive simulation results are provided through different scenarios which validate the proposed predictive control schemes and highlights their strengths and weakness in terms of global performances.

This thesis provides a first analysis for some problems related to the distributed control of cooperative systems based on the concepts from control, computer science, telecommunication and multi-agent theories. This joint approach to networked control systems (NCSs) will make possible the realization of robust and efficient control/supervision with strong constraints, as well as the emergence of new and attractive applications. However, although the layered approach adopted in this thesis holds the potential to solve complex problems using collective intelligence, there still exist many research issues to study and experimental validations to carry on.

Some perspectives of this work for future research are to:

- in the short term,
  - analyze quantitatively and qualitatively the characteristic of the distributed cooperative approach,
  - study the behavior of the control system in degraded mode; particularly, the contribution of the distributed cooperative approach with regards to the classical approach;
  - use more complex models of the irrigation systems and integrate the interaction with the environment (e.g., weather forecasting, water losses, etc.) to better represent the phenomena related to hydraulics of the water flow;
  - study the effects of uncertainties on the proposed control algorithms and the robustness against these uncertainties;
  - determine the convergence time of the consensus approach depending to the characteristics of the networks;
  - study the effects of the losses in communication networks and propose the possibility of network reconfiguration;
  - study the influence of the consensus on the performance of distributed cooperative control.
- for future projects,
  - perform the operational management of Bourne irrigation channel (extended over 46 km) for the optimal distribution of water resources; the optimal balance of electricity production and consumption (pumping versus turbine), which has represented a differential of 80 000 € in 2016 by SID - Syndicat d'Irrigation Drômois;
  - manage the architecture of networked control systems for the valves and pumping stations of the Bourne canal by a proprietary LoRa® network (actually, the communication equipped with redundant GSM links, and thus, depended on an operator has represented a communication budget of 60 000 €/year in 2015);

– modernize the irrigation and drainage systems in the Mekong Delta (Vietnam) with the scalability and complexity issues (e.g., CARE project). The Mekong Delta is a vast maze of rivers, swamps, islands, and villages surrounded by rice paddies. This region encompasses a large area of over $40,500\ km^2$ and 2.6 million hectares of irrigated land for agriculture.

References

[1] Minar El-Aaasser and Mohamed Ashour. "Energy Aware Classification for Wireless Sensor Networks Routing". In: *15th International Conference on Advanced Communication Technology (ICACT 2013)* (2013), pp. 66–71. ISSN: 1738-9445.

[2] Abdelkader Abdessameud, Abdelhamid Tayebi, and Ilia G. Polushin. "Leader-Follower Synchronization of Euler-Lagrange Systems With Time-Varying Leader Trajectory and Constrained Discrete-Time Communication". In: *IEEE Transactions on Automatic Control* 62.5 (2017), pp. 2539–2545.

[3] Aftab Ahmad and Shahbaz Khan. "Water and Energy Scarcity for Agriculture: Is Irrigation Modernization the Answer?" In: *Journal of Irrigation and Drainage* 66.1 (2017), pp. 34–44. ISSN: 15310361. DOI: 10.1002/ird.2021.

[4] Rajeev Alur et al. "Compositional modeling and analysis of multi-hop control networks". In: *IEEE Transactions on Automatic Control* 56.10 (2011), pp. 2345–2357. ISSN: 00189286. DOI: 10.1109/TAC.2011.2163873.

[5] Randal W. Beard. "Synchronization of Information in Distributed Multiple Vehicle Coordinated Control". In: *IEEE Conference on Decision and Control*. Maui, Hawaii, 2003.

[6] Gilles Belaud et al. "Hydraulic Modeling of an Automatic Upstream Water Level Control Gate for Submerged Flow Conditions". In: *Journal of Irrigation and Drainage Engineering* 134.3 (2008), pp. 315–326. ISSN: 0733-9437. DOI: 10.1061/(ASCE)0733-9437(2008)134:3(315).

[7] Alberto Bemporad, Maurice Heemels, and Mikael Johansson. *Networked Control Systems*. Springer-Verlag Berlin Heidelberg, 2010. ISBN: 9783540370116.

[8] Dimitri P. Bertsekas and John N. Tsitsiklis. *Parallel and Distributed Computation: Numerical Methods*. Prentice-Hall, Englewood Cliffs, NJ, 1989.

[9] Francesco Borrelli, Alberto Bemporad, and Manfred Morari. *Predictive Control for linear and hybrid systems*. Cambridge University Press, 2017.

[10] Julio H. Braslavsky, Richard H. Middleton, and James S. Freudenberg. "Feedback Stabilization over Signal-to-Noise Ratio Constrained Channels". In: *IEEE Transactions on Automatic Control* XX.8 (2007), pp. 1391–1403.

[11] Charles M . Burt and Styles W. Stuart. "Modern water control and management practices in irrigation: Impact on performance". In: *Water Report* 19 (1999), p. 244.

[12] Filipe A. D. M. Cadete. "Distributed LQG control of a water delivery canal". In: *19th Mediterraneam Control Conference on Control and Automation.* Corfu, Greece, 2011.

[13] Eduardo Camponogara et al. "Distributed model predictive control". In: *IEEE Control Systems Magazine* 22.1 (2002), pp. 44–52. ISSN: 02721708. DOI: 10.1109/37.980246.

[14] By Michael Cantoni et al. "Control of Large-Scale Irrigation Networks". In: *Proceedings of the IEEE*. Vol. 95. 1. 2007.

[15] Yongcan Cao et al. "An overview of recent progress in the study of distributed multi-agent coordination". In: *IEEE Transactions on Industrial Informatics* 9.1 (2013), pp. 427–438. ISSN: 15513203. DOI: 10.1109/TII.2012.2219061. arXiv: 1207.3231.

[16] Silvia Capone et al. "An Energy Efficient and Reliable Composite Metric for RPL Organized Networks". In: *Proceedings of International Conference on Embedded and Ubiquitous Computing* (2014), pp. 178–184. DOI: 10.1109/EUC.2014.33.

[17] Lin-Huang Chang et al. "Energy-Efficient Oriented Routing Algorithm in Wireless Sensor Networks". In: *IEEE International Conference on Systems, Man, and Cybernetics*. 2013, pp. 3813–3818. ISBN: 978-1-4799-0652-9. DOI: 10.1109/SMC.2013.651.

[18] Phillipe Charbonnaud, Francisco J. Carrillo, and Eric Duviella. "A supervised robust predictive multi-controller for large operating conditions of an open-channel system". In: *IFAC Proceedings Volumes* 18.PART 1 (2011), pp. 4620–4625. ISSN: 14746670. DOI: 10.3182/20110828-6-IT-1002.03203.

[19] Bastien Chopard and Michel Droz. *Cellular automata modeling of physical systems*. 2012. DOI: 10.1017/CBO9780511549755.

[20] Panagiotis D. Christofides et al. "Distributed model predictive control: A tutorial review and future research directions". In: *Computers and Chemical Engineering* 51 (2013), pp. 21–41. ISSN: 00981354. DOI: 10.1016/j.compchemeng.2012.05.011.

[21] Ahmad W. Al-Dabbagh and Tongwen Chen. "Design Considerations forWireless Networked Control Systems". In: *IEEE Transactions on Industrial Electronics* 63.9 (2016), pp. 2–209. DOI: 10.4271/610588.

[22] Zeleke A. Dejen. "Hydraulic and Operational Performance of Irrigation System in View of Interventions for Water Saving and Sustainability". PhD thesis. Wageningen University, 2014. ISBN: 9781138027671.

[23] Frederik Deroo et al. "Distributed control design with local model information and guaranteed stability". In: *19th World Congress The International Federation of Automatic Control*. Cape Town, South Africa, 2014, pp. 4010–4017.

[24] Gianni Di Girolamo, Alessandro D'Innocenzo, and Maria Domenica Di Benedetto. "Co-design of controller and routing redundancy over a wireless network". In: *IFAC-PapersOnLine* 48.22 (2015), pp. 100–105. ISSN: 24058963. DOI: 10.1016/j.ifacol.2015.10.314.

[25] Valerie Dos Santos Martins, Mickael Rodrigues, and Mamadou Diagne. "A multi-model approach to Saint-Venant Equations: A stability study by LMIs". In: *International Journal of Appl. Math. Comput. Science* 22.3 (2012), pp. 539–550. ISSN: 1641876X. DOI: 10.2478/v10006-012-0041-6.

[26] Ahmed Elmahdi et al. "Decentralized Control Framework and Stability Analysis for Networked Control Systems". In: *Journal of Dynamic Systems, Measurement, and Control* 137.5 (2015), p. 051006. ISSN: 0022-0434. DOI: 10.1115/1.4028789.

[27] Lei Fang. "Cooperative Control of Multi-Agent Systems with Information Flow Contraints". PhD thesis. University of Notre Dame, 2006.

[28] Lei Fang and Panos J. Antsaklis. "Information consensus of asynchronous discrete-time multi-agent systems". In: *Proceedings of the 2005, American Control Conference, 2005.* (2005), pp. 1883–1888. ISSN: 0743-1619. DOI: 10.1109/ACC.2005.1470243.

[29] Lei Fang and Panos J. Antsaklis. "On Communication Requirements for Multi-agent Consensus Seeking". In: *2005 Workshop on Networked Embedded Sensing and Control* (2005), pp. 53–68.

[30] Carlo Fischione et al. "Design principles of wireless sensor networks protocols for control applications". In: *Wireless Networking Based Control* 2010.May (2011), pp. 203–238. DOI: 10.1007/978-1-4419-7393-1_9.

[31] Giuseppe Franzè, Walter Lucia, and Francesco Tedesco. "A distributed model predictive control scheme for leader–follower multi-agent systems". In: *International Journal of Control* 7179.June (2017), pp. 1–14. ISSN: 0020-7179. DOI: 10.1080/00207179.2017.1282178.

[32] Andreas Frommer and Daniel B Szyld. “On asynchronous iterations”. In: *Journal of Computational and Applied Mathematics* 123.1-2 (2000), pp. 201–216. ISSN: 03770427. DOI: 10.1016/S0377-0427(00)00409-X.

[33] Lixin Gao et al. “Leader-following consensus for discrete-time descriptor multi-agent systems with observer-based protocols”. In: *Transactions of the Institute of Measurement and Control* 38.11 (2016), pp. 1353–1364. ISSN: 0142-3312. DOI: 10.1177/0142331215588807.

[34] Yanping Gao and Long Wang. “Asynchronous consensus of continuous-time multi-agent systems with intermittent measurements”. In: *International Journal of Control* 83.3 (2010), pp. 552–562. ISSN: 0020-7179. DOI: 10.1080/00207170903297192.

[35] Yanping Gao et al. “Asynchronous consensus of multiple second-order agents with partial state information”. In: *International Journal of Systems Science* 44.5 (2013), pp. 966–977. ISSN: 0020-7721. DOI: 10.1080/00207721.2011.651171.

[36] Igor Gejadze and Pierre-Olivier Malaterre. “Discharge estimation under uncertainty using variational methods with application to the full Saint-Venant hydraulic network model”. In: *International Journal for Numerical Methods in Fluids* 83 (2016), pp. 601–629. ISSN: 02712091. DOI: 10.1002/fld.4273. arXiv: fld.1 [DOI: 10.1002].

[37] Mohamed G. Gouda and Marco Schneider. “Maximizable routing metrics”. In: *IEEE/ACM Transactions on Networking* 11.4 (2003), pp. 663–675. ISSN: 10636692. DOI: 10.1109/TNET.2003.815294.

[38] Zhaoli Guo, Chuguang Zheng, and Baochang Shi. “Discrete lattice effects on the forcing term in the lattice Boltzmann method”. In: *Physical Review E - Statistical, Nonlinear, and Soft Matter Physics* 65.4 (2002), pp. 1–6. ISSN: 15393755. DOI: 10.1103/PhysRevE.65.046308.

[39] Rachana A. Gupta. *Hydrology and Hydraulic Systems: Fourth Edition*. 2016. ISBN: 9781478634218.

[40] Rachana Ashok Gupta and Mo-Yuen Chow. “Networked Control System: Overview and Research Trends”. In: *IEEE Transactions on Industrial Electronics* 57.7 (2010), pp. 2527–2535. ISSN: 0278-0046. DOI: 10.1109/TIE.2009.2035462.

[41] Xiaoyi He and Qisu Zou. “Analysis and boundary condition of the lattice Boltzmann BGK model with two velocity components”. In: *arXiv eprint* (1995), pp. 1–13. arXiv: 9507002 [comp-gas].

[42] W. P. Maurice H. Heemels et al. “Networked control systems with communication constraints: Tradeoffs between transmission intervals, delays and performance”. In: *IEEE Transactions on Automatic Control* 55.8 (2010), pp. 1781–1796. ISSN: 00189286. DOI: 10.1109/TAC.2010.2042352.

[43] Christopher D. Hollander. “Information Propagation Algorithms for Consensus Formation in Decentralized Multi-Agent Systems”. PhD thesis. University of Central Florida, 2015.

[44] Roger A. Horn and Charles R. Johnson. *Matrix analysis*. New York: Cambridge University Press, 2013, p. 607. ISBN: 978-0-521-54823-6. DOI: 10.1002/1521-3773(20010316)40:6<9823::AID-ANIE9823>3.3.CO;2-C. arXiv: arXiv:1011.1669v3.

[45] Klaudia Horvath et al. “New offset-free method for model predictive control of open channels”. In: *Control Engineering Practice* 41 (2015), pp. 13–25. ISSN: 09670661. DOI: 10.1016/j.conengprac.2015.04.002.

[46] Jose M. Igreja, Filipe M. Cadete, and Joao M. Lemos. “Application of distributed model predictive control to a water delivery canal”. In: *19th Mediterranean Conference on Control & Automation (MED)*. 2011, pp. 682–687. ISBN: 978-1-4577-0124-5. DOI: 10.1109/MED.2011.5983126.

[47] Ali Jadbabaie, Jie Lin, and Stephen A. Morse. "Coordination of mobile autonomous agents using nearest neighbor rules". In: *IEEE Transactions on Automatic Control* 48.9 (2003), pp. 988–1001. ISSN: 0018-9286. DOI: 10.1109/TAC.2003.812781.

[48] Patrick Olivier Kamgueu et al. *Energy-based routing metric for RPL*. Tech. rep. 2013, pp.14.

[49] Patrick Olivier Kamgueu et al. "Fuzzy-based routing metrics combination for RPL To cite this version :" in: *Doctoral Consortium Sensornets* (2014), p. 8.

[50] Karan Kansara et al. "Sensor based Automated Irrigation System with IOT : A Technical Review". In: *International Journal of Computer Science and Information Technologies* 6 (2016), pp. 2–5. DOI: 10.13140/RG.2.1.3342.3129.

[51] Panagiotis Karkazis et al. "Evaluating routing metric composition approaches for QoS differentiation in low power and lossy networks". In: *Wireless Networks* 19.6 (2013), pp. 1269–1284. ISSN: 10220038. DOI: 10.1007/s11276-012-0532-2.

[52] Yunseop Kim, Robert G. Evans, and William M. Iversen. "Remote Sensing and Control of an Irrigation System Using a Distributed Wireless Sensor Network". In: *IEEE Transactions on Instrumentation and Measurement* 57.7 (2008), pp. 1379–1387. ISSN: 0018-9456. DOI: 10.1109/TIM.2008.917198.

[53] Victor S. Kozyakin. "A short introduction to asynchronous systems". In: *Proceedings of the Sixth International Conference on Difference Equations* 00 (2004), pp. 153–165.

[54] Timm Kruger et al. *The Lattice Boltzmann Method*. 2017. ISBN: 978-3-319-44647-9. DOI: 10.1007/978-3-319-44649-3.

[55] Vinay Kumar and Sudarshan Tiwari. "Routing in IPv6 over low-power wireless personal area networks (6LoWPAN): A survey". In: *Journal of Computer Networks and Communications* (2012). ISSN: 20907141. DOI: 10.1155/2012/316839.

[56] Alexander L. Kupershtokh. "A lattice Boltzmann equation method for real fluids with the equation of state known in tabular form only in regions of liquid and vapor phases". In: *Computers and Mathematics with Applications* 61.12 (2011), pp. 3537–3548. ISSN: 08981221. DOI: 10.1016/j.camwa.2010.06.032.

[57] Yasuhiro Kuriki and Toru Namerikawa. "Consensus-based Cooperative Formation Control with Collision Avoidance for a Multi-UAV System". In: *American Control Conference (ACC)*. Portland, Oregon, USA, 2014, pp. 2077–2082. ISBN: 9781479932740.

[58] Kooktae Lee and Raktim Bhattacharya. "Convergence Analysis of Asynchronous Consensus in Discrete-time Multi-agent Systems with Fixed Topology". In: *eprint arXiv* (2016). arXiv: 1606.04156.

[59] Kooktae Lee and Raktim Bhattacharya. "Stability Analysis of Large-Scale Distributed Networked Control Systems with Random Communication Delays : A Switched System Approach". In: *Systems & Control Letters* 85 (2015), pp. 77–83. arXiv: arXiv:1503.03047v1.

[60] Lulu Li, Daniel Ho, and Jianquan Lu. "Event-based network consensus with communication delays". In: *Nonlinear Dynamics* 87.3 (2017), pp. 1847–1858. ISSN: 0924-090X. DOI: 10.1007/s11071-016-3157-7.

[61] Meng Li and Yong Chen. "Robust Tracking Control of Networked Control Systems With Communication Constraints and External Disturbance". In: *IEEE Transactions on Industrial Electronics* 64.5 (2017), pp. 4037–4047. ISSN: 0278-0046. DOI: 10.1109/TIE.2017.2652398.

[62] Mo Li, Zhenjiang Li, and Athanasios V Vasilakos. "A survey on topology control in wireless sensor networks: Taxonomy, comparative study, and open issues". In: *Proceedings of the IEEE* 101.12 (2013), pp. 2538–2557. ISSN: 00189219. DOI: 10.1109/JPROC.2013.2257631.

[63] Yuping Li and Bart De Schutter. "Performance analysis of irrigation channels with distributed control". In: *Proceedings of the IEEE International Conference on Control Applications*. 2010, pp. 2148–2153. ISBN: 9781424453627. DOI: 10.1109/CCA.2010.5611113.

[64] Zhongkui Li et al. "Designing Fully Distributed Consensus Protocols for Linear Multi-Agent Systems with Directed Graphs". In: *IEEE Transactions on Automatic Control* 60.4 (2015), pp. 1152–1157. ISSN: 00189286. DOI: 10.1109/TAC.2014.2350391. arXiv: 1312.7377.

[65] Xiao Liang, Juanjuan Xu, and Huanshui Zhang. "Optimal Control and Stabilization for Networked Control Systems with Packet Dropout and Input Delay". In: *IEEE Transactions on Circuits and Systems II: Express Briefs* 7747.c (2016), p. 1. ISSN: 1549-7747. DOI: 10.1109/TCSII.2016.2642986. URL: http://ieeexplore.ieee.org/document/7792690/.

[66] Peng Lin, Wei Ren, and Jay A. Farrell. "Distributed Continuous-time Optimization: Nonuniform Gradient Gains, Finite-time Convergence, and Convex Constraint Set". In: *IEEE Transactions on Automatic Control* PP.99 (2016), pp. 2239–2253. ISSN: 00189286. DOI: 10.1109/TAC.2016.2604324.

[67] Xavier Litrico and Vincent Fromion. *Modeling and Control of Hydrosystems*. Springer-Verlag London Limited, 2009. ISBN: 9781848826236.

[68] Xavier Litrico et al. "Experimental validation of a methodology to control irrigation canals based on Saint-Venant equations". In: *Control Engineering Practice* 13.11 (2005), pp. 1425–1437. ISSN: 09670661. DOI: 10.1016/j.conengprac.2004.12.010.

[69] Feng Liu, Chi Ying Tsui, and Ying Jun Zhang. "Joint routing and sleep scheduling for lifetime maximization of wireless sensor networks". In: *IEEE Transactions on Wireless Communications* 9.7 (2010), pp. 2258–2267. ISSN: 15361276. DOI: 10.1109/TWC.2010.07.090629.

[70] Haifei Liu et al. "Lattice Boltzmann method for the Saint-Venant equations". In: *Journal of Hydrology* 524.May (2015), pp. 411–416. ISSN: 00221694. DOI: 10.1016/j.jhydrol.2015.03.002.

[71] Xiaoyu Liu et al. "Leader-following consensus for discrete-time multi-agent systems with parameter uncertainties based on the event-triggered strategy". In: *Journal of Systems Science and Complexity* 30.1 (2017), pp. 30–45. ISSN: 15597067. DOI: 10.1007/s11424-017-6272-8.

[72] María Guinaldo Losada, Sebastián Dormido Bencomo, and Francisco Rodríguez Rubio. *Asynchronous Control for Networked Systems*. Switzerland: Springer International Publishing, 2015. ISBN: 978-3-319-21298-2 978-3-319-21299-9.

[73] David Lozano et al. "Simulation of automatic control of an irrigation canal". In: *Agricultural Water Management* 97.1 (2010), pp. 91–100. ISSN: 03783774. DOI: 10.1016/j.agwat.2009.08.016.

[74] Qingguo Lu, Huaqing Li, and Dawen Xia. "Distributed optimization of first-order discrete-time multi-agent systems with event-triggered communication". In: *Neurocomputing* 235.August 2016 (2017), pp. 255–263. ISSN: 18728286. DOI: 10.1016/j.neucom.2017.01.021.

[75] Boris Lubachevsky and Debasis Mitra. "A Chaotic Asynchronous Algorithm for Computing the Fixed Point of a Nonnegative Matrix of Unit Spectral Radius". In: *Journal of the ACM* 33.1 (Jan. 1986), pp. 130–150. ISSN: 0004-5411. DOI: 10.1145/4904.4801. URL: http://doi.acm.org/10.1145/4904.4801.

[76] Ji Ma et al. "Leader-following consensus of multi-agent systems with limited data rate". In: *Journal of the Franklin Institute* 354.1 (2017), pp. 184–196. ISSN: 00160032. DOI: 10.1016/j.jfranklin.2016.10.005.

[77] Pierre-Olivier Malaterre. "Control of irrigation canals: why and how?" In: *International Journal for Numerical Modeling of Hydrodynamics for Water Resources* (2007), pp. 271–292.

[78] Pierre-Olivier Malaterre, David Dorchies, and Jean-Pierre Baume. "La modernisation des canaux d'irrigation : apports de l'automatisation pour la gestion opérationnelle". In: *Sciences Eaux & Territoires n°11* (2013), pp. 44–47.

[79] Olivier Marcou. "Modélisation et contrôle d'écoulements à surface libre par la méthode de Boltzmann sur réseau". PhD thesis. Univ. de Genève, 2010.

[80] Iven Mareels et al. "Systems engineering for irrigation systems: Successes and challenges". In: *Annual Reviews in Control* 29.2 (2005), pp. 191–204. ISSN: 13675788. DOI: 10.1016/j.arcontrol.2005.08.001.

[81] Steven L. Markstrom et al. "GSFLOW—Coupled Ground-Water and Surface-Water Flow Model Based on the Integration of the Precipitation-Runoff Modeling System (PRMS) and the Modular Ground-Water Flow Model (MODFLOW-2005)". In: *U.S. Geological Survey* Techniques and Methods 6-D1 (2008), p. 240.

[82] Mortada Mehyar et al. "Distributed Averaging on Asynchronous Communication Networks". In: *IEEE/ACM Transactions on Networking* 15.3 (2007).

[83] Carl D. Meyer. "Chapter 8: Perron-Frobenius Theory of Nonnegative Matrices". In: *Matrix analysis and applied linear algebra*. Society for Industrial and Applied Mathematics, 2000, pp. 661–704. ISBN: 0898714540.

[84] Aliasghar Montazar and Saeed Isapoor. "Centralized Downstream PI controllers for the west canal of Aghili irrigation district". In: *Journal of Agricultural Science and Technology* 14.2 (2012), pp. 375–388. ISSN: 16807073.

[85] Luc Moreau. "Stability of multiagent systems with time-dependent communication links". In: *IEEE Transactions on Automatic Control* 50.2 (2005), pp. 169–182. ISSN: 00189286. DOI: 10.1109/TAC.2004.841888.

[86] Rudy R. Negenborn, Peter-Jules van Overloop, and Bart De Schutter. "Coordinated model predictive reach control for irrigation canals". In: *Proceedings of the European Control Conference*. Vol. 2009. August. 2009, pp. 1420–1425. ISBN: 9789633113691.

[87] Rudy Negenborn et al. "Distributed model predictive control of irrigation canals". In: *Networks and Heterogeneous Media* 4.2 (2009), pp. 359–380. ISSN: 1556-1801. DOI: 10.3934/nhm.2009.4.359.

[88] Lai Nguyen et al. "Distributed Model Predictive Control of Irrigation Systems using Cooperative Controllers". In: *IFAC 20th World Congress of the International Federation of Automatic Control*. 2017.

[89] Lai Nguyen et al. "Optimal reactive control of hybrid architectures : A case study on complex water transportation systems". In: *19th IEEE International Conference on Emerging Technologies and Factory Automation* 1 (2014). DOI: 10.1109/ETFA.2014.7005109.

[90] Lai Nguyen et al. "Signal-to-noise ratio for irrigation canal networked control system (MSC'2015)". In: *2015 IEEE Conference on Control and Applications, CCA 2015 - Proceedings* (2015), pp. 1637–1643. DOI: 10.1109/CCA.2015.7320844.

[91] Carlos Ocampo-Martinez et al. "Multi-layer Decentralized MPC of Large-scale Networked Systems". In: *Intelligent Systems, Control and Automation: Science and Engineering*. Vol. 69. 2014, pp. 495–515. ISBN: 9789400770058. DOI: 10.1007/978-94-007-7006-5_31.

[92] Tamoghna Ojha, Sudip Misra, and Narendra Singh Raghuwanshi. "Wireless sensor networks for agriculture: The state-of-the-art in practice and future challenges". In: *Computers and Electronics in Agriculture* 118 (2015), pp. 66–84. ISSN: 01681699. DOI: 10.1016/j.compag.2015.08.011. URL: http://dx.doi.org/10.1016/j.compag.2015.08.011.

[93] Reza Olfati-Saber, Alex J. Fax, and Richard M. Murray. "Consensus and Cooperation in Multi-Agent Networked Systems". In: *Proceedings of IEEE* 95.1 (2007), pp. 215–233. ISSN: 0018-9219. DOI: 10.1109/JPROC.2006.887293.

[94] Reza Olfati-Saber and Richard M. Murray. "Consensus problems in networks of agents with switching topology and time-delays". In: *IEEE Transactions on Automatic Control* 49.9 (2004), pp. 1520–1533. ISSN: 00189286. DOI: 10.1109/TAC.2004.834113.

[95] Diemer Anda Ondo, Laurent Lefèvre, and Bastien Chopard. "Discrete controllability of distributed parameters systems using lattice Boltzmann models: An application to the shallow water equations". In: *IFAC Proceedings Volumes (IFAC-PapersOnline)* 18 (2011). ISSN: 14746670. DOI: 10.3182/20110828-6-IT-1002.02546.

[96] Peter-Jules van Overloop et al. "Human-in-the-Loop Model Predictive Control of an Irrigation Canal". In: *IEEE Control Systems* 35.4 (2015), pp. 19–29. ISSN: 1066033X. DOI: 10.1109/MCS.2015.2427040.

[97] Pangun Park and Karl Henrik Johansson. "Wireless Networked Control System Co-Design". In: *International Conference on Networking, Sensing and Control*. April. 2011, pp. 11–13. ISBN: 9781424495733.

[98] van Thang Pham et al. "Study of the 1D lattice Boltzmann shallow water equation and its coupling to build a canal network". In: *Journal of Computational Physics* 229.19 (2010), pp. 7373–7400. ISSN: 00219991. DOI: 10.1016/j.jcp.2010.06.022.

[99] Van-Thang Pham, Clément Raïevsky, and Jean-Paul Jamont. "A multiagent approach using model-based predictive control for an irrigation canal". In: *Prism* (2013), pp. 1–8.

[100] Herve Plusquellec, Charles Burt, and Hans W. Vywpter. *Modern Water Control in Irrigation: Concepts, Issues, and Applications*. Tech. rep. 1994, p. 110.

[101] Matthias Pott. "On the convergence of asynchronous iteration methods for nonlinear paracontractions and consistent linear systems". In: *Linear Algebra and its Applications* 283.1-3 (1998), pp. 1–33. ISSN: 00243795. DOI: 10.1016/S0024-3795(98)10060-5.

[102] Vicenç Puig and Rudy R. Negenborn. "Model predictive control for combined water supply and navigability / sustainability in river systems". In: *Transport of Water versus Transport over Water*. Springer International Publishing, 2015, pp. 13–32.

[103] Vicenç Puig et al. "Model predictive control of combined irrigation and water supply systems: Application to the Guadiana river". In: *Proceedings of 9th IEEE International Conference on Networking, Sensing and Control*. 2012, pp. 85–90. ISBN: 978-1-4673-0390-3. DOI: 10.1109/ICNSC.2012.6204896.

[104] Vicenç Puig et al. "Optimal predictive control of water transport systems: Arrêt-Darré/Arros case study". In: *Water Science & Technology Technology* 60.8 (2009), pp. 2125–2133.

[105] Jiahu Qin, Changbin Yu, and Sandra Hirche. "Stationary consensus of asynchronous discrete-time second-order multi-agent systems under switching topology". In: *IEEE Transactions on Industrial Informatics* 8.4 (2012), pp. 986–994. ISSN: 15513203. DOI: 10.1109/TII.2012.2210430.

[106] Jiahu Qin et al. "Recent Advances in Consensus of Multi-Agent Systems: A Brief Survey". In: *IEEE Transactions on Industrial Electronics* 0046.c (2016), p. 1. ISSN: 0278-0046. DOI: 10.1109/TIE.2016.2636810.

[107] Aleksandar Ž. Rakie, Nikola S. Bežanié, and Ivan T. Popovié. "Novel Architecture for Networked Control Systems". In: *International Symposium on Industrial Electronics (INDEL)*. 2016. ISBN: 9781509023295.

[108] Jame B. Rawlings and David Q. Mayne. *Model Predictive Control : Theory and Design*. Nob Hill Pub, 2012, p. 669. ISBN: 9780975937709. DOI: 10.1109/TBME.2009.2039571. arXiv: arXiv:1011.1669v3.

[109] Biao Ren, Jian Ma, and Canfeng Chen. "The hybrid mobile wireless sensor networks for data gathering". In: *Proceeding of the 2006 international conference on Communications and mobile computing - IWCMC '06* (2006), p. 1085. DOI: 10.1145/1143549.1143766.

[110] Wei Ren and Randal W. Beard. "Consensus of information under dynamically changing interaction topologies". In: *Proceedings of the American Control Conference* 6 (2004), pp. 4939–4944. ISSN: 07431619. DOI: 10.1109/ACC.2004.249096.

[111] Wei Ren and Randal W Beard. "Consensus seeking in multiagent systems under dynamically changing interaction topologies". In: *IEEE Transactions on Automatic Control* 50.5 (2005), pp. 655–661. ISSN: 00189286. DOI: 10.1109/TAC.2005.846556.

[112] Wei Ren and Randal W. Beard. "Overview of Consensus Algorithms in Cooperative Control". In: *Distributed Consensus in Multi-Vehicle Cooperative Control: Theory and Applications*. Springer, 2008. ISBN: 978-1-84800-014-8.

[113] Wei Ren, Randal W. Beard, and Ella M. Atkins. "Information Consensus in Multivehicle Cooperative Control". In: *IEEE Control systems magazine* April (2007), pp. 71–82.

[114] Wei Ren and Yongcan Cao. *Distributed Coordination of Multi-agent Networks: Emergent Problems, Models, and Issues*. London: Springer-Verlag, 2011. ISBN: 9780857291684.

[115] Alejandro J. Rojas. "On the infimal Signal-to-Noise Ratio limitations for measurable disturbance rejection". In: *Proceedings of the American Control Conference*. Vol. 2015-July. 2015, pp. 2211–2217. ISBN: 9781479986842. DOI: 10.1109/ACC.2015.7171061.

[116] Alejandro J. Rojas, Julio H. Braslavsky, and Richard H. Middleton. "Fundamental Limitations in Control over a Communication channel". In: *Automatica* January 2008 (2008), pp. 1–13.

[117] Hasan Sajjadi et al. "Lattice Boltzmann method and RANS approach for simulation of turbulent flows and particle transport and deposition". In: *Particuology* 30.July (2017), pp. 62–72. ISSN: 16742001. DOI: 10.1016/j.partic.2016.02.004.

[118] Laura Sanchez and Miguel A. Ridao. "Distributed Control of Irrigation Canals". In: *HD-MPC*. 2010, p. 46.

[119] Salam Sawadogo et al. "Decentralized Predictive Controller for Delivery Canals". In: *Journal des Sciences* (2001).

[120] Pallavi Sethi and Smruti R. Sarangi. "Internet of Things : Architecture, Protocols, and Applications". In: *Journal of Electrical and Computer Engineering* 1.1 (2017), pp. 9–19.

[121] Yilun Shang and Yamei Ye. "Leader-Follower Fixed-Time Group Consensus Control of Multiagent Systems under Directed Topology". In: *Hindawi Complexity* 2017 (2017).

[122] Zach Shelby and Carsten Bormann. *6LoWPAN: the wireless embedded internet*. Vol. 43. John Wiley and Sons, Ltd., 2011. ISBN: 9780470747995.

[123] Long Sheng, Ya-Jun Pan, and Xiang Gong. "Consensus Formation Control for a Class of Networked Multiple Mobile Robot Systems". In: *Journal of Control Science and Engineering* 2012 (2012), pp. 1–12. ISSN: 1687-5249. DOI: 10.1155/2012/150250. URL: http://www.hindawi.com/journals/jcse/2012/150250/.

[124] Zhengguo Sheng et al. "A survey on the IETF protocol suite for the internet of things: Standards, challenges, and opportunities". In: *IEEE Wireless Communications* 20.6 (2013), pp. 91–98. ISSN: 15361284. DOI: 10.1109/MWC.2013.6704479.

[125] Ahmed Sobeih et al. "J-Sim: A simulation and emulation environment for wireless sensor networks". In: *IEEE Wireless Communications* 13.4 (2006), pp. 104–119. ISSN: 15361284. DOI: 10.1109/MWC.2006.1678171.

[126] Joao Luis Sobrinho. "Algebra and algorithms for QoS path computation and hop-by-hop routing in the Internet". In: *IEEE/ACM Transactions on Networking* 10.4 (2002), pp. 541–550. ISSN: 10636692. DOI: 10.1109/TNET.2002.801397.

[127] João Luis Sobrinho. "Network routing with path vector protocols". In: *Proceedings of the conference on Applications, technologies, architectures, and protocols for computer communications - SIGCOMM '03*. 2003, p. 49. ISBN: 1581137354. DOI: 10.1145/863955.863963.

[128] John C. Strikwerda. "A convergence theorem for chaotic asynchronous relaxation". In: *Linear Algebra and its Applications* 253.1-3 (1997), pp. 15–24. ISSN: 00243795. DOI: 10.1016/0024-3795(95)00698-2.

[129] Yangfeng Su et al. "Further results on convergence of asynchronous linear iterations". In: *Linear Algebra and its Applications* 281.1-3 (1998), pp. 11–24. ISSN: 00243795. DOI: 10.1016/S0024-3795(98)10030-7.

[130] Imam Sutrisno, Y. Salmah, and Indah E. Wijayanti. "Distributed model predictive control and application to irrigation canal". In: *IEEE Conference on Control, Systems & Industrial Informatics (ICCSII)*. Vol. 1. 978. 2012, pp. 126–130. ISBN: 9781467310239.

[131] Cheng Tan and Huanshui Zhang. "Necessary and Sufficient Stabilizing Conditions for Networked Control Systems with Simultaneous Transmission Delay and Packet Dropout". In: *IEEE Transactions on Automatic Control* 9286.c (2016), p. 1. ISSN: 0018-9286. DOI: 10.1109/TAC.2016.2614887.

[132] Andrew S. Tanenbaum and David J. Wetherall. *Computer Networks*. Vol. 52. 169. 2011, pp. 349–351. ISBN: 0130661023. DOI: 10.1016/j.comnet.2008.04.002. arXiv: 1011.1529.

[133] Xin Tian et al. "Distributed model predictive control for multi-objective water system management". In: *Proceedings of the 10th International Conference on Hydroinformatics*. Hamburg, Germany, 2012, p. 175.

[134] Yodyium Tipsuwan and Mo Yuen Chow. "Control methodologies in networked control systems". In: *Control Engineering Practice* 11.10 (2003), pp. 1099–1111. ISSN: 09670661. DOI: 10.1016/S0967-0661(03)00036-4.

[135] Claire Tomlin, George J. Pappas, and Shankar Sastry. "Conflict resolution for air traffic management: a study in multiagent hybrid systems". In: *IEEE Transactions on Automatic Control* 43.4 (1998), pp. 509–521. ISSN: 00189286. DOI: 10.1109/9.664154.

[136] Panagiotis Trakadas et al. "Routing metric selection and design for multi-purpose WSN". In: *IWSSIP 21st International Conference on Systems, Signals and Image Processing* May (2014), pp. 12–15. ISSN: 21578702.

[137] Peter-Jules P.-J. Van Overloop. "Model Predictive Control on Open Water Systems". PhD thesis. Delft University Press, 2006, p. 182. ISBN: 1586036386.

[138] José Vasquez. *Hydraulique a surface libre*. Tech. rep. École Nationale du Génie de l'Eau et de l'Environnement de Strasbourg (ENGEES), 2011, p. 105.

[139] Jean Phillippe Vasseur et al. "Routing Metrics Used for Path Calculation in Low-Power and Lossy Networks". 2012.

[140] Tamas Vicsek et al. "Novel Type of Phase Transition in a System of Self-Driven Particles". In: *Physical Review Letters* 75.6 (1995).

[141] Dong Wang et al. "Cooperative Containment Control of Multiagent Systems Based on Follower Observers With Time Delay". In: *IEEE Transactions on Systems, Man, and Cybernetics* 47.1 (2017), pp. 13–23.

[142] Qingling Wang et al. "An overview of consensus problems in constrained multi-agent coordination". In: *Systems Science & Control Engineering* 2.1 (2014), pp. 275–284. ISSN: 2164-2583. DOI: 10.1080/21642583.2014.897658.

[143] Yangling Wang, Jinde Cao, and Jianqiang Hu. "Pinning consensus for multi-agent systems with non-linear dynamics and time-varying delay under directed switching topology". In: *IET Control Theory & Applications* 8.17 (2014), pp. 1931–1939. ISSN: 17518652. DOI: 10.1049/iet-cta.2014.0032.

[144] Erik Weyer. "Control of irrigation channels". In: *IEEE Transactions on Control Systems Technology* 16.4 (2008), pp. 664–675. ISSN: 10636536. DOI: 10.1109/TCST.2007.912122.

[145] Tim Winter et al. "RPL: IPv6 Routing Protocol for Low-Power and Lossy Networks". 2012.

[146] Steven Wollkind, John Valasek, and Thomas R. Ioerger. "Automated conflict resolution for air traffic management using cooperative multiagent negotiation". In: *AIAA guidance, navigation, and control conference and exhibit* 4992.August (2004), pp. 1–11. DOI: 10.2514/6.2004-4992.

[147] Michael Wooldridge. *An Introduction to MultiAgent Systems*. London: John Wiley & Sons Ltd., 2002.

[148] Feng Xia. "QoS Challenges and Opportunities in Wireless Sensor/Actuator Networks". In: *Sensors* 8.2 (2008), pp. 1099–1110. ISSN: 1424-8220. DOI: 10.3390/s8021099. arXiv: 0806.0128.

[149] Feng Xiao and Long Wang. "Asynchronous consensus in continuous-time multi-agent systems with switching topology and time-varying delays". In: *IEEE Transactions on Automatic Control* 53.8 (2008), pp. 1804–1816. ISSN: 00189286. DOI: 10.1109/TAC.2008.929381. arXiv: 0611932 [math].

[150] Feng Xiao, Long Wang, and Aiping Wang. "Consensus problems in discrete-time multiagent systems with fixed topology". In: *Journal of Mathematical Analysis and Applications* 322.2 (2006), pp. 587–598. ISSN: 0022247X. DOI: 10.1016/j.jmaa.2005.08.094.

[151] Wenying Xu et al. "Event-Triggered Schemes on Leader-Following Consensus of General Linear Multiagent Systems Under Different Topologies". In: *IEEE Transactions on Cybernetics* 47.1 (2017), pp. 212–223. ISSN: 2168-2267. DOI: 10.1109/TCYB.2015.2510746.

[152] Yang Yaling and Wang Jun. "Design guidelines for routing metrics in multihop wireless networks". In: *Proceedings of IEEE INFOCOM* (2008), pp. 2288–2296. ISSN: 0743166X. DOI: 10.1109/INFOCOM.2007.222.

[153] Ke-you You and Li-Hua Xie. "Survey of Recent Progress in Networked Control Systems". In: *ACTA Automatica Sinica* 39.2 (2013).

[154] Xiaoqing Yu et al. "A survey on wireless sensor network infrastructure for agriculture". In: *Computer Standards & Interfaces* 35.1 (2013), pp. 59–64. ISSN: 09205489. DOI: 10.1016/j.csi.2012.05.001.

[155] Theodore Zahariadis and Panagiotis Trakadas. "Design Guidelines for Routing Metrics Composition in LLN". 2012.

[156] Xian-Ming Zhang, Qing-Long Han, and Yu-Long Wang. "A brief survey of recent results on control and filtering for networked systems". In: *12th World Congress on Intelligent Control and Automation (WCICA)*. 2016, pp. 64–69. ISBN: 978-1-4673-8414-8. DOI: 10.1109/WCICA.2016.7578665.

[157] Xianming Zhang, Qing-Long Han, and Xinghuo Yu. "Survey on Recent Advances in Networked Control Systems". In: *IEEE Transactions on Industrial Informatics* 3203.c (2015), p. 1. ISSN: 1551-3203. DOI: 10.1109/TII.2015.2506545.

[158] Xiaona Zhang, Jie Feng, and Tao Yang. "Lattice Boltzmann method for overland flow studies and its experimental validation". In: *Journal of Hydraulic Research* 53.5 (2015), pp. 561–575. ISSN: 0022-1686. DOI: 10.1080/00221686.2015.1110625.

[159] Ming Zhao, Ivan Wang Hei Ho, and Peter Han Joo Chong. "An Energy-Efficient Region-Based RPL Routing Protocol for Low-Power and Lossy Networks". In: *IEEE Internet of Things Journal* 3.6 (2016), pp. 1319–1333. ISSN: 23274662. DOI: 10.1109/JIOT.2016.2593438.

[160] Wei Zhao, Renfu Li, and Huaipin Zhang. "Leader–follower optimal coordination tracking control for multi-agent systems with unknown internal states". In: *Neurocomputing* 249 (2017), pp. 171–181. ISSN: 09252312. DOI: 10.1016/j.neucom.2017.03.066.

[161] Bo Zhou et al. "Constrained consensus of asynchronous discrete-time multi-agent systems with time-varying topology". In: *Information Sciences* 320 (2015), pp. 223–234. ISSN: 00200255. DOI: 10.1016/j.ins.2015.05.024.

[162] Jian G. Zhou. "A lattice Boltzmann model for the shallow water equations". In: *Computer Methods in Applied Mechanics and Engineering* 191.32 (2002), pp. 3527–3539. ISSN: 00457825. DOI: 10.1016/S0045-7825(02)00291-8.

[163] Xiangtao Zhuan and Xiaohua Xia. "Models and Control Methodologies in Open Water Flow Dynamics: A Survey". In: *Africon* (2007), pp. 1–7. DOI: 10.1109/AFRCON.2007.4401525.